lubricants

MDPI

Article

Stability and Ageing Behaviour of SiO_2 Nanoparticle-Modified Lubricants and Biolubricants: An Experimental–Numerical Investigation

Homeyra Piri [1], Salar Moradi [1], Massimiliano Renzi [1,*] and Marco Bietresato [1,2]

[1] Faculty of Engineering, Free University of Bozen-Bolzano, 39100 Bolzano, Italy; homeira.piri@gmail.com (H.P.); salar.moradi@unibz.it (S.M.); marco.bietresato@uniud.it (M.B.)
[2] Department of Agricultural, Food, Environmental and Animal Sciences (DI4A), University of Udine, 33100 Udine, Italy
* Correspondence: massimiliano.renzi@unibz.it; Tel.: +39-0471-017-816

Abstract

This study comparatively investigated the ageing behaviour of a conventional lubricant and a biolubricant modified with 0.25–1.00 wt.% KH570-coated SiO_2 nanoparticles. Nanolubricants and nanobiolubricants were prepared using a two-step dispersion method and subjected to accelerated thermal ageing at 220 and 260 °C for exposure times ranging from 120 to 240 h. Density, kinematic viscosity at 40 and 100 °C, viscosity index, Total Acid Number (TAN), Total Base Number (TBN), Fourier Transform Infrared Spectroscopy (FTIR), and Inductively Coupled Plasma Optical Emission Spectroscopy (ICP-OES) were used to evaluate their physicochemical and chemical degradation. The results showed that increasing temperature and exposure time generally intensified density growth, viscosity thickening, viscosity-index deterioration, and oxidation, whereas SiO_2-containing formulations exhibited more moderate changes in several responses under severe ageing conditions. At 260 °C and 168 h, the viscosity at 40 °C of the conventional lubricant decreased from 193.7 $mm^2 \cdot s^{-1}$ without nanoparticles to 135.1 $mm^2 \cdot s^{-1}$ with 1.00 wt.% SiO_2, corresponding to a reduction of 30.25%. For the biolubricant, viscosity decreased from 312.9 $mm^2 \cdot s^{-1}$ to 98.6 and 116.8 $mm^2 \cdot s^{-1}$ with 0.75 and 1.00 wt.% SiO_2, corresponding to reductions of 68.49% and 62.67%, respectively. Under the same severe ageing conditions, oxidation in the conventional lubricant decreased by 27.19% at 1.00 wt.% SiO_2, while oxidation in the biolubricant decreased by 34.11% and 22.08% at 0.75 and 1.00 wt.% SiO_2, respectively. Response Surface Methodology combined with ANOVA and backward elimination identified temperature, exposure time, nanoparticle concentration, and their interactions as response-dependent controlling factors. The resulting reduced regression models provided high goodness of fit; for example, the coefficients of determination ranged from 0.9976 to 0.9981 for density and from 0.9954 to 0.9999 for viscosity at 40 °C. The response surfaces confirmed that temperature and time generally promoted degradation, whereas SiO_2 addition was associated with lower excessive viscosity and oxidation increases under specific concentrations at high thermal severity, with a more pronounced effect in the biolubricants. Overall, KH570-modified SiO_2 nanoparticles showed potential for mitigating changes associated with accelerated thermo-oxidative ageing, although the optimum concentration depended on the lubricant formulation and the investigated response. Because all formulations were tested under identical nominal ageing conditions, the observed differences support a comparative assessment of nanoparticle

Received: 22 September 2026
Revised: 26 October 2026
Accepted: 28 October 2026
Published: 30 October 2026

Copyright: © 2026 by the authors. Licensee MDPI, Basel, Switzerland. This article is an open access article distributed under the terms and conditions of the Creative Commons Attribution (CC BY) license.

effects; however, the contribution of evaporation and concentration effects could not be independently quantified.

Keywords: SiO_2 nanoparticles; lubricants; biolubricants; thermal ageing; oxidation; viscosity; response surface methodology

1. Introduction

The potential of nanotechnology to improve lubrication performance and reduce the demand for conventional additives has made its application in lubricant formulations increasingly widespread in recent years [1–3]. Incorporating appropriate nanoparticles into lubricants (to obtain the so-called "nanolubricants") represents a viable method for significantly improving their oxidative stability, anti-wear, anti-friction, and anti-corrosion properties [4]. Amongst all possible materials for nanoparticles, SiO_2 has shown significant promise as a lubricant additive [5–8]. These nanoparticles are appropriate for this application because of a number of distinctive characteristics they have, such as

- Heat Resistance: SiO_2 has a high heat resistance and the ability to absorb light and heat [9,10];
- Low coefficient of friction: Interposed SiO_2 nanoparticles can reduce friction between moving parts. This may reduce wear in mechanical components lubricated with nanolubricants and improve energy efficiency [11,12];
- Good biocompatibility: SiO_2 nanoparticles are safe to be employed in lubricants that are already thought to come into contact with food or living beings, since they are known to be biocompatible [12].

Silicon dioxide (SiO_2) nanoparticles, for example, find versatile applications in different types of agricultural machinery lubricants. They contribute to improving wear resistance and lower friction when incorporated into engine lubricant, which eventually extends engine life and increases fuel efficiency [5,13]. Comparably, adding SiO_2 nanoparticles to gear lubricant improves wear resistance and lowers noise, which prolongs gear life and improves machinery performance [14,15]. Moreover, incorporating them into hydraulic oil also increases, in this case, the wear resistance of all the involved systems, which extends the longevity of hydraulic systems and improves the overall machinery performance [16,17].

There are several advantages associated with using SiO_2 nanoparticles in lubricants. By reducing wear and tear on machinery components, these nanoparticles can increase the equipment's lifespan and lower maintenance expenses [5,18]. Additionally, by lowering wear and friction, the use of SiO_2 nanoparticles improves fuel efficiency [19]. As a result, by enhancing engine performance and reducing fuel usage, emissions are also reduced. SiO_2 nanoparticles are notably a more environmentally friendly lubricant additive than many other conventional additives [20,21].

Mohd Farid Ismail et al. [22] demonstrate that nanoparticle additives improve the coefficient of friction (COF) at low volume concentrations. Specifically, the COF of nanolubricants with a volume concentration of nanoparticles below 0.010 vol.% for TiO_2 and less than 0.005 vol.% for SiO_2 is lower than that of pure polyvinyl ether (PVE) lubricant. Yeou et al. [23] indicate that the abrasion loss of a nano-SiO_2 lubricant containing 3.5 wt.% SiO_2 dropped by 42.43% on average in tribology tests. Meghana et al. [13] report that SiO_2 nanoparticles decreased the average coefficient of friction by 8.69%, while extending the mixed lubrication regime of a Pongamia-based lubricant (*Pongamia pinnata* L.). Furthermore, DPPH (2,2-diphenyl-1-picrylhydrazyl) analysis was used to evaluate the

antioxidant capabilities of SiO_2, and the results showed DPPH inhibition of 74.38% at the highest concentration (700 $\mu g \cdot mL^{-1}$). A study on the rheological and tribological characteristics of polyethylsiloxane containing SiO_2 nanoparticles is presented by Tuyana et al. [7]; SiO_2 nanoparticles were added, and this increased the lubricating film's tear strength and tribological performance. There was a favourable effect of SiO_2 nanoparticles on the friction coefficient. The shear modulus and mechanical loss angle of the SiO_2 nanoparticle suspensions in polyethylsiloxane, as well as other viscoelastic parameters, were evaluated in another study by Fatima et al. [11], which investigated the tribological characteristics of polyalphaolefin 6 (PAO6) lubricant incorporated with SiO_2 nanoparticles modified with stearic acid (SiO_2-SA) as additives, at concentrations ranging from 0.05% to 0.30% in mass. When compared to PAO6 alone, the tribological tests showed that all nanolubricants had better anti-friction properties. In both tribological circumstances, 0.30% in mass was shown to be the ideal concentration for reducing friction. The combination of PAO6 + 0.20% in mass of SiO_2-SA showed the best anti-wear performance in pure sliding conditions, with wear track width, wear track depth, and wear area reduced by 55%, 86%, and 92%, respectively. Mohd Farid Ismail et al. [24] distributed SiO_2 and TiO_2 nanoparticles at different concentrations and temperatures in a polyvinyl ether (PVE) lubricant. As the concentration of nanoparticles increased, the thermal conductivity showed an increase, but conductivity also showed a decrease with increased temperature. The experimental data showed an average deviation of less than 0.29% from the regression model, and this model had a high R-square of more than 0.9952. The COF decreased by 15% while using SiO_2/PVE nanolubricant at 0.003 vol.%, in comparison to the baseline. Interestingly, when the concentration values for SiO_2 and TiO_2 exceeded the thresholds of 0.010 vol.% and 0.020 vol.%, respectively, the COF values for nanolubricants exceeded those of base lubricants. The ideal concentration of SiO_2 and TiO_2 nanoparticles improved the PVE lubricant's thermal and tribological characteristics, indicating possible benefits for use in refrigeration systems. Sankar and Duraivelu [25] conducted a groundbreaking study in which they ingeniously blended nanoparticles of SiO_2, Al_2O_3, and TiO_2, seamlessly infusing them into a light grade base oil (SN 500). Their research reveals that an optimal composition of 1 wt.% SiO_2, 1 wt.% TiO_2, and 0.05 wt.% Al_2O_3 stands out as remarkably effective, demonstrating unparalleled friction-reduction properties when employed as a lubricant. The judicious use of these nanoparticles not only mitigates shearing stress but also curtails friction and wear on surfaces, making it a standout solution for enhanced lubrication performance. In the study by Abhisek et al. [16], a hydraulic oil with an optimal volume fraction of 1.8% multi-walled carbon nanotubes (MWCNT)/SiO_2 nanomaterials at a ratio of 20:80 showed notable decreases in wear scar diameter (WSD) and friction coefficient, by 14.00% and 92.99%, respectively, when compared to the pure lubricant. When compared to base sunflower lubricant, Vicente et al. [5] demonstrated that the addition of SiO_2 and TiO_2 nanoparticles reduced the coefficients of friction by 77.7% and 93.7%, respectively. Moreover, the inclusion of SiO_2 and TiO_2 nanoparticles, respectively, reduced the volume loss by 74.1% and 70.1%. The authors concluded that a modified sunflower lubricant augmented with nanoparticles has the potential to be used as an effective biodegradable lubricant, based on the experimental results. Sumit et al. [19] conducted a comprehensive study to assess the impacts of different nanoparticles (SiO_2, WS_2, Cu, CuO, and graphite) on the tribological properties of a 15W40 lubricating oil. SiO_2 nanolubricant exhibited the maximum reduction of COF, equal to 15–25%, followed by graphite (≈15–18%), WS_2 (≈13–21%), Cu (≈9–20%), and CuO (≈1.5–17%). WSD reduction was most prominent with SiO_2 nanolubricant (≈50–59%), followed by graphite (≈45–57%), WS_2 (≈17–26%), Cu (≈33–49%), and CuO (≈13–28%). As reported by Kok-Hou Tan et al. [26], zeolite nanoparticles have been shown to be capable of preventing the oxidation of lubricants based on palm oil. According to the TAN study, the quantity of acidic chemicals produced during

the oxidation of palm oil lubricant is likewise decreased by 35–50% in the presence of nanosized zeolites. Thachnatharen et al. [27] have extensively investigated the use of microwave-synthesized MoS2-graphene nanohybrid additives to enhance the tribological properties of 20W40 lubricant for diesel engines. Their findings reveal that even a minimal addition of 0.05 wt.% MoS2-graphene nanohybrid yields significant improvements: a remarkable 58.82% reduction in friction coefficient and a substantial 36.26% decrease in the average wear scar diameter. Furthermore, the study indicates a notable enhancement in oxidation resistance by 19.21%, along with a remarkable increase in thermal conductivity by 19.83% (at 100 °C).

Building on our previous investigations into nanoparticle dispersion stability, real-engine biolubricant ageing, oxidation inhibition in nanobiolubricants, and the thermal–oxidative behaviour of conventional and bio-based lubricants [28–31], the present study provides a systematic comparative assessment of the accelerated ageing behaviour of both lubricant classes. Whereas the previous studies separately addressed dispersion stability, real-engine ageing, oxidation resistance, or thermal stability, the present work evaluates the combined effects of ageing temperature, exposure time, and KH570-modified SiO_2 nanoparticle concentration on the degradation of a conventional lubricant and a biolubricant under identical experimental conditions. This design enables a direct comparison of the ageing responses of the two lubricant formulations and supports the development of response-surface models describing the influence of the investigated factors.

KH570-modified SiO_2 nanoparticles were incorporated at concentrations ranging from 0.25 to 1.00 wt.% into both conventional lubricant and biolubricant formulations. The resulting samples were subjected to accelerated thermal ageing at 220 and 260 °C for exposure times between 120 and 240 h. Density, kinematic viscosity at 40 and 100 °C, viscosity index, Total Acid Number (TAN), Total Base Number (TBN), Fourier Transform Infrared Spectroscopy (FTIR), and Inductively Coupled Plasma Optical Emission Spectroscopy (ICP-OES) were employed to evaluate changes in physicochemical properties, acid–base reserves, oxidation, molecular structure, and elemental composition. Response Surface Methodology was subsequently applied to quantify the individual and interactive effects of temperature, exposure time, and nanoparticle concentration. This integrated experimental–numerical approach was used to determine whether SiO_2 nanoparticles could mitigate thermo-oxidative degradation and preserve the functional properties of both lubricant types during prolonged thermal exposure.

The present study focuses on physicochemical and chemical ageing behaviour. No direct tribological measurements, including friction or wear tests, were performed; therefore, the results should not be interpreted as direct evidence of improved anti-friction, anti-wear, or overall tribological performance.

2. Materials and Methods

2.1. Used Lubricants and Nanoparticles

NILS S.p.A. (Postal, Bolzano, Italy; https://www.nils.eu/en/ (accessed on 1 September 2026)) and FUCHS LUBRICANTS GERMANY GmbH (Mannheim, Germany, https://www.fuchs.com/de/en/ (accessed on 1 September 2026)) supplied the two lubricants used in this study, respectively: the "Mistral 15W40", by NILS, a conventional (mineral) lubricant, and "PLANTO MOT SAE 10W40", a biolubricant produced by FUCHS LUBRICANTS GERMANY. The technical specifications for these lubricants are detailed in Table 1. Silicon dioxide (SiO_2) nanoparticles with an average particle size of 18–35 nm and coated with KH570-Silane coupling agent were acquired from Nanografi Inc. (Çankaya/Ankara, Türkiye; https://nanografi.com/ (accessed on 1 September 2026)). Table 2 outlines the key characteristics of the nanoparticles used; Table 3 presents the elemental analysis. It should be noted that the two investigated lubricants are commercial

formulations with different SAE grades, initial physicochemical properties, additive packages, and base-oil chemistries. Therefore, the differences observed during ageing cannot be attributed solely to the mineral- versus bio-based nature of the lubricants and may also reflect formulation-specific effects.

Table 1. Technical specifications of the lubricants used.

Properties	Measurement Unit	Reference	NILS Mistral 15W40	PLANTO MOT SAE 10W40
Kinematic viscosity at 40 °C	[$mm^2 \cdot s^{-1}$]	ASTM D445-24 [32]	97.3	87.0
Kinematic viscosity at 100 °C	[$mm^2 \cdot s^{-1}$]	ASTM D445-24 [32]	13.5	13.7
Viscosity index	[-]	ISO 2909:2002 [33]	138	160
Density at 15 °C	[$g \cdot cm^{-3}$]	ASTM D4052-22 [34]	0.8769	0.8719
TBN	[$mg(KOH) \cdot g^{-1}$]	ASTM D4739-17 [35]	10.5	9.7
TAN	[$mg(KOH) \cdot g^{-1}$]	ASTM D664-18e2 [36]	2.2	1.7

Table 2. Properties of SiO_2 nanoparticles.

Technical Properties	Unit of Measurement	Value/Appearance
Purity	[%]	95.9+
Colour	[-]	white
Average Particle Size	[nm]	18–35
Specific Surface Area	[$m^2 \cdot g^{-1}$]	150–550
Bulk Density	[$g \cdot cm^{-3}$]	<0.1
True Density	[$g \cdot cm^{-3}$]	2.2

Table 3. Elemental Analysis of SiO_2 nanoparticles.

Elements	wt.%
SiO_2	95.9
KH570	3–4
Fe	0.032
Ca	0.056
Mg	0.0085
S	0.025

2.2. Experimental Procedure for Nanolubricant Samples: Preparation and Artificial Ageing

Nanoparticles were dispersed in both Mistral 15W40 lubricant and PLANTO MOT SAE 10W40 biolubricant at four different concentrations (0.25, 0.50, 0.75, and 1.00 weight percent). The recommendations in the literature for the most effective ranges of SiO_2 nanoparticles in lubricants were used to choose these concentrations [5,37]. In our previous study [28], we evaluated the stability and dispersion of nanoparticles at the same concentrations and with the same lubricant and biolubricant used in the present study. FTIR, UV–Vis spectrophotometric analysis, and sedimentation photography were used to evaluate their dispersion stability. We found that longer sonication times (hence: 2.5 h) considerably improved the stability of nanolubricants and nanobiolubricants, demonstrating the critical importance of optimizing the sonication time. So, after the addition of the nanoparticles, the samples underwent magnetic stirring at 1500 rpm for 1.5 h at ambient temperature. Subsequently, ultrasonic processing was performed using an ultrasonic cleaner (VWR USC600THD (Avantor, Inc., Radnor Township, PA, USA); https://sg.vwr.com/store/product/10694225/null (accessed on 1 September 2026)) with a power output of 120 W and a frequency of 45 kHz for 2.5 h. The ultrasonication process aimed to achieve a dispersion of nanoparticles as uniform as practicable.

After the preparation described above, the base lubricants used for the study, i.e., the Mistral 15W40 and PLANTO MOT SAE 10W40 biolubricant, along with all prepared nanolubricants, underwent an artificially induced degradation process. This was achieved by heating the samples in a hot-air oven (TCF 120 PLUS (TC Farmer Co., LLC, Canandaigua, NY, USA); https://www.tcfarmer.com/ (accessed on 1 September 2026)) at 220 °C and 260 °C for 120, 168 and 240 h. These temperatures and time durations were determined following preliminary screening tests designed to produce measurable lubricant oxidation. Those preliminary tests started from a minimum temperature of 90 °C, with temperature increments of 20–30 °C and a minimum duration of 30 h, in 30 h increments. Based on these tests, it was observed that oxidation primarily occurred at 220 °C.

The selected temperatures were intentionally higher than typical bulk lubricant temperatures encountered during normal engine operation and were used to provide accelerated, severe thermal–oxidative ageing conditions within a practicable experimental time. The 220 °C condition was selected as the lowest temperature at which measurable oxidation was clearly observed during the preliminary screening tests, while 260 °C was included as a more severe ageing condition to amplify degradation responses and enable comparison of lubricant formulations under stronger thermal stress. In the present oven experiments, these temperatures represent the bulk temperature of the lubricant samples rather than localized hot-spot temperatures. Therefore, the applied temperature–time combinations should be interpreted as accelerated laboratory ageing conditions and not as direct representations of lubricant service intervals or engine operating temperatures. No direct conversion between the applied ageing times and real service life was established. An Arrhenius-type acceleration analysis was deliberately not applied because the experimental design was intended for comparative degradation assessment rather than kinetic lifetime prediction, and the available temperature levels and measurements were insufficient to establish a validated temperature-dependent degradation rate model.

The inner ventilation of the oven was active to ensure a consistent temperature and air circulation throughout the ageing period. The experiments were conducted on nanolubricant samples put in open 100 mL bottles without lids. Periodically, samples were withdrawn to perform the required analyses.

For each lubricant type, 20 distinct experimental conditions were investigated, five fresh formulations and 15 aged formulations, resulting in 40 experimental conditions across the two lubricant types. Each condition was represented by one independently prepared sample ($n = 1$). Independent open bottles containing approximately 100 mL of lubricant were used for each ageing condition and exposure time, including the 120, 168, and 240 h conditions. Aliquots required for the subsequent analyses were taken from the corresponding independently aged bottles. Each reported analytical value represents a single measurement rather than the mean of replicate measurements. Mass loss during ageing was not quantified. The primary objective of the ageing protocol was comparative rather than the prediction of absolute lubricant lifetime. All lubricant and biolubricant formulations, including the nanoparticle-free references and the SiO_2-containing samples, were subjected to the same nominal ageing conditions, including temperature, exposure time, vessel configuration, and initial sample volume. Therefore, the observed differences between formulations provide a comparative indication of their relative behaviour under identical accelerated-ageing conditions. Nevertheless, because sample mass loss was not quantified, the individual contributions of evaporation, concentration effects, chemical degradation, and nanoparticle addition cannot be quantitatively separated.

2.3. Analyses Performed on the Lubricant Samples

The ageing of lubricant samples was quantified by observing the variation of some properties of interest after their exposure to heat for set periods of time, as declared before.

In this study, viscometric analysis was conducted to assess key properties of lubricants. The kinematic viscosity at 40 °C and 100 °C was measured to determine the lubricants' resistance to flow under the influence of gravity [32]. Additionally, the viscosity index, indicating the change in viscosity with temperature [33], and the density of lubricants at 15 °C, representing the mass per unit volume at the indicated temperature [34], were determined using an "SVM 3001" kinematic viscometer manufactured by Anton Paar (Graz, Austria; https://www.anton-paar.com/corp-en/ (accessed on 1 September 2026)).

A comprehensive spectroscopic analysis was conducted, employing Fourier Transform Infrared (FTIR) Spectroscopy to delve into the molecular intricacies of the lubricants. The FTIR technique, facilitated by FTIR Spectrometer from Perkin Elmer, Spectrum 100 (Waltham, MA, USA; https://content.perkinelmer.com/ (accessed on 1 September 2026)), allowed the researchers to scrutinize both fresh and aged lubricant samples. FTIR spectroscopy played a crucial role in identifying molecular changes resulting from interactions with nanoparticles and from the degradation of lubricants over time. By exposing the samples to infrared radiation, this technique induced molecular vibrations, which were then recorded as spectra. This provided valuable information into the functional groups present in the lubricants, aiding in the detection of subtle alterations due to ageing and nanoparticle interactions.

The analysis of Total Acid Number (TAN) and Total Base Number (TBN) [35,36] yielded valuable insights into the oxidation resistance of the lubricants, and used state-of-the-art titration methods, utilizing a T50 Titrator from Mettler Toledo (Columbus, OH, USA; https://www.mt.com/us/en/home.html (accessed on 1 September 2026)). The examination of TBN involved considerations of nanoparticle influence, with outcomes varying depending on the type of nanoparticles and their interaction with the lubricant's antioxidants. It is noteworthy that ageing processes generally led to a decrease in TBN, which was primarily attributed to the depletion of antioxidants over time.

The quantification of metal concentrations in lubricants, which can provide information on elemental composition, contamination, additive behaviour, and, in engine-service studies, wear-related elements, was accomplished through Inductively Coupled Plasma Optical Emission Spectroscopy (ICP-OES) utilizing a Perkin Elmer OPTIMA 8000. ICP-OES analysis was also used to assess changes in elemental composition associated with nanoparticle addition and ageing conditions.

The methods and instruments employed in this study are outlined in Table 4.

Table 4. Techniques and equipment used for evaluating degradation and analysing nanoparticle effects.

Measured Parameter Type of Analysis	**Instrument**	**Manufacturer, Model**	**Precision**
Density Viscosity 40–100 °C Viscosity Index	Viscometer	Anton Paar, SVM 3001	Density = 0.0001 [g·cm^{-3}] Viscosity = 0.001 [mm^2·s^{-1}]
IR Nitration Oxidation	FT-IR Spectrometer	Perkin Elmer, Spectrum 100	0.1 [au·cm^{-1}]
TBN TAN	Titrator	Mettler Toledo, T50	TBN = 0.01 [mg(KOH)·g^{-1}] TAN = 0.001 [mg(KOH)·g^{-1}]
Metals	ICP-OES	Perkin Elmer, OPTIMA 8000	1 [ppm]

Wear Elements
Pollution Elements
Additives Elements

2.4. Data Analysis and Mathematical Modelling

The data was statistically analysed using Design-Expert 13.0.5.0 software (by Stat-Ease Inc., Minneapolis, MN, USA) to identify the mathematical relationships in accordance with the Response Surface Methodology (RSM). In fact, RSM was subsequently used to help the experimenters mathematically describe the effects of the statistically significant independent variables (factors) on the dependent variables (responses), using explicit regression functions [38].

A preliminary Analysis of Variance (ANOVA) was performed to ascertain the statistical significance of each independent variable in order to improve the analysis. By ensuring that only the most significant features were incorporated into the next regression models, this step improved the process of data processing. By removing non-significant components, the ANOVA results improved the accuracy and efficiency of the model by shedding light on the contributions of each factor to the response variables [39,40].

For both nanolubricants and nanobiolubricants, the first-attempt model proposed by the software was selected for data fitting. Based on the *p*-values for each numerical coefficient in the regression model, the ANOVA on the first model identified a large number of non-significant terms, i.e., those having associated *p*-values greater than 0.1000. Instead, *p*-values less than 0.0500 were said to indicate model terms were significant [39]. Model reduction can help a model, especially if it has a lot of unnecessary terms (aside from those needed to maintain hierarchy). Based on the *p*-values of the regression coefficients, terms with $p < 0.05$ were considered statistically significant, whereas terms with $p > 0.10$ were considered candidates for removal. Terms for which $0.05 \leq p \leq 0.10$ were retained when required to preserve model hierarchy or when retained by the backward-elimination criterion. Model hierarchy was preserved throughout the reduction procedure; therefore, lower-order terms were retained whenever their corresponding interaction or higher-order terms remained in the model. Backward elimination was performed iteratively, with *p*-values recalculated after each term removal.

The regression equations are reported in terms of actual factors, where T is the ageing temperature (°C), t is the exposure time (h), and $CSiO_2$ is the SiO_2 nanoparticle concentration (wt.%). Although Design-Expert internally uses coded factor levels for the ANOVA, the equations presented in the manuscript are the actual-factor equations.

Each design point was evaluated once, and no replicated experimental runs were performed. Therefore, pure error could not be independently estimated, and a conventional lack-of-fit test was not available for the fitted models.

3. Results and Discussion

3.1. Evolution of Physicochemical Properties in Lubricants and Biolubricants with Ageing

The experimental results, their interpretation, and any inferred empirical conclusions are briefly and precisely explained in this section. The following features were examined in the tests:

- Density, defined as the mass of the liquid per unit volume [41–43]; composition, temperature, and pressure all affect density.
- Viscosity, defined as the liquid's resistance to flow and shear; temperature, contamination, and lubricant ageing all have an impact on this property; in particular, kinematic viscosity is a measurement of the lubricant's rate of flow in response to force [44–47].

- Viscosity index (VI), defined as a measurement of how a liquid's viscosity varies with changes in temperature, is an arbitrary, unitless number that describes how lubricating oils behave in relation to viscosity and temperature, and is calculated according to ISO 2909:2002 [33]. The higher the VI, the more stable the viscosity is over a range of temperatures, and the lower the VI, the more sensitive to temperature changes [48–50].

Depending on their structure and quality, lubricants and biolubricants have varying viscosity, density, and viscosity index values. Biolubricants are often more resilient to temperature-related changes in viscosity because they have a higher natural VI than mineral lubricants. Nevertheless, compared to mineral lubricants, biolubricants may also be less oxidatively stable, which could have an impact on their durability and performance [51–54].

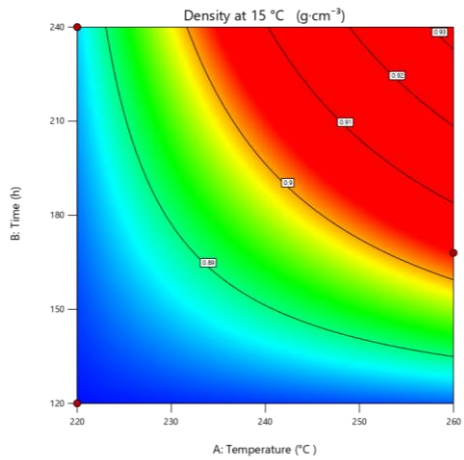
3.1.1. Evaluation of Density

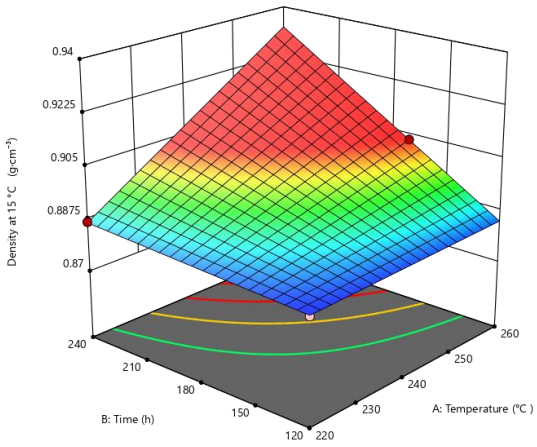
This study investigates the density variations of a lubricant and a biolubricant at different concentrations (wt.%) of SiO_2 nanoparticle and under varying conditions (aged lubricants after 120, 168 and 240 h at 220 °C and 260 °C).

In order to fit the data, the software first suggested starting with a full-cubic model for density. Non-significant terms were eliminated using the ANOVA and backward elimination process outlined in Section 2.4. Table 5 shows the numerical regression models as they resulted after the term-selection procedure. The graphical (2D/3D) representation of these equations is provided in Figures 1 and 2, which enable the viewing of absolute values as well as trends.

Table 5. Main data on both nanolubricants and nanobiolubricants for a response-surface reduced cubic model based on density data.

Quantity	Nanolubricants Regression Equation	Nanobiolubricants Regression Equation
Density at 15 °C [g·cm^{-3}]	$+1.11483 - 0.00107643 \cdot T - 0.00201534 \cdot t - 0.36756 \cdot C_{SiO2} + 9.32049 \cdot 10^{-6} \cdot T \cdot t + 0.00165998 \cdot T \cdot C_{SiO2} + 0.00156894 \cdot t \cdot C_{SiO2} + 0.148724 \cdot C_{SiO2}^2 - 7.10278 \cdot 10^{-6} \cdot T \cdot t \cdot C_{SiO2} - 0.00066381 \cdot T \cdot C_{SiO2}^2$	$+0.919017 - 0.000228173 \cdot T - 0.000731951 \cdot t - 0.116282 \cdot C_{SiO2} + 3.48160 \cdot 10^{-6} \cdot T \cdot t + 0.000547881 \cdot T \cdot C_{SiO2} + 0.00148456 \cdot t \cdot C_{SiO2} - 0.107581 \cdot C_{SiO2}^2 - 6.78889 \cdot 10^{-6} \cdot T \cdot t \cdot C_{SiO2} + 0.000480952 \cdot T \cdot C_{SiO2}^2$
Fit Statistics, Std. Dev.	0.0006	0.0003
Mean	0.8890	0.8782
C.V. %	0.0673	0.0384
R^2	0.9976	0.9981
Adjusted R^2	0.9932	0.9946





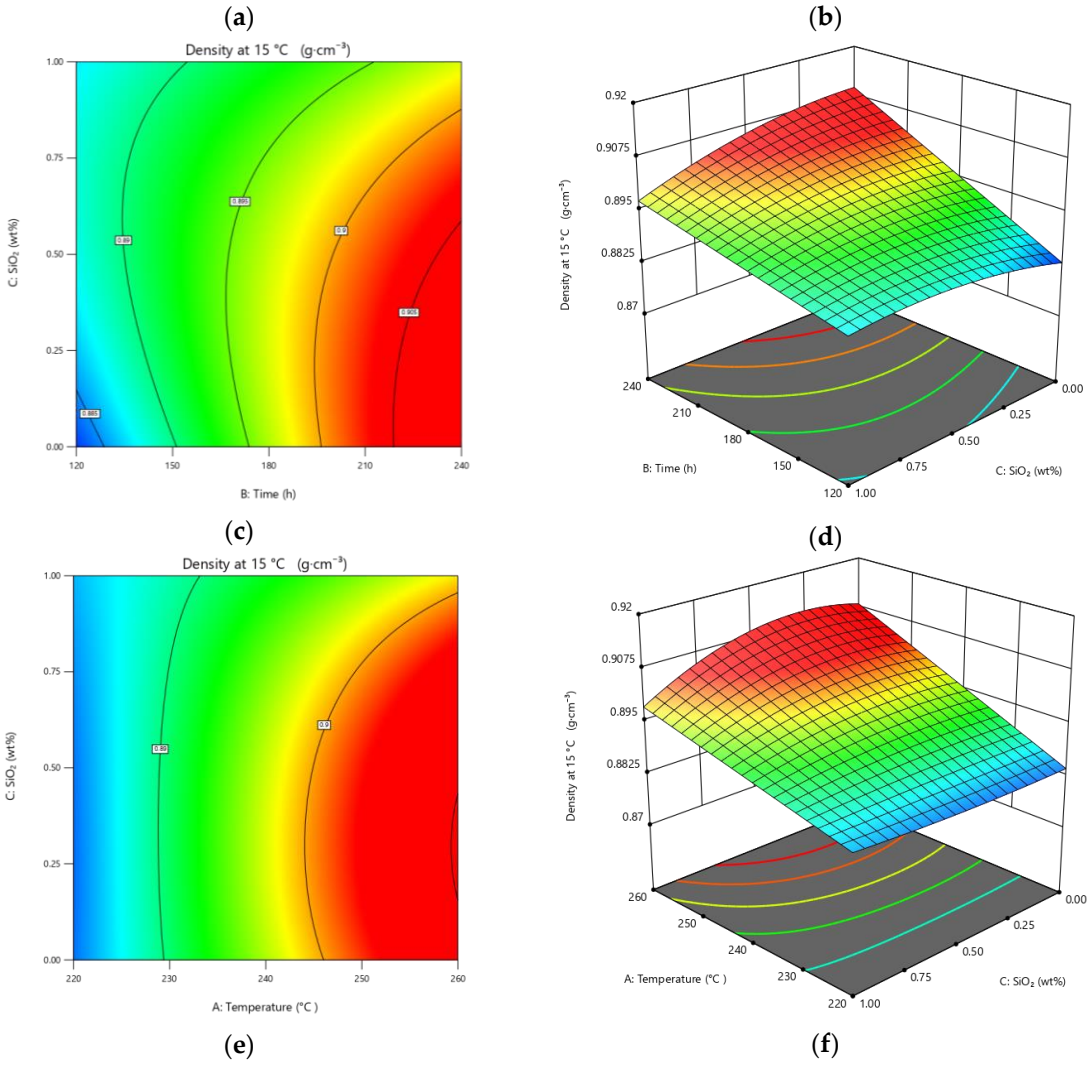
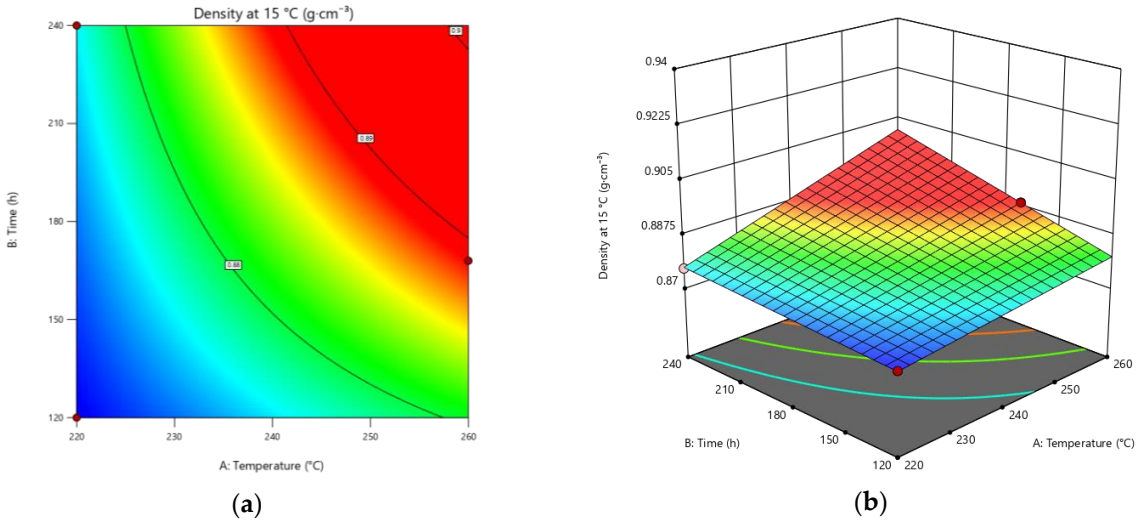


Figure 1. Contour plots (**left**) and the 3D surfaces (**right**) of the regression function for the density at 15 °C, varying the temperature and the heat-exposure time for a conventional lubricant ((**a**,**b**); in this case the SiO_2 concentration is set at 0.00%), the time and concentration of SiO_2 nanoparticles ((**c**,**d**); in this case the temperature is set at 240 °C); and the temperature and concentration of SiO_2 nanoparticles ((**e**,**f**); in this case the time is set at 180 h).



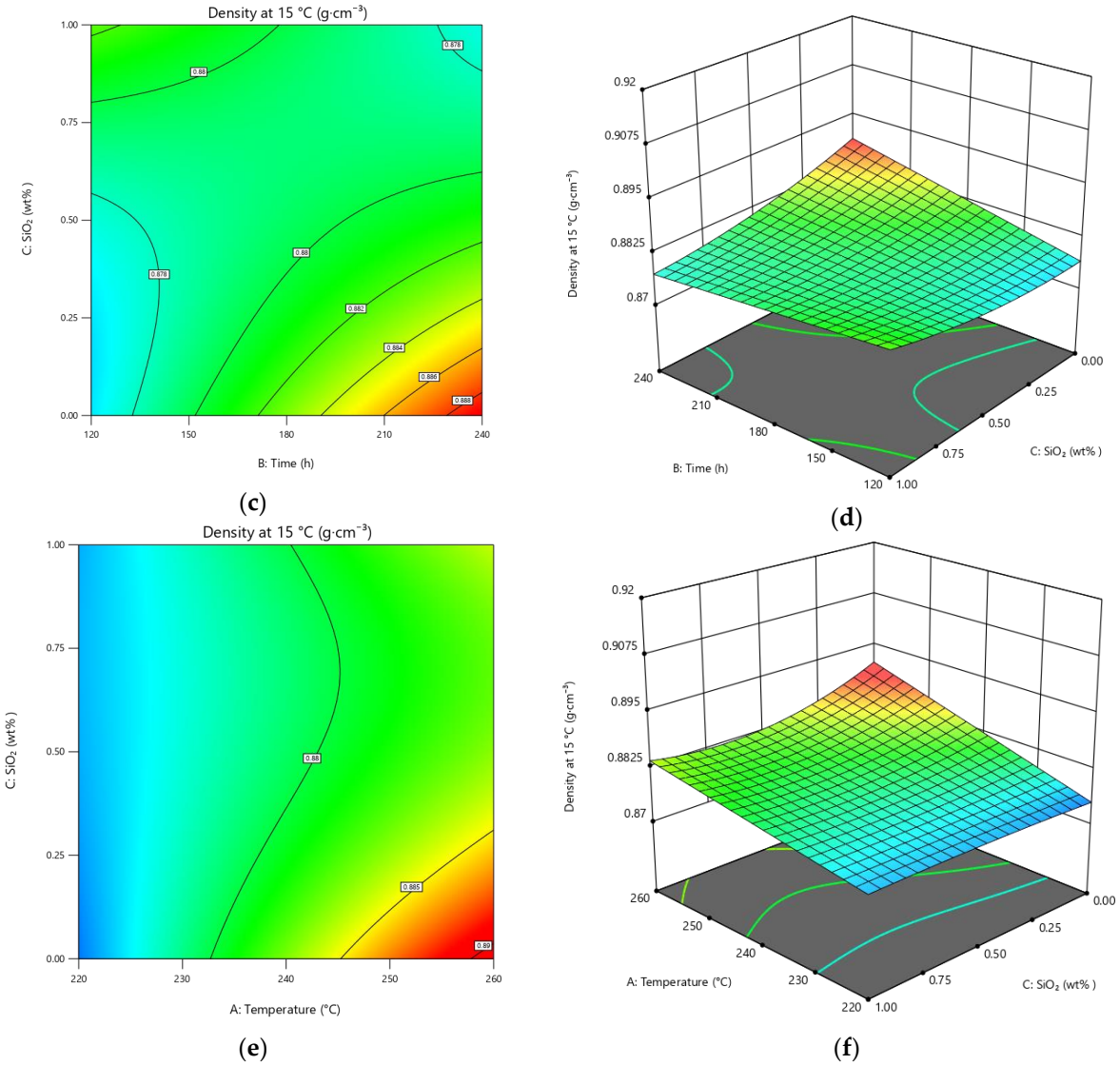


Figure 2. Contour plots (**left**) and the 3D surfaces (**right**) of the regression function for the density at 15 °C, varying the temperature and the heat-exposure time for a biolubricant ((**a**,**b**); in this case the SiO_2 concentration is set at 0.00%); the time and concentration of SiO_2 nanoparticles ((**c**,**d**); in this case the temperature is set at 240 °C); and the temperature and concentration of SiO_2 nanoparticles ((**e**,**f**); in this case the time is set at 180 h).

The contour plot (Figures 1a and 2a) and 3D surface (Figures 1b and 2b) illustrate how density is affected by temperature and time in lubricants and biolubricants, both without the inclusion of SiO_2 nanoparticles. Density consistently rises as temperature increases from 220 °C to 260 °C in both the lubricant and biolubricant. As can be seen from the steep slopes in the contour and surface plots, the lubricant is more sensitive to temperature, achieving a higher maximum density (0.9035 g·cm^{-3}) than the biolubricant (0.8888 g·cm^{-3}) within the factors' variation ranges. Longer exposure at higher temperatures leads to a more pronounced density rise, means that time is also important with the lubricant. The biolubricant also follows the same trend, but its reaction is more gradual and stable.

The effects of time and concentration of SiO_2 nanoparticles on density in nanolubricants and nanobiolubricants are illustrated in Figures 1c,d and 2c,d. In both lubricants and biolubricants, the surface and contour plots show that an increase in time increases the resulting density. However, the increase in SiO_2 nanoparticles (e.g., 0.75% and 1%) in longer times balances this increase. The contour plot of lubricant shows that the density

has increased significantly over longer times in the absence of SiO_2 nanoparticles. However, the addition of SiO_2 nanoparticles reduces this abrupt increase. The biolubricant plots exhibit a controlled and steady increase in density as the concentration of SiO_2 rises, thereby averting over-density.

Figures 1e,f and 2e,f demonstrate the effects of temperature and SiO_2 nanoparticle concentration on density in nanolubricants and nanobiolubricants. As we mentioned in our earlier work [28], the density of the fresh lubricants and biolubricants tends to increase as the percentage of SiO_2 nanoparticles increases. However, under severe ageing conditions, SiO_2 addition partially offset the ageing-associated increase in density relative to the fresh lubricant. Indeed, the plots demonstrate that temperature has a major impact on density for both lubricants and biolubricants. The density of the biolubricant increased from 0.8731 $g \cdot cm^{-3}$ without SiO_2 to 0.8745 $g \cdot cm^{-3}$ with 1.0 wt.% SiO_2, corresponding to an increase of 0.16% per percentage point of SiO_2 added. Similarly, at 220 °C, the density of the conventional lubricant increased from 0.8819 $g \cdot cm^{-3}$ without SiO_2 to 0.8830 $g \cdot cm^{-3}$ with 1.0 wt.% SiO_2, corresponding to an increase of 0.12% per percentage point of SiO_2 added. Although this trend is completely different at higher temperatures and the stabilizing effect of SiO_2 nanoparticles can be clearly seen, at a temperature of 260 °C, the density of lubricants drops from 0.9035 $g \cdot cm^{-3}$ (0 wt.% SiO_2) to 0.9031 $g \cdot cm^{-3}$ (0.75 wt.% SiO_2) and 0.8970 $g \cdot cm^{-3}$ (1.0 wt.% SiO_2), and for biolubricants drops from 0.8888 $g \cdot cm^{-3}$ (0 wt.% SiO_2) to 0.8829 $g \cdot cm^{-3}$ (0.75 wt.% SiO_2) at 168 h, and then slightly increases to 0.8853 $g \cdot cm^{-3}$ (1.0 wt.% SiO_2).

By comparing the two types of lubricants, it is evident that the conventional lubricant's density is more sensitive to temperature, increasing more sharply as the temperature rises. By comparison, biolubricants react to temperature variations in a more controlled manner. Under the investigated severe ageing conditions, SiO_2-containing formulations exhibited lower measured density values than the corresponding nanoparticle-free samples, particularly in the biolubricant. This trend indicates a possible moderating effect on ageing-associated density changes, although the underlying mechanism cannot be established from the present measurements. In comparison to conventional lubricant, the biolubricant is more resistant to density variations brought on by thermal stress, since it generally maintains a more balanced density across a range of temperatures and nanoparticle concentrations.

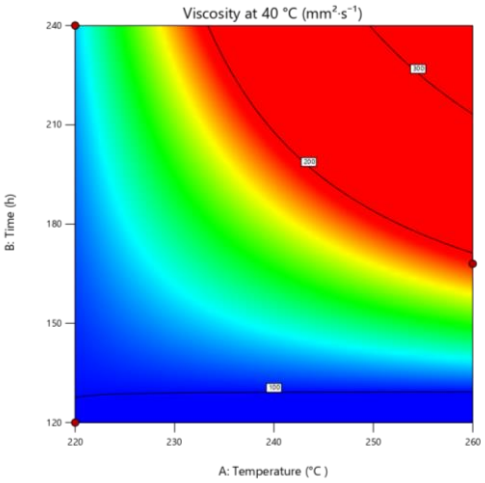
3.1.2. Evaluation of Kinematic Viscosity at 40° C

The effect of nanoparticles on the kinematic viscosity at 40 °C was examined at various mass concentrations (wt.%) of SiO_2 nanoparticle and under various conditions of time–temperature exposure (aged lubricants after 120, 168, and 240 h at 220 °C and 260 °C). The best software-proposed model to fit the data for both nanolubricants and nanobiolubricants was the full-cubic for this response as well. Using the ANOVA and backward elimination process outlined in Section 2.4, non-significant terms were eliminated. The numerical regression models are displayed in Table 6 and Figures 3 and 4 provide a graphical (2D/3D) depiction of these equations that makes absolute values and trends observable.

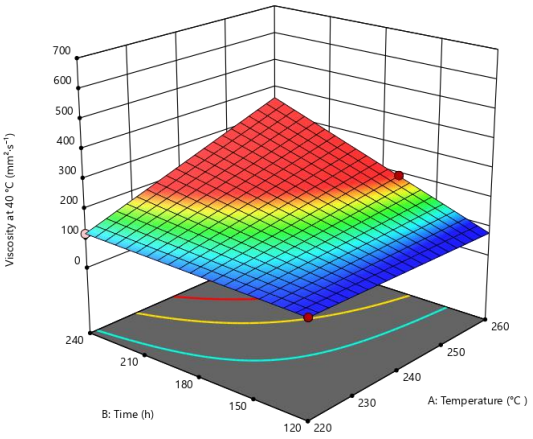
Table 6. Main data for both nanolubricants and nanobiolubricants for a response-surface reduced cubic model based on viscosity at 40 °C data.

Quantity	Nanolubricants Regression Equation	Nanobiolubricants Regression Equation
Viscosity at 40 °C [$mm^2 \cdot s^{-1}$]	$+1661.47 - 7.19034 \cdot T - 12.0642 \cdot t - 963.461 \cdot C_{SiO_2} + 0.0555643 \cdot T \cdot t + 4.65504 \cdot T \cdot C_{SiO_2} - 0.45852 \cdot t \cdot C_{SiO_2} + 1291.97 \cdot C_{SiO_2}^2 - 6.14897 \cdot T \cdot C_{SiO_2}^2 + 0.474953 \cdot t \cdot C_{SiO_2}^2$	$+2466.91 - 10.8758 \cdot T - 21.8929 \cdot t - 2820.22 \cdot C_{SiO_2} + 0.0996267 \cdot T \cdot t + 12.8348 \cdot T \cdot C_{SiO_2} + 35.0301 \cdot t \cdot C_{SiO_2} -$

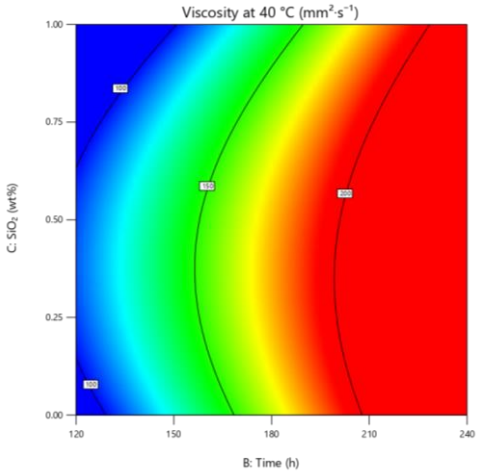
		$1992.73 \cdot C_{SiO2}^2 - 0.159261 \cdot T \cdot t \cdot C_{SiO2} + 9.04333 \cdot T \cdot C_{SiO2}^2$
Fit Statistics, Std. Dev.	3.49	0.9269
Mean	120.53	98.72
C.V. %	2.89	0.9389
R^2	0.9954	0.9999
Adjusted R^2	0.9871	0.9998



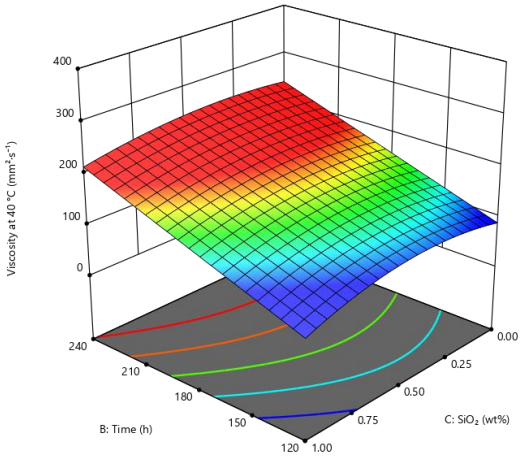
(**a**)



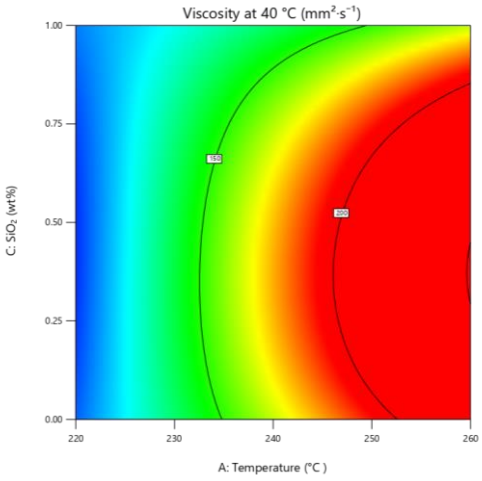
(**b**)



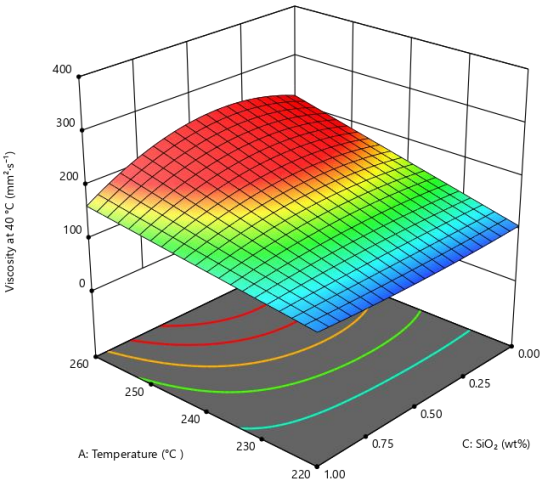
(**c**)



(**d**)



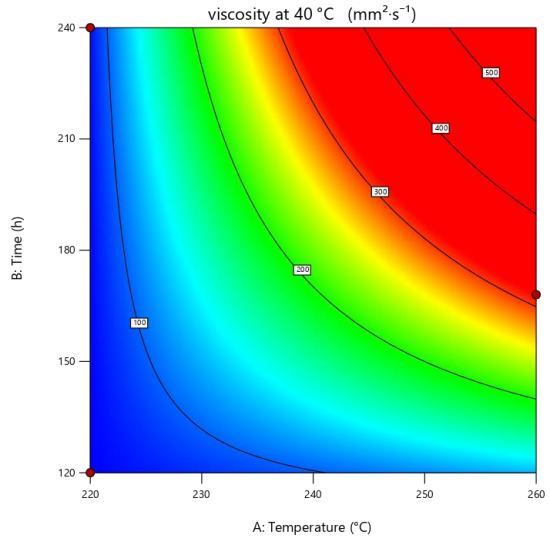
(**e**)



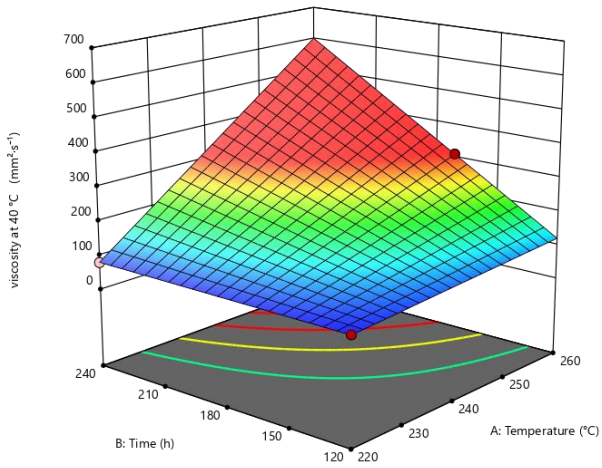
(**f**)

https://doi.org/10.3390/lubricants14110416

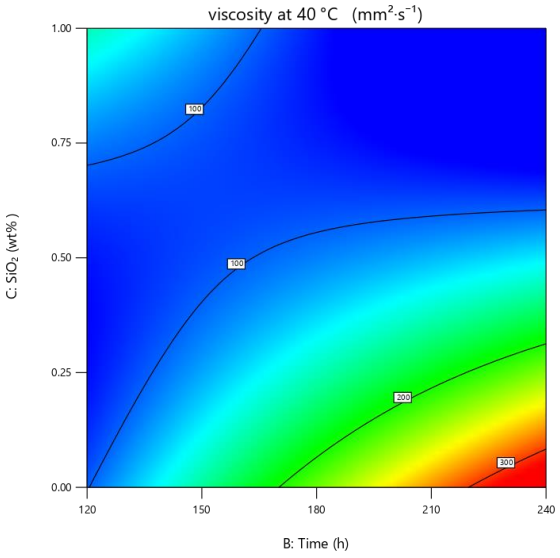
Figure 3. Contour plots (**left**) and the 3D surfaces (**right**) of the regression function for the viscosity at 40 °C varying the temperature and the heat-exposure time for a conventional lubricant ((**a**,**b**); in this case the SiO_2 concentration is set at 0.00%); the time and concentration of SiO_2 nanoparticles ((**c**,**d**); in this case the temperature is set at 240 °C); and the temperature and concentration of SiO_2 nanoparticles ((**e**,**f**); in this case the time is set at 180 h).



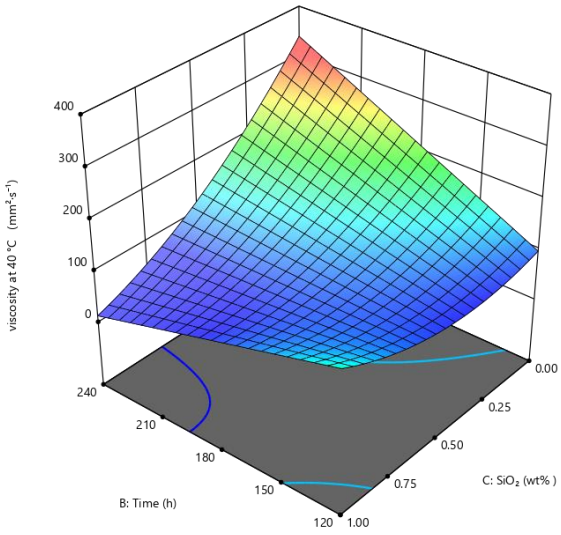
(**a**)



(**b**)

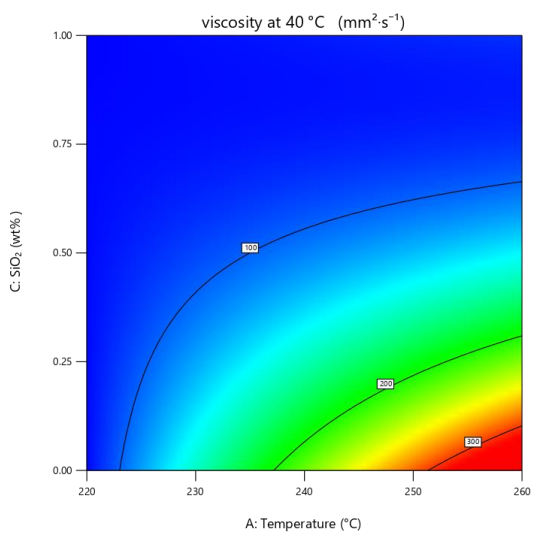


(**c**)

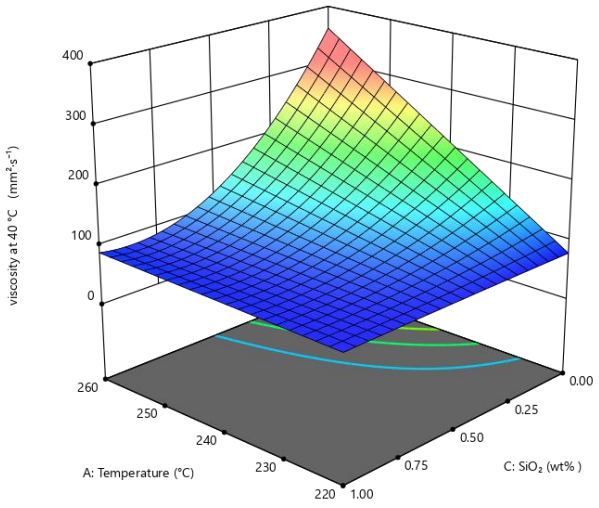


(**d**)

https://doi.org/10.3390/lubricants14110416



(**e**)



(**f**)

Figure 4. Contour plots and the 3D surfaces of the regression function for the viscosity at 40 °C varying the temperature and the heat-exposure time for a biolubricant ((**a**,**b**); in this case the SiO_2 concentration is set at 0.00%); the time and concentration of SiO_2 nanoparticles ((**c**,**d**); in this case the temperature is set at 240 °C); and the temperature and concentration of SiO_2 nanoparticles ((**e**,**f**); in this case the time is set at 180 h).

The influence of time and temperature on viscosity at 40 °C in the lubricants and biolubricants, both without SiO_2 nanoparticles, is shown in the contour plot (Figures 3a and 4a) and 3D surface (Figures 3b and 4b). The viscosity of both lubricants and biolubricants is greatly influenced by the interaction of temperature and time. Over the 120–240 h period at 220 °C, the viscosity increased from 99.4 $mm^2 \cdot s^{-1}$ at 120 h to 117.3 $mm^2 \cdot s^{-1}$ at 240 h for the lubricant without SiO_2, corresponding to an average relative increase of 0.150% per hour. For the biolubricant without SiO_2, the viscosity increased from 77.8 to 79.2 $mm^2 \cdot s^{-1}$ over the same period, corresponding to an average relative increase of 0.015% per hour. The effect of severe thermal ageing was particularly evident at 260 °C. After 168 h of exposure, the viscosity of the conventional lubricant without SiO_2 increased from its fresh-oil value of 97.3 to 193.7 $mm^2 \cdot s^{-1}$, corresponding to an increase of approximately 99.1%. Under the same ageing conditions, the viscosity of the biolubricant increased from 87.0 to 312.9 $mm^2 \cdot s^{-1}$, representing an increase of approximately 259.7%. These results indicate that prolonged exposure to high temperature strongly accelerated viscosity-increasing degradation processes, with a substantially greater effect observed for the biolubricant. Such pronounced viscosity growth is consistent with advanced thermo-oxidative degradation, which may involve oxidation-induced polymerization, molecular association, and the formation of higher-molecular-weight degradation products during prolonged exposure.

Figures 3c,d and 4c,d indicate the behaviour of the nanolubricants and nanobiolubricants by showing how time and SiO_2 nanoparticle concentration affect viscosity at 40 °C. Viscosity tends to increase with time in both lubricants and biolubricants, particularly when SiO_2 nanoparticles are not present. Nonetheless, the gradual increase in SiO_2 nanoparticles' mass (0.75% and 1.00%) counteracts this elevation in viscosity, averting the abrupt spike seen in lubricants without nanoparticles, indicating that the nanoparticles assist in stabilizing viscosity under extended temperature exposure.

The combined effects of temperature and SiO_2 nanoparticles on viscosity in nanolubricants and nanobiolubricants are shown in Figures 3d,e and 4d,e. According to our earlier research, adding SiO_2 nanoparticles to fresh lubricants and biolubricants causes

viscosity to rise slightly [28]. The interaction between temperature and nanoparticle concentration has more intricate implications during ageing. Interestingly, viscosity without nanoparticles increases dramatically to 193.7 $mm^2 \cdot s^{-1}$ and 312.9 $mm^2 \cdot s^{-1}$ at its highest temperature and longest period in lubricants and biolubricants, respectively. On the other hand, compared with the corresponding samples aged at 260 °C for 168 h without SiO_2, the addition of 0.75 wt.% and 1.00 wt.% SiO_2 nanoparticles reduced the viscosity of the conventional lubricant to 190.5 $mm^2 \cdot s^{-1}$ (−1.65%) and 135.1 $mm^2 \cdot s^{-1}$ (−30.25%), respectively. For the biolubricant, the viscosity decreased to 98.6 $mm^2 \cdot s^{-1}$ (−68.49%) and 116.8 $mm^2 \cdot s^{-1}$ (−62.67%) with 0.75 wt.% and 1.00 wt.% SiO_2, respectively. These results are consistent with a possible influence of SiO_2 nanoparticles on oxidation products or molecular association under severe ageing conditions, which may contribute to limiting excessive viscosity increases.

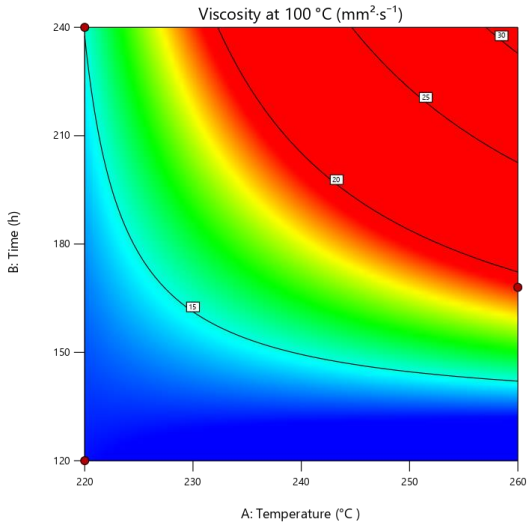
The pronounced viscosity increase observed after severe thermal ageing may be associated with oxidation-induced molecular association or polymerization. The lower viscosity measured in some SiO_2 containing samples is consistent with a possible influence of the nanoparticles on these degradation processes. However, the present measurements do not directly establish the underlying mechanism, and further molecular, particle-size, and structural analyses would be required to confirm it.

3.1.3. Evaluation of Kinematic Viscosity at 100° C

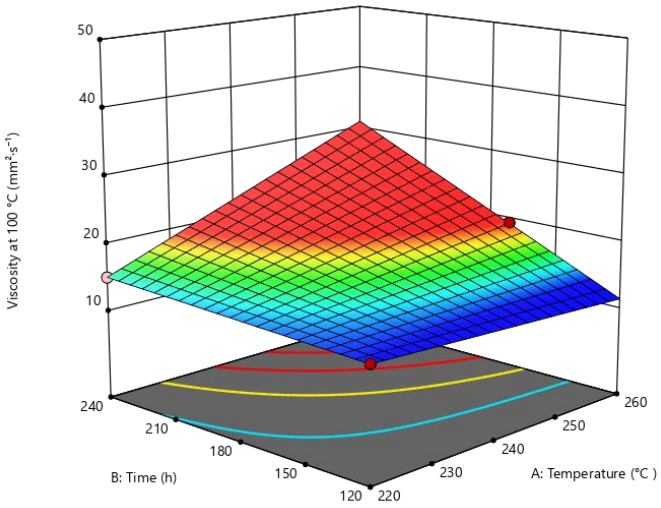
This study also examined the effects of SiO_2 nanoparticles at different concentrations and ageing conditions (120, 168, and 240 h at 220 °C and 260 °C) on the viscosity of lubricants at 100 °C. This reference temperature is considered by the international standards [32] to be as important as the temperature of 40 °C because it offers vital information on the lubricant's performance in high-temperature scenarios that are pertinent to engine operation. As done for data referring to the other reference temperature, a first full-cubic regression model was initially used to fit the data for nanolubricants and nanobiolubricants. An ANOVA performed on the terms of the full-cubic model, however, revealed that several components were not statistically significant. A backward elimination procedure was then used to improve the model, keeping only the significant terms. Table 7 provides a summary of the numerical regression models that were achieved. A 2D/3D graphical depiction of these models is shown in Figures 5 and 6, emphasizing important trends and overall values.

Table 7. Main data on both nanolubricants and nanobiolubricants for a response-surface reduced cubic model based on viscosity at 100 °C data.

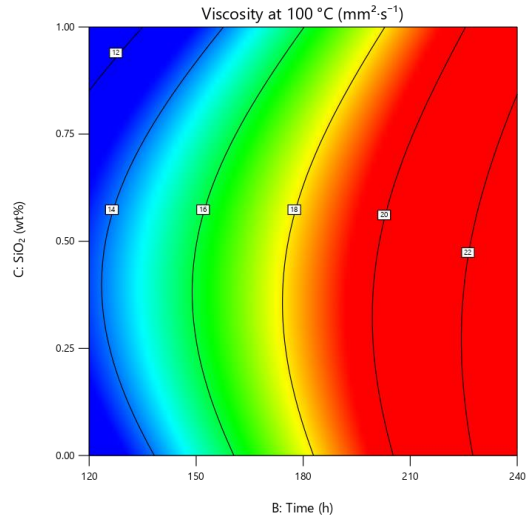
Quantity	Nanolubricants Regression Equation	Nanobiolubricants Regression Equation
Viscosity at 100 °C [$mm^2 \cdot s^{-1}$]	$+122.726 - 0.504635 \cdot T - 0.819061 \cdot t - 65.9658 \cdot C_{SiO2} + 0.00378601 \cdot T \cdot t + 0.325488 \cdot T \cdot C_{SiO2} - 0.0446275 \cdot t \cdot C_{SiO2} + 87.7353 \cdot C_{SiO2}^2 - 0.42264 \cdot T \cdot C_{SiO2}^2 + 0.0434278 \cdot t \cdot C_{SiO2}^2$	$+170.671 - 0.721458 \cdot T - 1.44303 \cdot t - 182.717 \cdot C_{SiO2} + 0.0065691 \cdot T \cdot t + 0.834167 \cdot T \cdot C_{SiO2} + 2.26122 \cdot t \cdot C_{SiO2} - 133.867 \cdot C_{SiO2}^2 - 0.0102889 \cdot T \cdot t \cdot C_{SiO2} + 0.606667 \cdot T \cdot C_{SiO2}^2$
Fit Statistics, Std. Dev.	0.2560	0.0866
Mean	14.75	13.84
C.V. %	1.74	0.6257
R^2	0.9940	0.9998
Adjusted R^2	0.9832	0.9995



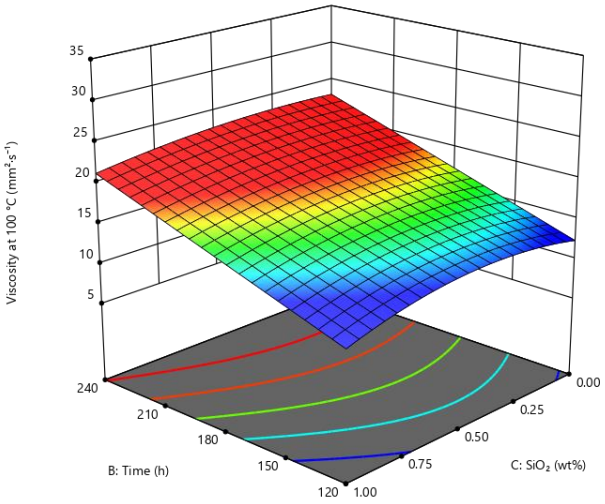
(**a**)



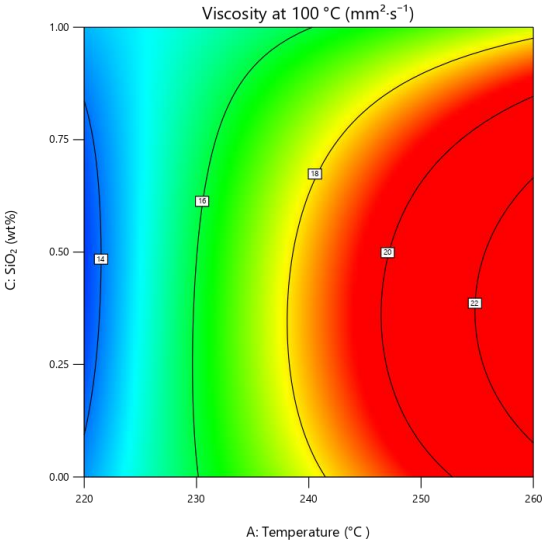
(**b**)



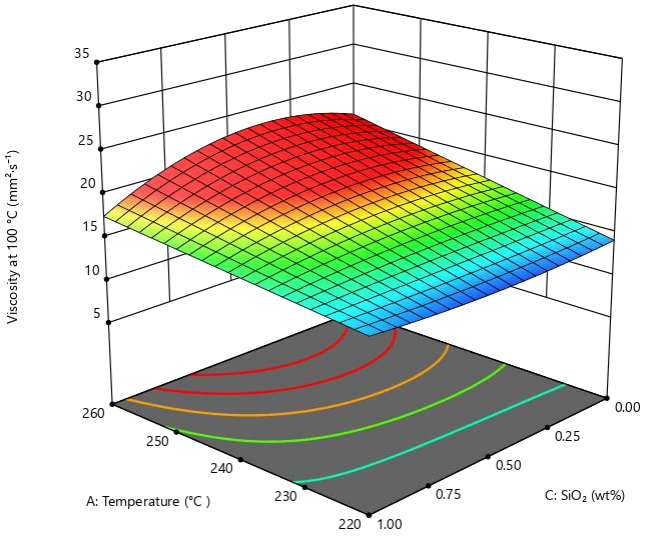
(**c**)



(**d**)



(**e**)



(**f**)

Figure 5. Contour plots (**left**) and the 3D surfaces (**right**) of the regression function for the viscosity at 100 °C, varying the temperature and the heat-exposure time for a conventional lubricant ((**a**,**b**); in this case the SiO_2 concentration is set at 0.00%); the time and concentration of SiO_2 nanoparticles

((**c**,**d**); in this case the temperature is set at 240 °C); and the temperature and concentration of SiO_2 nanoparticles ((**e**,**f**); in this case the time is set at 180 h).

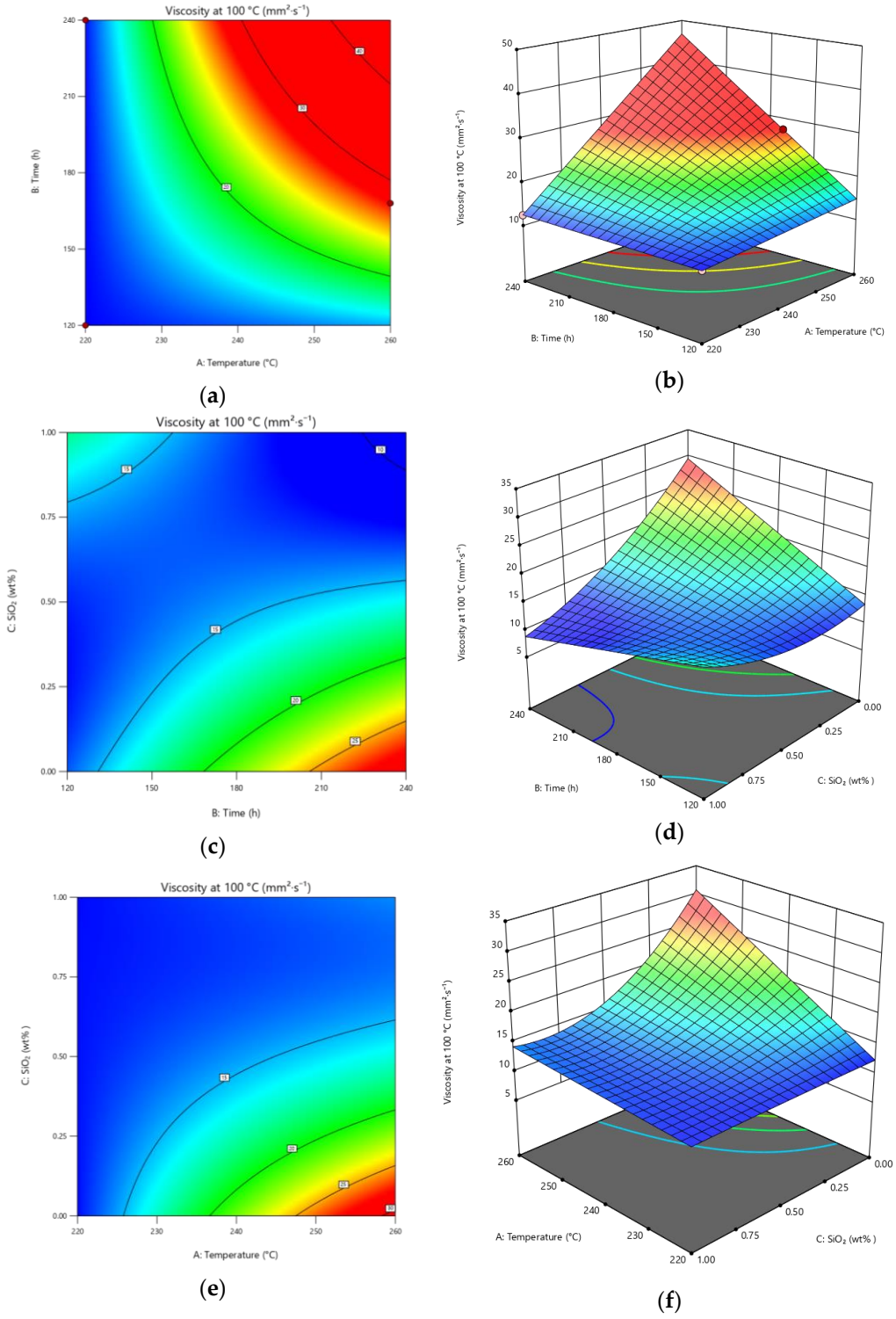


Figure 6. Contour plots (**left**) and the 3D surfaces (**right**) of the regression function for the viscosity at 100 °C, varying the temperature and the heat-exposure time for a biolubricant ((**a**,**b**); in this case the SiO_2 concentration is set at 0.00%); the time and concentration of SiO_2 nanoparticles ((**c**,**d**); in this case the temperature is set at 240 °C); and the temperature and concentration of SiO_2 nanoparticles ((**e**,**f**); in this case the time is set at 180 h).

The contour plot (Figures 5a and 6a) and the 3D surface plot (Figures 5b and 6b) show the effects of temperature and time on the viscosity at 100 °C for both lubricants and

biolubricants. In the absence of nanoparticles, at 220 °C, the viscosity measured at 100 °C increased only slightly with ageing time. For the conventional lubricant, the viscosity increased from 13.4 to 15.0 $mm^2 \cdot s^{-1}$ between 120 and 240 h, corresponding to an increase of 11.94% over 120 h, or an average relative increase of 0.100% h^{-1}. Under the same conditions, the viscosity of the biolubricant increased only marginally, from 12.2 to 12.4 $mm^2 \cdot s^{-1}$, corresponding to an increase of 1.64%, or 0.014% h^{-1}. As anticipated, the viscosity increases significantly at 260 °C, reaching 19.4 $mm^2 \cdot s^{-1}$ for lubricants and 27.6 $mm^2 \cdot s^{-1}$ for biolubricants after 168 h. This pattern shows that although viscosity is fairly constant over time at 220 °C, it increases dramatically at 260 °C with prolonged exposure, underscoring the important impact of temperature on viscosity, especially at higher temperatures and longer exposure times.

The effects of time and concentration of SiO_2 nanoparticles on viscosity at 100 °C are displayed in the contour plot (Figures 5c and 6c) and the 3D surface plot (Figures 5d and 6d). In both lubricants and biolubricants, viscosity increases over time in the absence of nanoparticles. SiO_2 nanoparticles seem effective in preventing the thickening of the lubricant over time: and this is particularly evident when they are not present. For instance, when the conventional lubricant contained 1.00 wt.% SiO_2, its viscosity increased only moderately, from 13.6 $mm^2 \cdot s^{-1}$ at 120 h to 15.2 $mm^2 \cdot s^{-1}$ at 240 h, corresponding to an increase of 11.76% over 120 h, or an average relative increase of 0.098%·h^{-1}. By contrast, when 1.00 wt.% SiO_2 was added to the biolubricant, the viscosity remained nearly constant over the same period, decreasing slightly from 12.4 to 12.3 $mm^2 \cdot s^{-1}$, corresponding to a reduction of approximately 0.81%.

Figures 5d,e and 6d,e illustrate how temperature and SiO_2 nanoparticles affect viscosity in both lubricants and biolubricants. The viscosity of both lubricants and biolubricants is greatly affected by temperature variations and the presence of SiO_2 nanoparticles. Viscosity is rather constant at lower temperatures (220 °C) and is very slightly affected by the presence of nanoparticles, regardless of concentration. But the impact of the nanoparticles intensifies when the temperature rises to 260 °C. Interestingly, in the absence of nanoparticles, the viscosity rises noticeably at 260 °C and 168 h, but the addition of SiO_2 nanoparticles reduces this rise. For example, the viscosity of lubricants increases to 19.4 $mm^2 \cdot s^{-1}$ at 0.0 wt.%; by adding 1.0 wt.% SiO_2 nanoparticles, it decreases instead to 15.6 $mm^2 \cdot s^{-1}$, and for biolubricants it increases to 27.6 $mm^2 \cdot s^{-1}$ at 0.0 wt.% nanoparticles but decreases to 16.1 $mm^2 \cdot s^{-1}$ at 1.0 wt.% nanoparticles. This implies that SiO_2 nanoparticles assist in regulating the viscosity of the lubricants in which they are put at elevated temperatures, averting the possibility of extreme thickening brought on by heat exposure.

3.1.4. Evaluation of Viscosity Index

A full-cubic regression model provided the best match to the viscosity index data for nanolubricants and nanobiolubricants at various concentrations and ageing conditions (120, 168, and 240 h at 220 °C and 260 °C). However, an ANOVA on the full cubic model showed that several of the components were not statistically significant. The model was improved by employing a backward elimination process, which retained just the crucial terms. A summary of the achieved numerical regression models is given in Table 8. Figures 7 and 8 display a 2D/3D graphical representation of these models that highlights significant patterns and overall values.

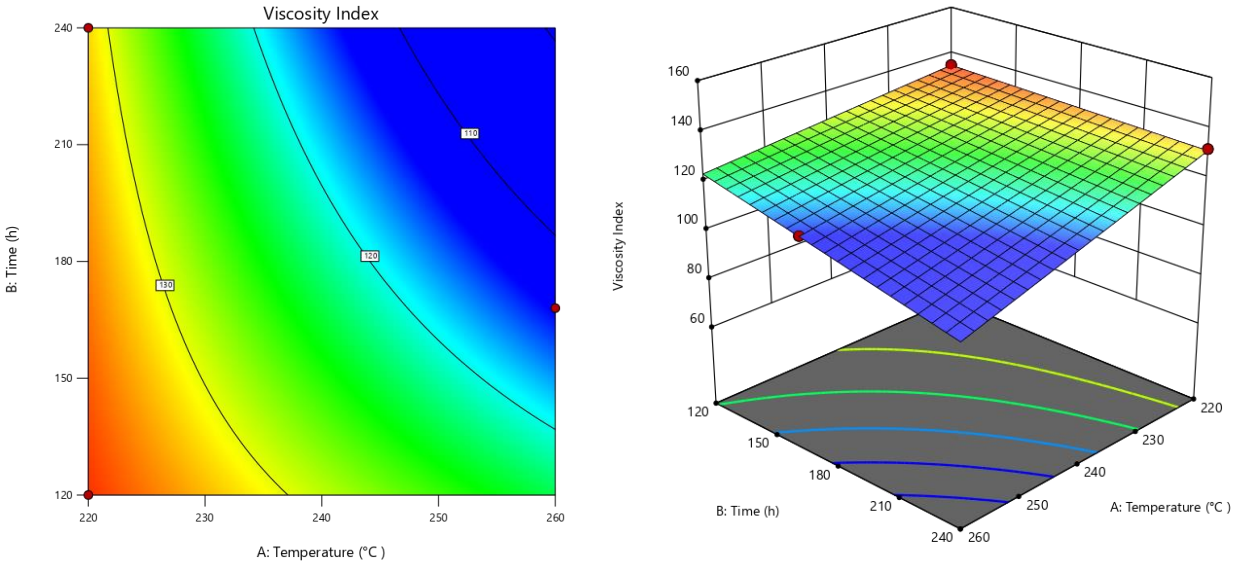
Table 8. Main data on both nanolubricants and nanobiolubricants for a response-surface reduced cubic model based on viscosity index data.

Quantity	Nanolubricants Regression Equation	Nanobiolubricants Regression Equation
Viscosity Index	$+89.6223 + 0.222366 \cdot T + 0.907865 \cdot t + 62.0964 \cdot C_{SiO2} - 0.00426302 \cdot T \cdot t -$	$-211.767 + 1.67667 \cdot T + 3.36736 \cdot t + 594.533 \cdot C_{SiO2} - 0.0153819 \cdot T \cdot t - 2.65333 \cdot T \cdot C$

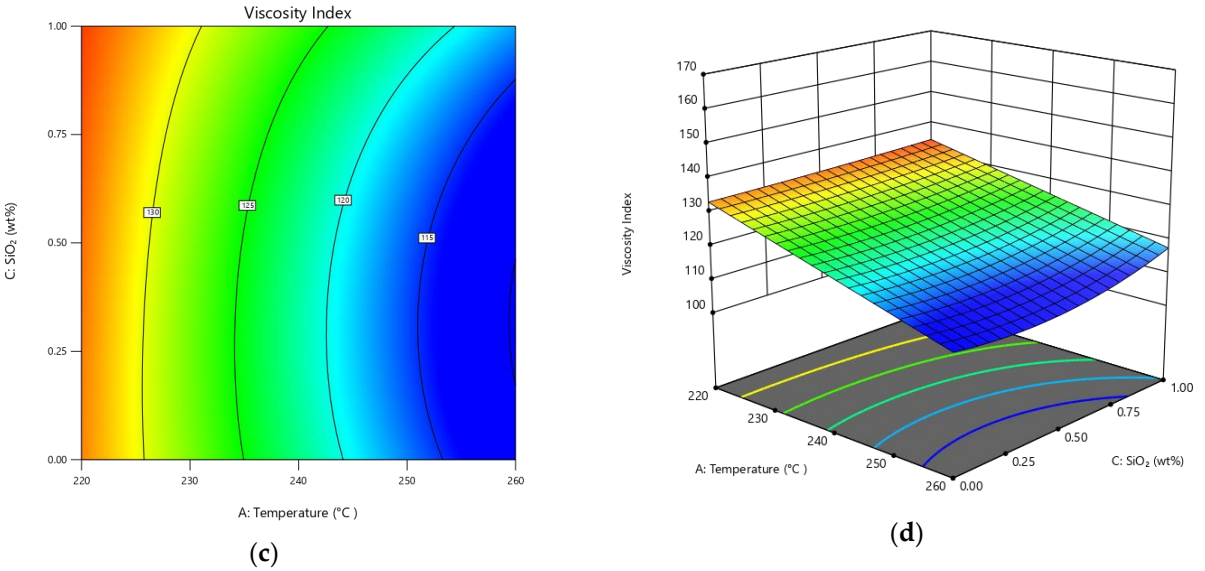
	$0.280179 \cdot T \cdot C_{SiO_2} - 86.0714 \cdot C_{SiO_2}^2 + 0.396429 \cdot T \cdot C_{SiO_2}^2$	$_{SiO_2} - 6.30611 \cdot t \cdot C_{SiO_2} + 311.333 \cdot C_{SiO_2}^2 + 0.0285278 \cdot T \cdot t \cdot C_{SiO_2} - 1.43333 \cdot T \cdot C_{SiO_2}^2$
Fit Statistics, Std. Dev.	0.8542	1.07
Mean	128.73	151.80
C.V. %	0.6635	0.7064
R^2	0.9941	0.9957
Adjusted R^2	0.9883	0.9879

The effects of temperature and time on viscosity index in lubricants and biolubricants without the inclusion of SiO_2 nanoparticles are displayed in the contour plot (Figures 7a and 8a) and the 3D surface plot (Figures 7b and 8b). In the lubricant and biolubricant, the viscosity index continuously drops as temperature rises from 220 °C to 260 °C. The contour and surface plots' steep slopes indicate that the lubricant is more temperature-sensitive than the biolubricant, as demonstrated by its lower viscosity index. The viscosity index decreases more sharply with longer exposure times at higher temperatures, suggesting that time is a significant factor as well, particularly for the lubricant. The biolubricant exhibits the same pattern, albeit with a more gradual and consistent decline in viscosity index.

Figure 8c,d show how time and SiO_2 nanoparticle concentration affect viscosity index in biolubricants. But regarding the lubricants, the combined impact of time and SiO_2 nanoparticle concentration is not presented, because no comparable plots were produced, because the cubic model in the Design-Expert software did not find this interaction to be significant. According to the plots, the viscosity index normally falls with time; however, this loss can be lessened by adding SiO_2 nanoparticles (0.75 wt.% and 1.0 wt.%). With increasing nanoparticle concentration, the biolubricants show a more controlled decline in viscosity index, indicating that SiO_2 contributes to viscosity stability, particularly during extended exposure intervals.

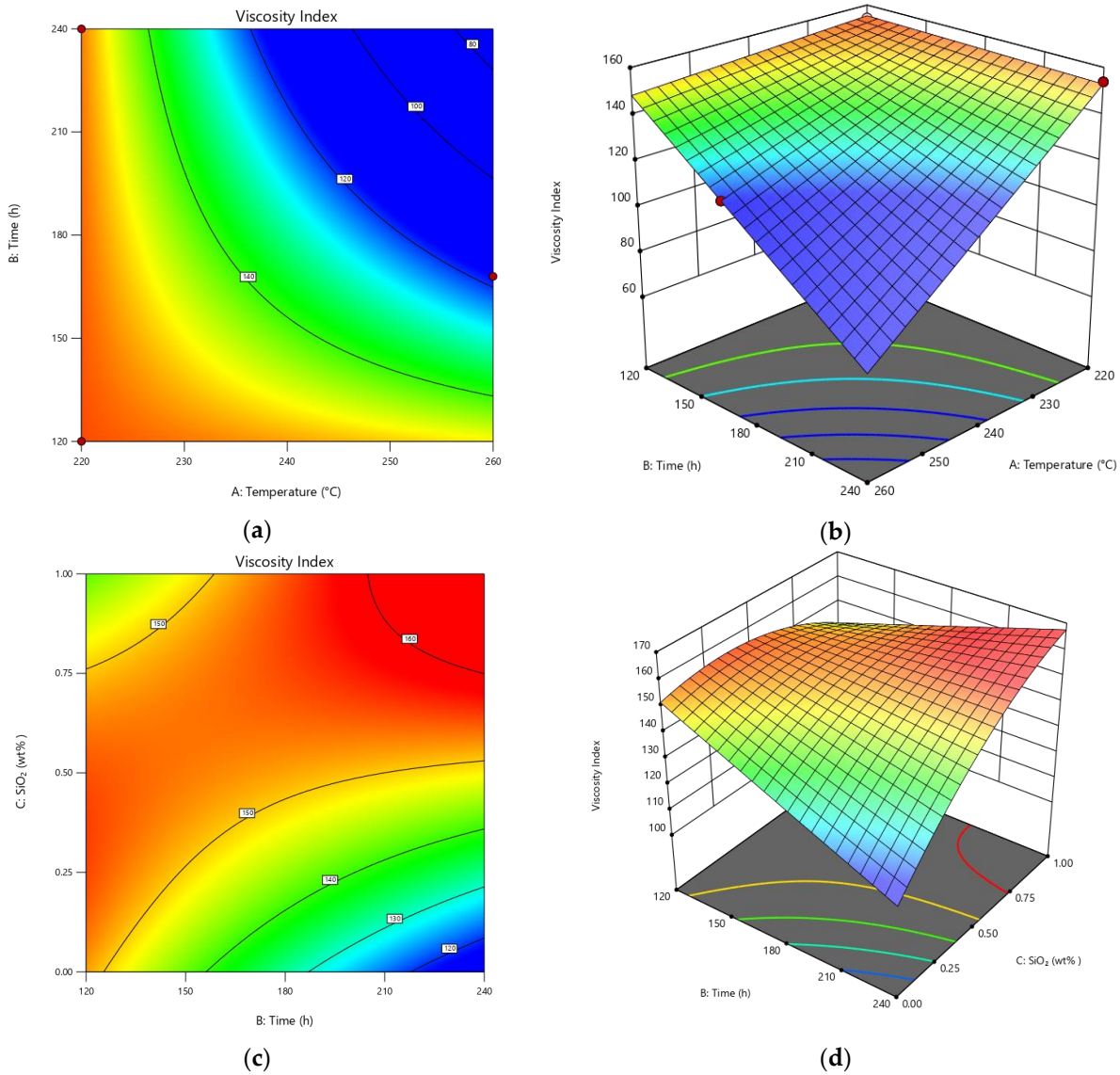


(**a**) (**b**)



(**c**) (**d**)

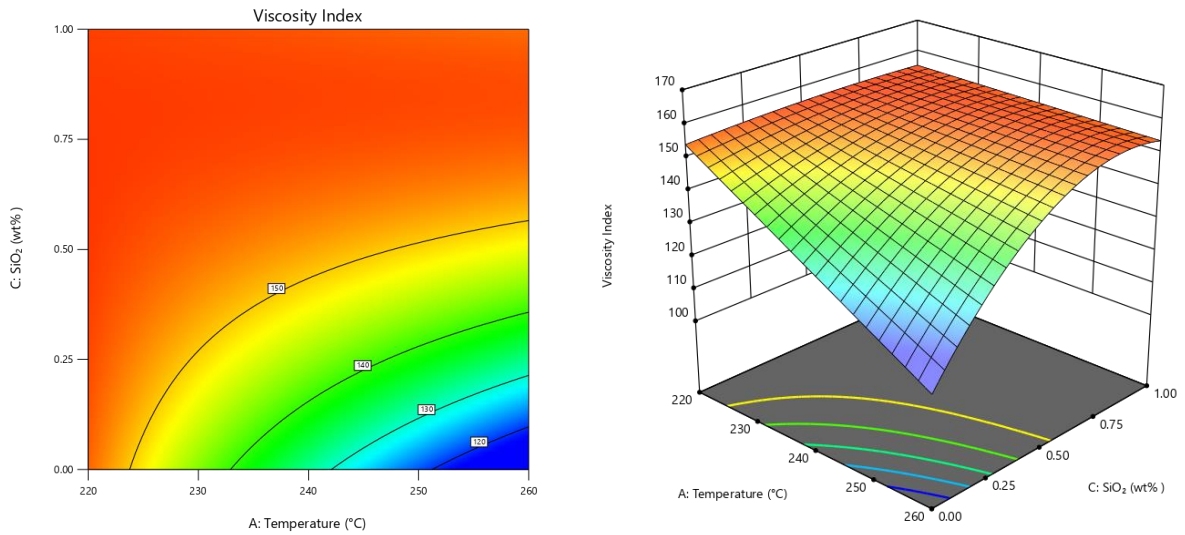
Figure 7. Contour plots (**left**) and the 3D surfaces (**right**) of the regression function for the viscosity index varying the temperature and the heat-exposure time for a conventional lubricant ((**a**,**b**); in this case the SiO_2 concentration is set at 0.00%) and the temperature and concentration of SiO_2 nanoparticles ((**c**,**d**); in this case the time is set at 180 h).



(**a**) (**b**)

(**c**) (**d**)

https://doi.org/10.3390/lubricants14110416



(**e**) (**f**)

Figure 8. Contour plots (**left**) and the 3D surfaces (**right**) of the regression function for the viscosity index, varying the temperature and the heat-exposure time for a biolubricant ((**a**,**b**); in this case the SiO_2 concentration is set at 0.00%); the time and concentration of SiO_2 nanoparticles ((**c**,**d**); in this case the temperature is set at 240 °C); and the temperature and concentration of SiO_2 nanoparticles ((**e**,**f**); in this case the time is set at 180 h).

The effects of temperature and SiO_2 nanoparticle concentration on viscosity index are depicted in Figure 7c,d for lubricants, and for biolubricants in Figure 8e,f. As previously reported, the addition of SiO_2 nanoparticles increased the viscosity index of the fresh conventional lubricant from 138 to 143 (+3.62%) and that of the fresh biolubricant from 160 to 166 (+3.75%). Without nanoparticles, the viscosity index at 220 °C is 154; however, as nanoparticle concentrations increase (up to 1.0 wt.%), the index rises to 158, indicating an improvement in the thermal stability of the biolubricant. While the lubricant varies from 135 to 136 under the same temperature conditions, these variations are extremely small. Without nanoparticles, the viscosity index dramatically decreases to 114 for lubricants, and 118 for biolubricants, at 260 °C. The viscosity index is 115 for lubricants and 152 for biolubricants when 0.75 wt.% is added, and when 1.0 wt.% of nanoparticles are added, the values are 120 and 148 for lubricants and biolubricants, respectively. It is clear from comparing the two types of lubricants that the viscosity index of the conventional lubricant is more temperature-sensitive, declining more steeply as the temperature rises. Biolubricants, on the other hand, respond to temperature changes in a more controlled way. SiO_2 nanoparticles are added to both lubricants to help stabilize the viscosity index, although the impact is more pronounced in the biolubricant because of the important role the nanoparticles play in avoiding excessive viscosity index degradation. Since biolubricants often retain a more constant viscosity index over a range of temperatures and nanoparticle concentrations, they are more resilient to viscosity index fluctuations caused by thermal stress than conventional lubricants.

The different ageing responses of the conventional lubricant and the biolubricant may be related to differences in their base-oil chemistry, molecular structure, polarity, initial viscosity index, and additive packages. The biolubricant exhibited a higher initial viscosity index, which may contribute to its comparatively smaller viscosity-index variation under some ageing conditions. In addition, differences in molecular architecture and additive formulation can influence thermal stability, oxidation behaviour, and viscosity evolution. However, because the two investigated products are commercial formulations with different SAE grades and proprietary additive packages, the present data do not

allow the contribution of individual compositional or molecular factors to be isolated. Therefore, the observed differences should be interpreted as formulation-dependent rather than being attributed solely to the bio-based or mineral nature of the base oil.

3.2. TAN and TBN Analysis

Acidification of engine lubricants can affect their longevity and performance. Total Acid Number (TAN) and Total Base Number (TBN), which are both expressed in milligrams of potassium hydroxide (KOH) per gram of lubricant, are widely used to quantify this characteristic. The TAN is defined as the mass (in milligrams) of a standard base (e.g., potassium hydroxide, KOH) that is required to neutralise all of the acidic components within the lubricant. TBN determines how effective the battle will be against any acids formed during the combustion process. Higher TBN means the oil has more reserve alkalinity available, which can be used to reduce the corrosive effects of acids [55]. As the lubricant ages, TBN typically declines while TAN increases. It is advised to replace the lubricant after the TBN has decreased to around 50% of the initial value. But this rule may not always apply, particularly when it comes to biodiesel and low-sulphur fuels, which might produce a variety of acid types in the lubricant [56,57].

At different concentrations and ageing conditions (120, 168, and 240 h at 220 °C and 260 °C), the software used suggests a two-factor with interactions (2FI) model for nanolubricants, and a linear model for nanobiolubricants, to give the best fit to the TAN data. ANOVA on the full 2FI model showed that the effects of temperature and time were not statistically significant (*p*-values bigger than 0.0500) so the model was improved by employing a backward elimination process, which retained just the crucial terms, and on the linear model, confirmed that all of the items were statistically significant. Table 9 provides a summary of the developed numerical regression models. The 2D/3D graphical depictions of these models are shown in Figures 9 and 10, emphasizing important patterns and overall values.

Table 9. Main data on both nanolubricants and nanobiolubricants for a response-surface reduced 2FI and full linear model based on TAN data.

Quantity	Nanolubricants Regression Equation	Nanobiolubricants Regression Equation
TAN [mg(KOH)·g^{-1}]	$+0.671849 + 0.00337838 \cdot T + 0.000527266 \cdot t - 3.31219 \cdot C_{SiO2} + 0.0130648 \cdot T \cdot C_{SiO2} + 0.00454403 \cdot t \cdot C_{SiO2}$	$-9.66355 + 0.0483065 \cdot T + 0.0112903 \cdot t - 0.312258 \cdot C_{SiO2}$
Fit Statistics, Std. Dev.	0.1021	0.1936
Mean	1.81	3.37
C.V. %	5.65	5.75
R^2	0.9370	0.9701
Adjusted R^2	0.9020	0.9619

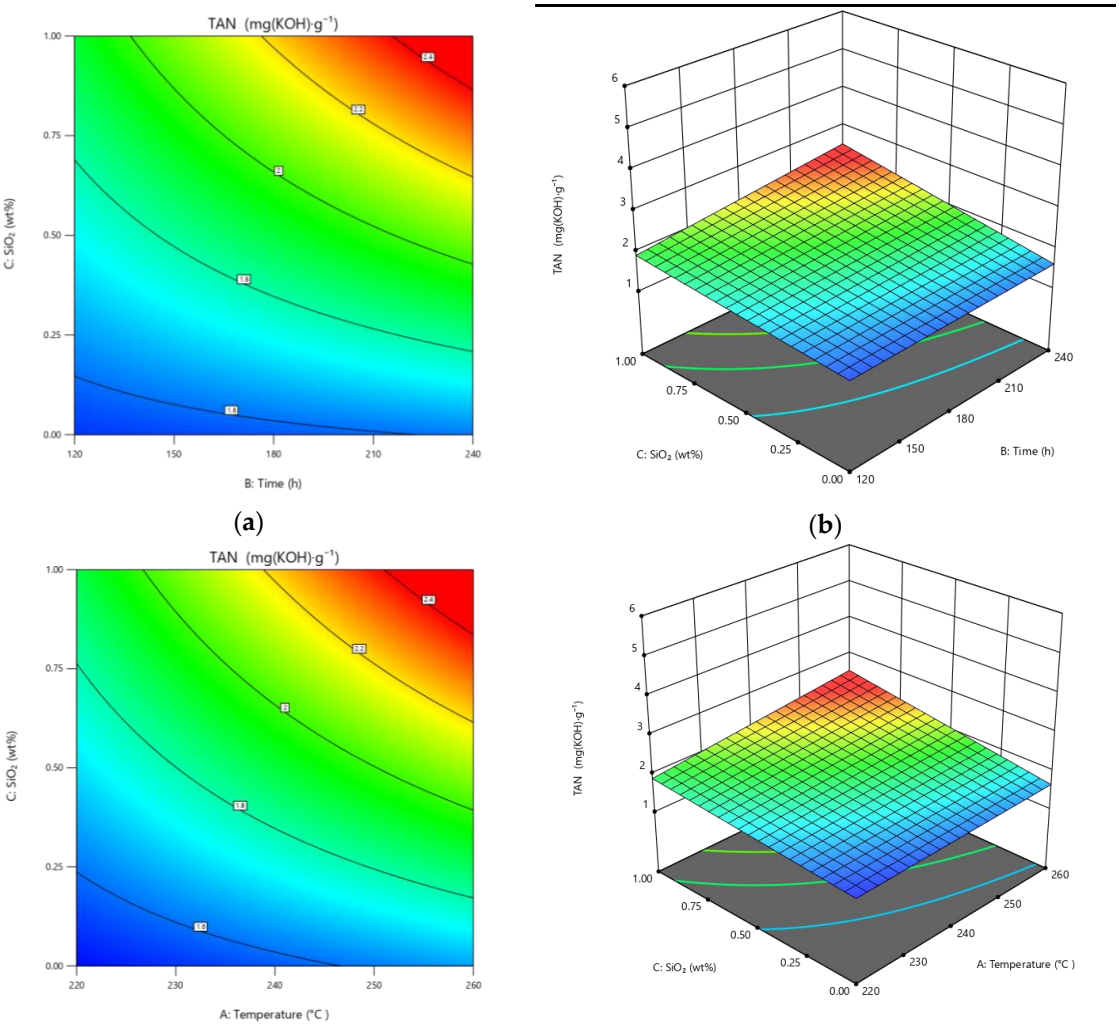
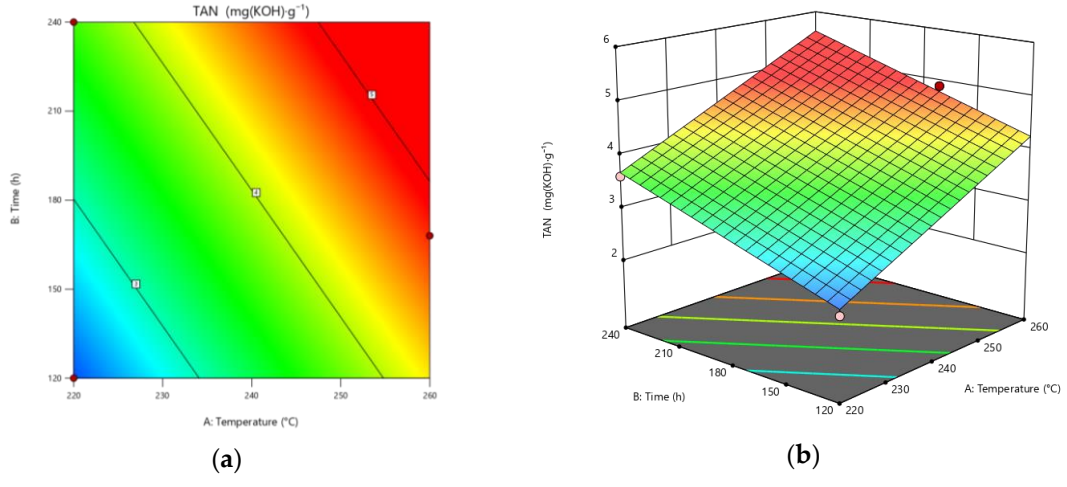
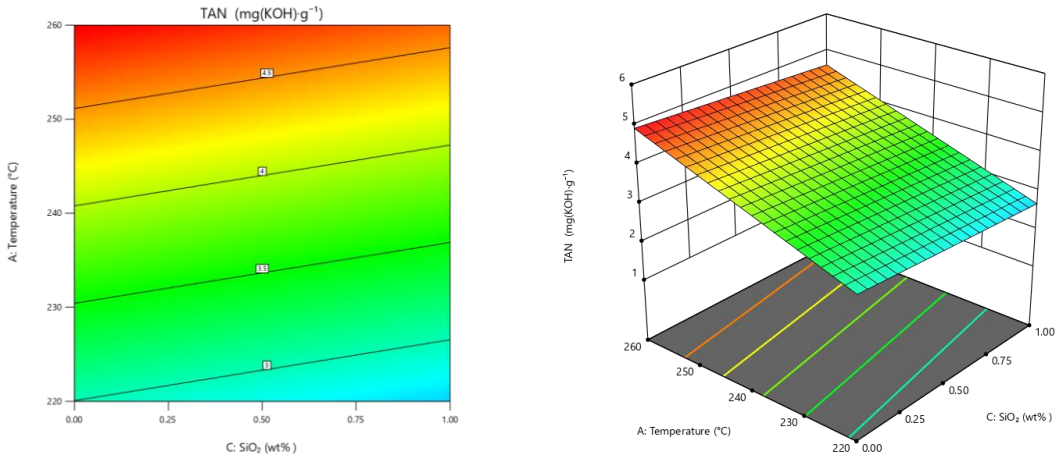


Figure 9. Contour plots (**left**) and the 3D surfaces (**right**) of the regression function for the TAN varying the time and concentration of SiO_2 nanoparticles for a conventional lubricant ((**a**,**b**); in this case the temperature is set at 240 °C) and the temperature and concentration of SiO_2 nanoparticles ((**c**,**d**); in this case the time is set at 180 h).





(**c**) (**d**)

Figure 10. Contour plots (**left**) and the 3D surfaces (**right**) of the regression function for the TAN varying the temperature and the heat-exposure time for a biolubricant ((**a**,**b**); in this case the SiO_2 concentration is set at 0.00%) and the temperature and concentration of SiO_2 nanoparticles ((**c**,**d**); in this case the time is set at 180 h).

The contour plot (Figure 10a) and the 3D surface plot (Figure 10b) indicate how temperature and time affect TAN for biolubricants without SiO_2 nanoparticles, while for lubricants, the combined impact of temperature and time is not covered, because the 2FI model in the Design-Expert program did not find this interaction to be significant. There is a noticeable rise in TAN, in the case of biolubricants. After 120 h at 220 °C, TAN was 2.2 mg(KOH)·g^{-1}; after 240 h, it rose to 3.6 mg(KOH)·g^{-1}. After 168 h, TAN achieved 4.9 mg(KOH)·g^{-1} at 260 °C. These findings show that TAN rises with temperature and time, with the rise being more noticeable at higher temperatures. The period of exposure almost exactly determines the increase in TAN, but the effect is noticeably more pronounced at 260 °C than it is at 220 °C.

The contour plot (Figure 9a) and the 3D surface plot (Figure 9b) indicate how time and SiO_2 nanoparticle concentration affect TAN for lubricants. However, these plots are not defined for biolubricants. Remarkably, in lubricants, SiO_2 nanoparticles raise TAN, indicating that the presence of SiO_2 was associated with higher measured TAN values under these conditions. This increase may reflect oxidation-related acid formation, surface-acidity effects, titration-matrix effects, or sample heterogeneity, rather than a demonstrated catalytic mechanism. At 220 °C and 240 h, for instance, the addition of 1.0% SiO_2 nanoparticles causes TAN to rise from 1.6 mg(KOH)·g^{-1} (without nanoparticles) to 2.2 mg(KOH)·g^{-1}.

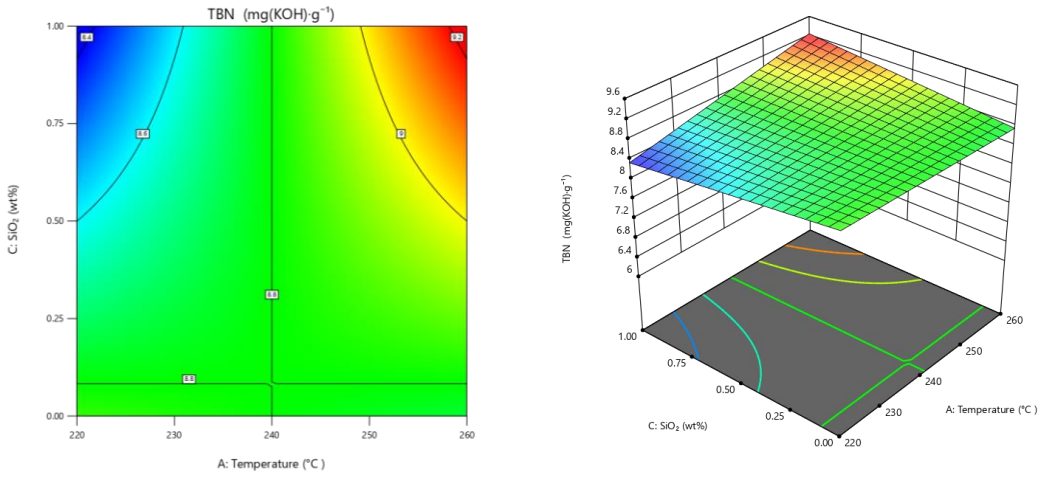
Figures 9c,d and 10c,d demonstrate the effects of temperature and SiO_2 nanoparticle concentration on TAN, for both lubricants and biolubricants. As temperatures rise, the addition of SiO_2 nanoparticles to lubricants causes TAN to rise. The TAN at 260 °C is 1.7 mg(KOH)·g^{-1} in the absence of nanoparticles, but increases to 2.4 mg(KOH)·g^{-1} in the presence of 1% SiO_2, indicating that SiO_2 addition was associated with higher TAN values in the conventional lubricant under these conditions. SiO_2 nanoparticle addition, on the other hand, has the reverse effect in biolubricants; it lowers the TAN as temperature rises. For example, at 260 °C, TAN decreases to 4.4 mg(KOH)·g^{-1} with 1.0% SiO_2 from 4.9 mg(KOH)·g^{-1} without nanoparticles. This indicates that SiO_2 nanoparticles, probably by increasing their oxidative stability at high temperatures, aid in lowering the production of acids in biolubricants.

A 2FI and linear model provided the best fit to the TBN data for nanolubricants and nanobiolubricants, respectively, at various concentrations and ageing conditions (120, 168,

and 240 h at 220 °C and 260 °C). It was verified by an ANOVA on the full 2FI model and full linear model that only SiO_2 concentration and temperature had statistically significant *p*-values, those less than 0.05. Consequently, a backward elimination procedure was used to improve the model, retaining only the most significant terms. A summary of the constructed numerical regression models is given in Table 10. Figures 11 and 12 provide a 2D/3D graphical representation of these models that highlights significant patterns and overall values.

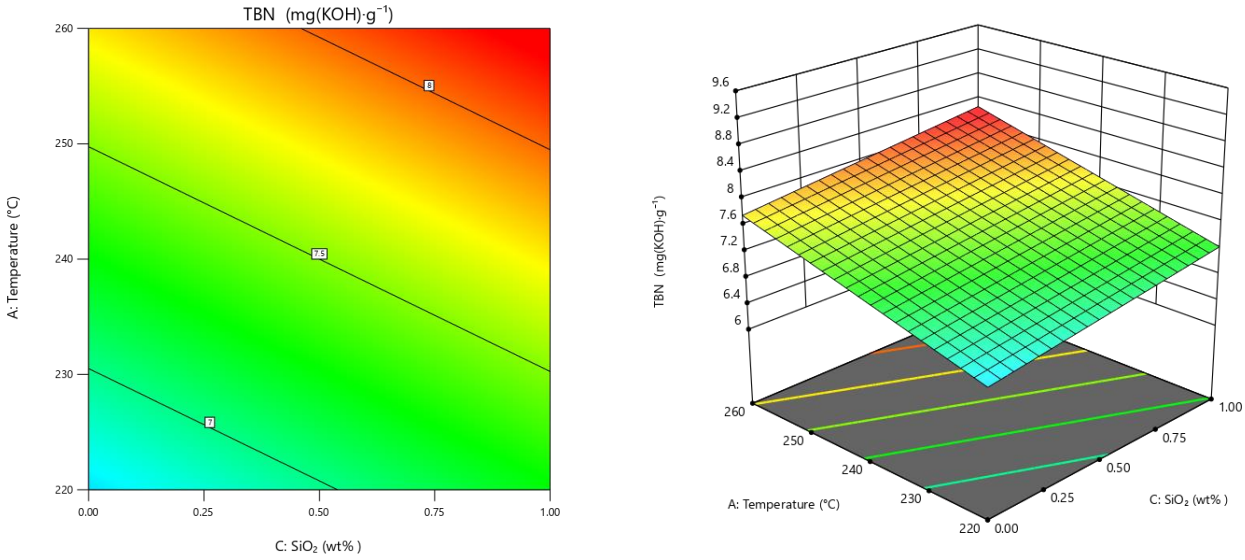
Table 10. Main data on both nanolubricants and nanobiolubricants for a response-surface reduced 2FI and reduced linear model based on TBN data.

Quantity	Nanolubricants Regression Equation	Nanobiolubricants Regression Equation
TBN [mg(KOH)·g^{-1}]	$+9.28 - 0.002 \cdot T - 5.76 \cdot C_{SiO2} + 0.024 \cdot T \cdot C_{SiO2}$	$+1.00667 + 0.026 \cdot T + 0.506667 \cdot C_{SiO2}$
Fit Statistics, Std. Dev.	0.0661	0.1535
Mean	8.73	7.33
C.V. %	0.7564	2.09
R^2	0.9526	0.9353
Adjusted R^2	0.9397	0.9245



(**a**) (**b**)

Figure 11. Contour plot (**left**) and the 3D surface (**right**) of the regression function for the TBN varying the temperature and concentration of SiO_2 nanoparticles for a conventional lubricant ((**a**,**b**); in this case the time is set at 180 h).



(**a**) (**b**)

Figure 12. Contour plot (**left**) and the 3D surface (**right**) of the regression function for the TBN varying the temperature and concentration of SiO_2 nanoparticles for a biolubricant ((**a**,**b**); in this case the time is set at 180 h).

The effects of temperature and SiO_2 nanoparticle concentration on TBN are depicted in the contour plot (Figures 11a and 12a) and the 3D surface plot (Figures 11b and 12b), for both lubricants and biolubricants. According to the plots that have been supplied, TBN behaviour exhibits distinctive trends. TBN generally decreases in lubricants as SiO_2 nanoparticle concentration rises, particularly at lower temperatures, at 220 °C from 8.9 mg(KOH)·g^{-1} to 8.4 mg(KOH)·g^{-1}. On the other hand, TBN either increases or stabilizes at higher temperatures, specifically, at 260 °C, especially at greater concentrations of nanoparticles (0.75% and 1.0%), from 8.8 mg(KOH)·g^{-1} to 9.2 mg(KOH)·g^{-1}. This implies that adding SiO_2 at high temperatures could improve the lubricants' alkaline reserves.

Similar temperature-dependent patterns are seen for biolubricants, while overall TBN values are lower than for lubricants. TBN progressively increases at 220 °C as the SiO_2 content rises; from 6.3 mg(KOH)·g^{-1} without nanoparticles to 7.2 mg(KOH)·g^{-1} with 1.0% nanoparticles. The TBN values increase slightly around 260 °C at greater concentrations of nanoparticles, from 7.9 mg(KOH)·g^{-1} with 0.0 wt.% SiO_2 to 8.2 mg(KOH)·g^{-1} with 1.0 wt.% SiO_2. This suggests that both adding SiO_2 and raising the temperature enhance the base reserve of biolubricants, especially when used for longer periods of time. These figures show that while SiO_2 nanoparticles in lubricants and biolubricants have a favourable effect on TBN, the effect is stronger at higher temperatures and concentrations of nanoparticles.

3.3. Oxidation of Lubricant and Biolubricant

Oxidation is one of the main degradation mechanisms that affect the longevity and efficacy of lubricants. When the lubricant is exposed to oxygen, it oxidizes and changes its chemical composition. Contaminants, metal catalysts, high temperatures, and water can speed up this process. Increased acidity, increased viscosity, sludge development, and corrosion on metal surfaces can all result from this process [51,58,59]. Lubricant samples' FT-IR absorbance changes over time, indicating changes in oxidation and serving as an indicator of ageing.

In the present study, the FTIR oxidation index was calculated by baseline-corrected integration of the absorbance area in the carbonyl region, using Spectrum OilExpress v.

4.0 software. Accordingly, oxidation values are reported as integrated absorbance in absorbance units per centimetre (au·cm^{-1}), rather than as dimensionless point absorbance.

The oxidation of nanolubricants and nanobiolubricants at different concentrations and ageing settings (120, 168, and 240 h at 220 °C and 260 °C) was best matched by a cubic model. ANOVA on the full cubic model, however, revealed that a number of the components lacked statistical significance. By using a backward elimination method, the model was refined and only the most significant terms were kept. Table 11 provides a summary of the developed numerical regression models. A 2D/3D graphical depiction of these models is shown in Figures 13 and 14, emphasizing important patterns and overall values.

The contour plot (Figures 13a and 14a) and the 3D surface plot (Figures 13b and 14b) illustrate how temperature and time affect oxidation, in the absence of SiO_2 nanoparticles, for both lubricants and biolubricants. The oxidation increased significantly from 6.6 to 18.3 au·cm^{-1} in the conventional lubricant, corresponding to an increase of approximately 177.3%, and from 11.7 to 27.0 au·cm^{-1} in the biolubricant, corresponding to an increase of approximately 130.8%, over the 120–240 h exposure period at 220 °C. The aforementioned findings suggest that oxidation can be enhanced by time, especially under moderate temperature conditions. When the temperature reaches 260 °C, the effect increases. Significantly greater oxidation levels, ranging from 25.6 au·cm^{-1} to 53.7 au·cm^{-1} (+109.8%) in lubricants and from 34.0 au·cm^{-1} to 55.7 au·cm^{-1} (+63.8%) in biolubricants, are seen at both time intervals (120 h and 168 h). These findings indicate that longer exposure times and higher temperatures accelerate oxidation, while the biolubricant reaches higher absolute oxidation values under severe ageing conditions.

Figures 13c,d and 14c,d depict how oxidation is influenced by time and the concentration of SiO_2 nanoparticles for both lubricants and biolubricants. Time tends to increase the oxidation level in both cases. But, the addition of SiO_2 nanoparticles helps reduce this oxidation rise, particularly at higher concentrations. When SiO_2 nanoparticles are absent from the lubricant graphs, oxidation accelerates more sharply with time, reaching a peak of 53.7 au·cm^{-1} at 260 °C for 168 h in the absence of nanoparticles. Under the same conditions, the inclusion of SiO_2 nanoparticles at 1.0% reduces the oxidation to 39.1 au·cm^{-1} (−27.19%). The biolubricant shows a more controlled increase in oxidation; it peaks at 55.7 au·cm^{-1} with 0% SiO_2 at 260 °C and 168 h, then decreases to 36.7 au·cm^{-1} (−34.11%) and 43.4 au·cm^{-1} (−22.08%), respectively, as SiO_2 concentration rises to 0.75 wt.% and 1.0 wt.%, respectively.

Table 11. Main data on both nanolubricants and nanobiolubricants for a response-surface reduced cubic model based on oxidation data.

Quantity	Nanolubricants Regression Equation	Nanobiolubricants Regression Equation
Oxidation [au·cm^{-1-1}]	$+510.262 - 2.33889 \cdot T - 4.35696 \cdot t - 869.777 \cdot C_{SiO2} + 0.0202271 \cdot T \cdot t + 3.93914 \cdot T \cdot C_{SiO2} + 3.66417 \cdot t \cdot C_{SiO2} + 336.057 \cdot C_{SiO2}^2 - 0.016625 \cdot T \cdot t \cdot C_{SiO2} - 1.51714 \cdot T \cdot C_{SiO2}^2$	$-7.9644 + 0.0202798 \cdot T - 1.08613 \cdot t - 181.035 \cdot C_{SiO2} + 0.00551424 \cdot T \cdot t + 0.870262 \cdot T \cdot C_{SiO2} + 3.18294 \cdot t \cdot C_{SiO2} - 288.962 \cdot C_{SiO2}^2 - 0.0147528 \cdot T \cdot t \cdot C_{SiO2} + 1.3119 \cdot T \cdot C_{SiO2}^2$
Fit Statistics, Std. Dev.	1.06	0.3948
Mean	21.92	26.22
C.V. %	4.82	1.51
R^2	0.9985	0.9997
Adjusted R^2	0.9958	0.9991

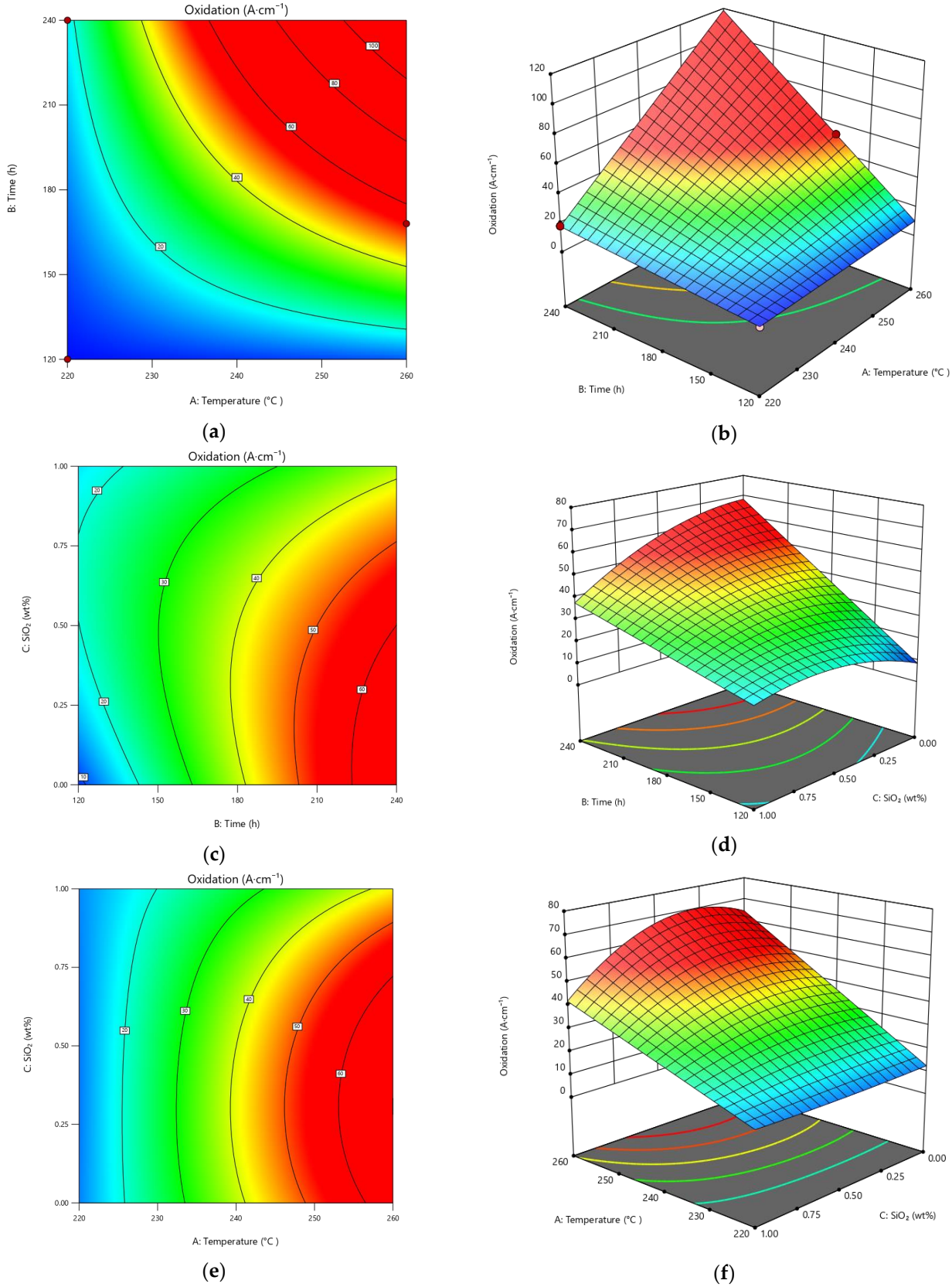


Figure 13. Contour plots (**left**) and the 3D surfaces (**right**) of the regression function for the oxidation, varying the temperature and the heat-exposure time for a conventional lubricant ((**a**,**b**); in this case the SiO_2 concentration is set at 0.00%); the time and concentration of SiO_2 nanoparticles ((**c**,**d**); in this case the temperature is set at 240 °C); and the temperature and concentration of SiO_2 nanoparticles ((**e**,**f**); in this case the time is set at 180 h).

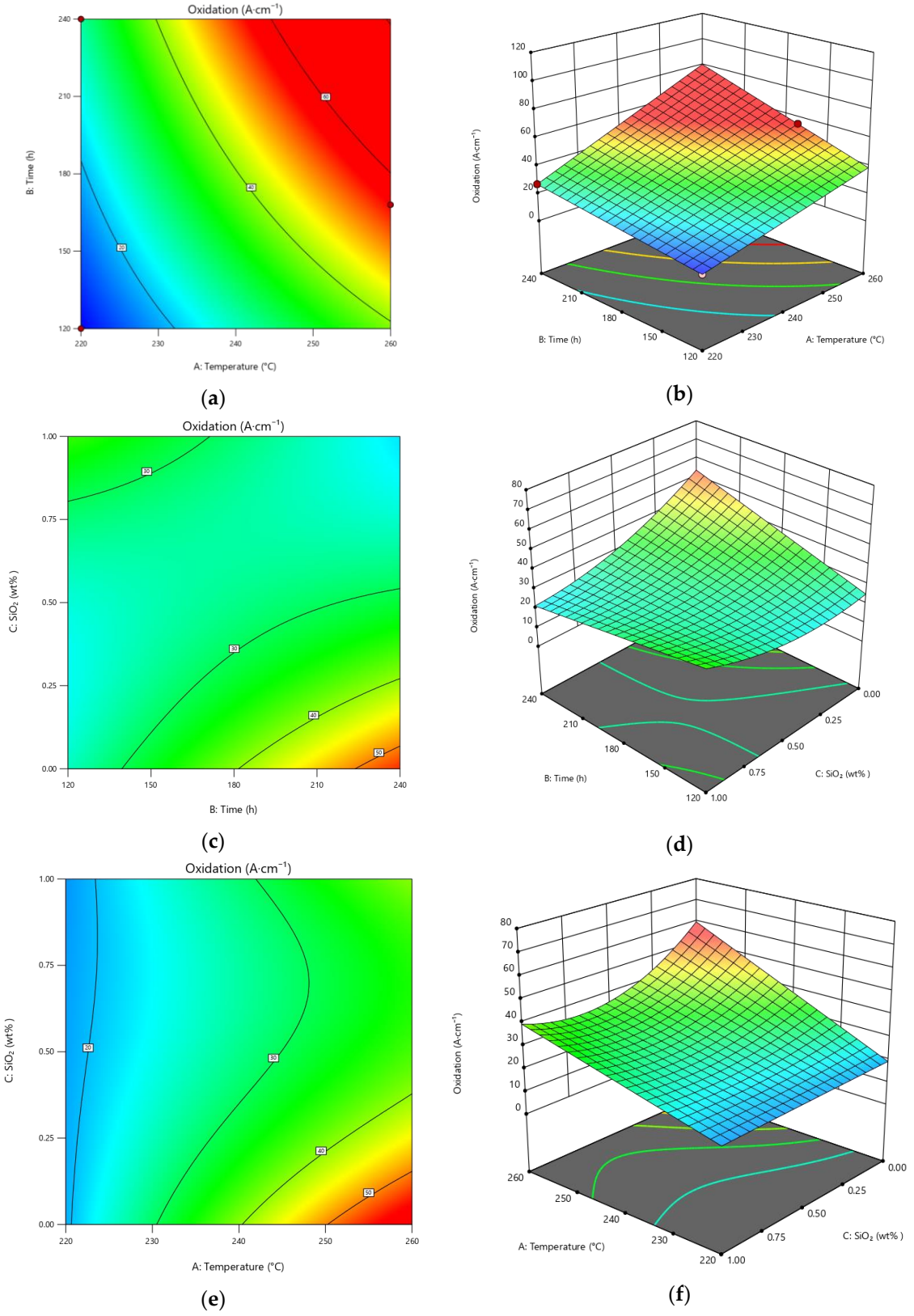


Figure 14. Contour plots (**left**) and the 3D surfaces (**right**) of the regression function for the oxidation, varying the temperature and the heat-exposure time for a biolubricant ((**a**,**b**); in this case the SiO_2 concentration is set at 0.00%); the time and concentration of SiO_2 nanoparticles ((**c**,**d**); in this case the temperature is set at 240 °C); and the temperature and concentration of SiO_2 nanoparticles ((**e**,**f**); in this case the time is set at 180 h).

The relationships between oxidation and temperature, as well as those involving SiO_2 nanoparticle concentration, in both lubricants and biolubricants, are illustrated in Figures 13e,f and 14e,f. Both lubricants and biolubricants exhibit an increase in oxidation at higher temperatures, as would have been predicted. SiO_2 nanoparticles, on the other hand, stabilize the system and lower oxidation levels at higher temperatures.

At 220 °C and 120 h, lubricants exhibit steady oxidation at 6.6 au·cm^{-1} in the absence of nanoparticles and 1.0% SiO_2. This implies that at shorter exposure times, SiO_2 has a minor effect on oxidation. After 240 h at the same temperature, however, oxidation drops from 18.3 au·cm^{-1} in the absence of nanoparticles to 16.6 au·cm^{-1} with 0.75 wt.% SiO_2 (−9.29%), then somewhat rises to 19.4 au·cm^{-1} with 1.0 wt.% SiO_2 (+6.01% relative to the nanoparticle-free sample). This suggests that SiO_2 can suppress oxidation over long exposure times at specific concentrations, though it exhibits some variability at higher concentrations. Without SiO_2, oxidation peaks at 260 °C and 168 h, with a value of 53.7 au·cm^{-1}. Oxidation drops to 39.1 au·cm^{-1} (27.19% decrease) as the SiO_2 concentration rises to 1.0 wt.%, respectively. Our findings validate the function of SiO_2 as an oxidation stabilizer by showing that it can reduce oxidation at both temperatures over extended exposure times (240 h and 168 h), though its impact varies with concentration.

In biolubricants, at 220 °C and 120 h, oxidation increases from 11.7 au·cm^{-1} (without nanoparticles) to 14.1 au·cm^{-1} (+20.51%) as the SiO_2 concentration climbs from 0.0% to 1.0%. This implies that SiO_2 slightly increases oxidation at shorter exposure durations. On the other hand, oxidation drops from 27 au·cm^{-1} to 22.2 au·cm^{-1} (−17.78%) after 240 h as the SiO_2 rises, suggesting that SiO_2 can suppress oxidation during extended exposure. Oxidation peaks at 55.7 au·cm^{-1} with 0% SiO_2 at 260 °C and 168 h. Oxidation decreases to 36.7 au·cm^{-1} (34.11% decrease) and 43.4 au·cm−1 (22.08% decrease), respectively, as SiO_2 concentrations rise to 0.75 wt.% and 1.0 wt.%, respectively. SiO_2 generally reduces oxidation during lengthy exposure intervals, although the effect remains concentration-dependent, indicating that it functions as a stabilizer.

In general, SiO_2 shows potential as an oxidation stabilizer for biolubricants as well as lubricants, especially when exposed to high temperatures for extended periods as well. The fact that it can lower oxidation in both types of lubricants indicates that it is important for improving the thermal stability of these materials, even if its effect is more noticeable in biolubricants.

3.4. Analysis of Pollution and Additives Through ICP-OES

One particularly effective method for determining the metal content of lubricant samples is the ICP-OES. Metals found in lubricating oil may accumulate from a variety of sources, such as wear, pollution, and outside additions. During an engine's operating life, wear metal particles are produced by friction or corrosion on parts like piston rings and bearings. The total contamination is caused by elements like leaks, impurities, and leftover metal pieces. In addition to offering significant information regarding the effectiveness and quality of the lubricating oil, a lubricant's metal content assessment can reveal important details about the state of the machinery it lubricates [60,61].

3.4.1. Analysis of Silicon

The addition of SiO_2 nanoparticles to both nanolubricants and nanobiolubricants results in distinct trends in elemental concentrations, as revealed by the ICP-OES analysis. Higher SiO_2 concentrations are correlated with a large increase in silicon levels, which is to be expected and validates the presence of SiO_2 nanoparticles. This rise is not a sign of contamination, but rather of the deliberate addition of SiO_2 nanoparticles, which act as a source of silicon, as demonstrated in our previous study [28]. Silicon was already present in the fresh commercial formulations at 65 ppm in the conventional lubricant and 2 ppm

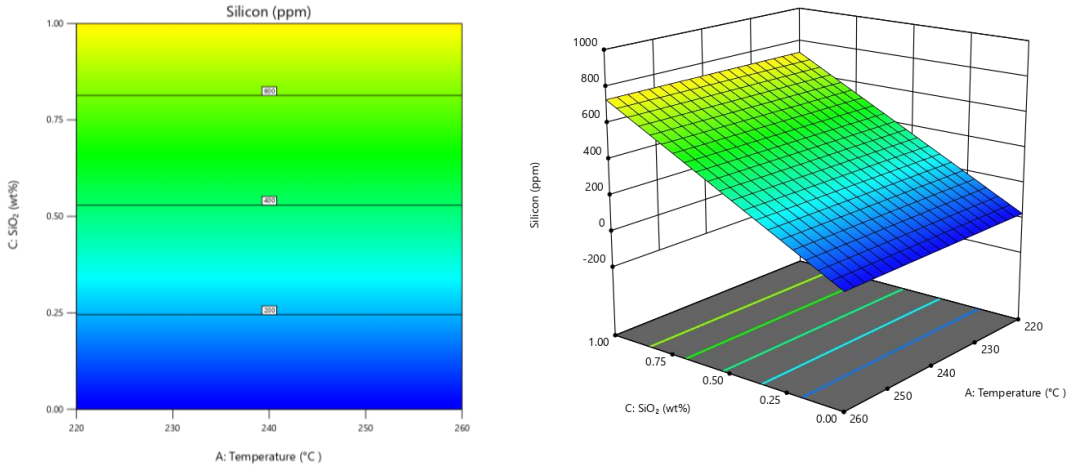
in the biolubricant; therefore, baseline silicon should be distinguished from the additional silicon introduced through the SiO_2 nanoparticles.

A linear regression model provided the best match to the silicon data for nanolubricants and nanobiolubricants at various concentrations and ageing conditions (120, 168, and 240 h at 220 °C and 260 °C). However, an ANOVA on the linear model showed that some of the terms were not statistically significant. The model was improved by employing a backward elimination process, which retained just the crucial terms. A summary of the achieved numerical regression models is given in Table 12. Figures 15 and 16 display 2D/3D graphical representations of these models that highlight significant patterns and overall values.

The contour plot (Figures 15a and 16a) and the 3D surface plot (Figures 15b and 16b) illustrate how the concentration of SiO_2 nanoparticles influences silicon levels for both lubricants and biolubricants. Figures 15 and 16 demonstrate a direct and clear relationship between the concentration of silicon and the concentration of SiO_2 nanoparticles. This linear dependency implies that the amount of SiO_2 injected effectively controls the silicon concentration in the samples, with little to no influence from ageing time or temperature. By illustrating the durability of SiO_2 nanoparticles under various circumstances and confirming their function as a reliable supply of silicon in both nanolubricants and nano-biolubricants, the plots visually validate that SiO_2 concentration is the primary factor influencing silicon levels.

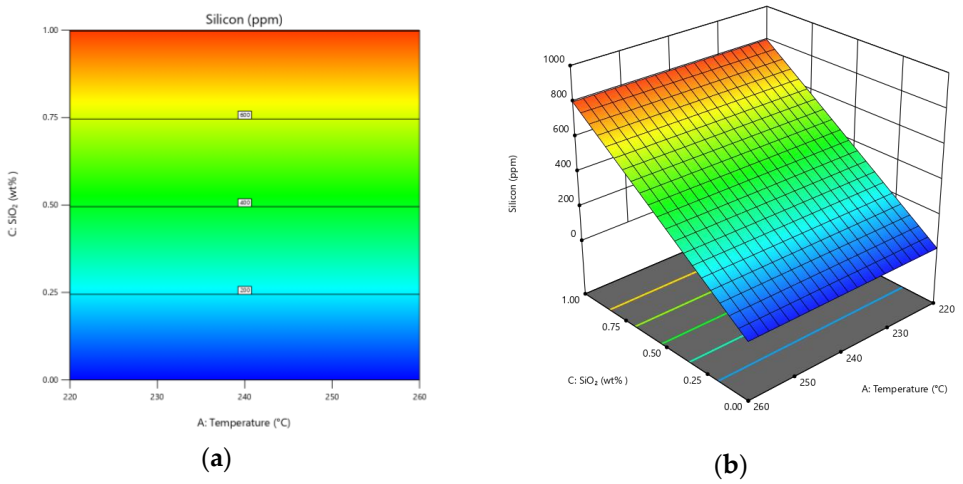
Table 12. Main data on both nanolubricants and nanobiolubricants for a response-surface reduced linear model based on the silicon data.

Quantity	Nanolubricants Regression Equation	Nanobiolubricants Regression Equation
Silicon [ppm]	+27.2667 + 704.133 · C $_{SiO2}$	+4.86667 + 797.733 · C $_{SiO2}$
Fit Statistics, Std. Dev.	89.71	22.73
Mean	379.33	403.73
C.V. %	23.65	5.63
R^2	0.8988	0.9944
Adjusted R^2	0.8911	0.9940
Predicted R^2	0.8549	0.9923
Adeq Precision	21.4959	96.0944



(**a**) (**b**)

Figure 15. Contour plot (**left**) and the 3D surface (**right**) of the regression function for the silicon varying the temperature and the concentration of SiO_2 nanoparticles for a conventional lubricant ((**a**,**b**); in this case the time is set at 180 h).



(**a**) (**b**)

Figure 16. Contour plot (**left**) and the 3D surface (**right**) of the regression function for the silicon varying the temperature and the concentration of SiO_2 nanoparticles for a biolubricant ((**a**,**b**); in this case the time is set at 180 h).

3.4.2. Analysis of Sodium

Sodium was not detected in either fresh lubricant (0 ppm in both the conventional lubricant and the biolubricant). Therefore, the sodium measured after ageing cannot be attributed to an initially measurable sodium content in the fresh oils. Its appearance and increase during ageing may reflect external contamination, evaporation-related concentration effects, interactions with the ageing environment, additive decomposition or redistribution, or changes in matrix composition. The present ICP-OES measurements do not allow the specific source of sodium to be uniquely identified.

A linear regression model provided the best match to the sodium data for nanolubricants and nanobiolubricants at various concentrations and ageing conditions (120, 168, and 240 h at 220 °C and 260 °C). An ANOVA on the linear model showed that all of the terms were statistically significant. A summary of the achieved numerical regression models is given in Table 13. Figures 17 and 18 display 2D/3D graphical representations of these models that highlight significant patterns and overall values.

Regardless of the SiO_2 content, the contour plot (Figures 17a and 18a) and the 3D surface plot (Figures 17b and 18b) show how temperature and time impact sodium in both lubricants and biolubricants. Both lubricants and biolubricants exhibit an increase in sodium concentrations with increasing temperature and exposure duration. However, this increase should not be interpreted as direct evidence of improved sodium uptake or retention. It may instead reflect evaporation-related concentration effects, additive decomposition or redistribution, contamination, or changes in the lubricant matrix.

Table 13. Main data on both nanolubricants and nanobiolubricants for a response-surface reduced linear model based on the sodium data.

Quantity	Nanolubricants Regression Equation	Nanobiolubricants Regression Equation
Sodium [ppm]	$-148.76 + 0.622 \cdot T + 0.0730769 \cdot t + 19.1323 \cdot C_{SiO2}$	$-83.2755 + 0.311065 \cdot T + 0.0590571 \cdot t + 31.222 \cdot C_{SiO2}$
Fit Statistics, Std. Dev.	4.99	5.04
Mean	18.33	14.93
C.V. %	27.22	33.73
R^2	0.9057	0.8951
Adjusted R^2	0.8799	0.8665
Predicted R^2	0.8114	0.7956

Adeq Precision	18.4414	17.8742

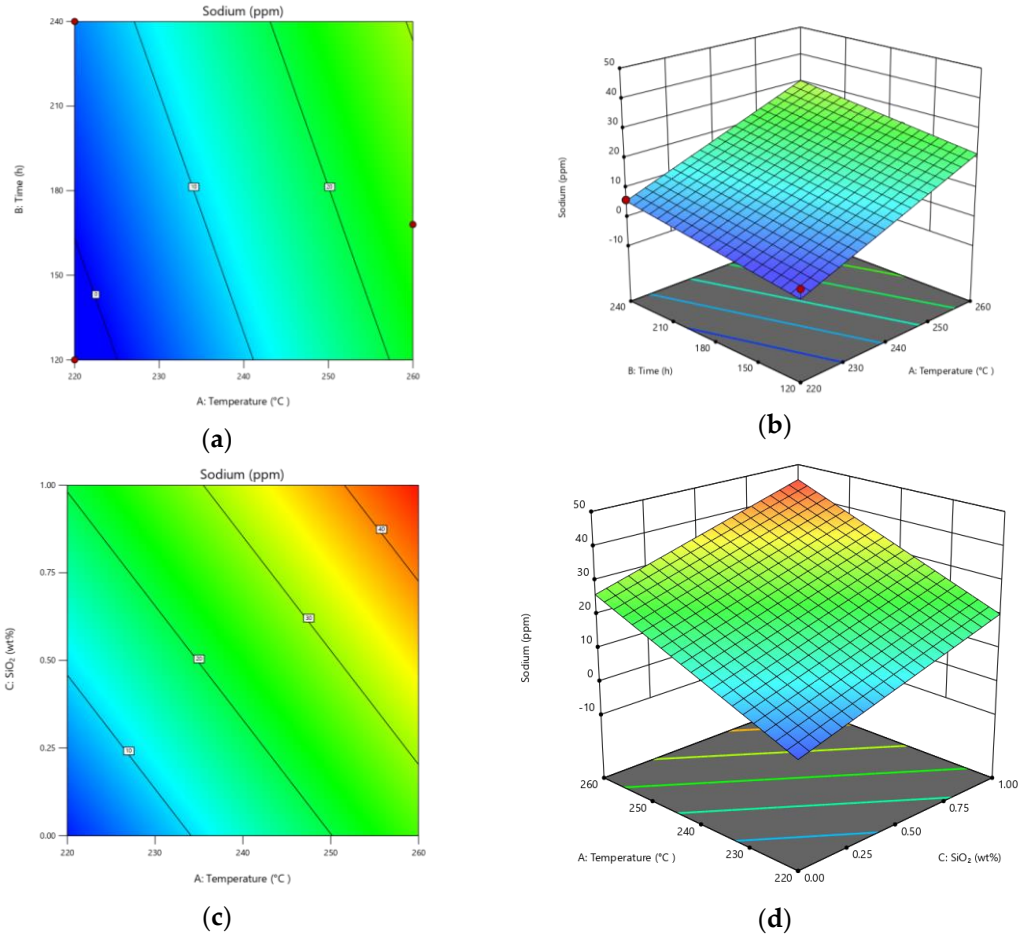
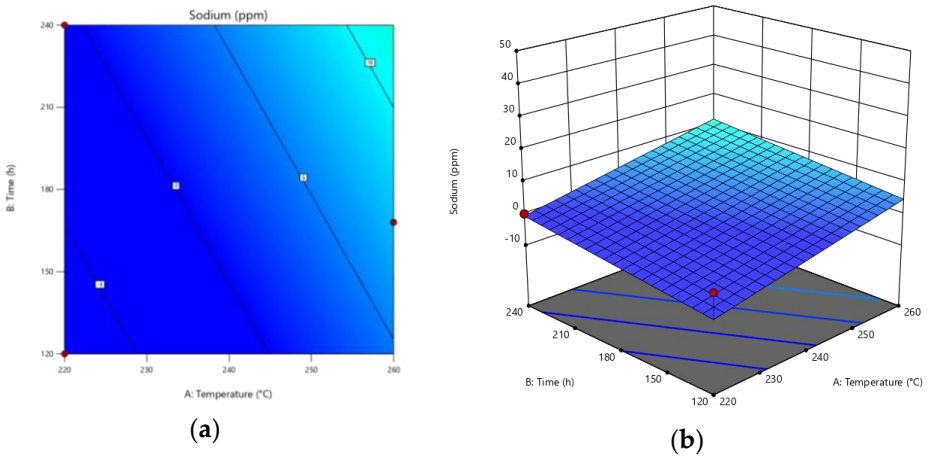
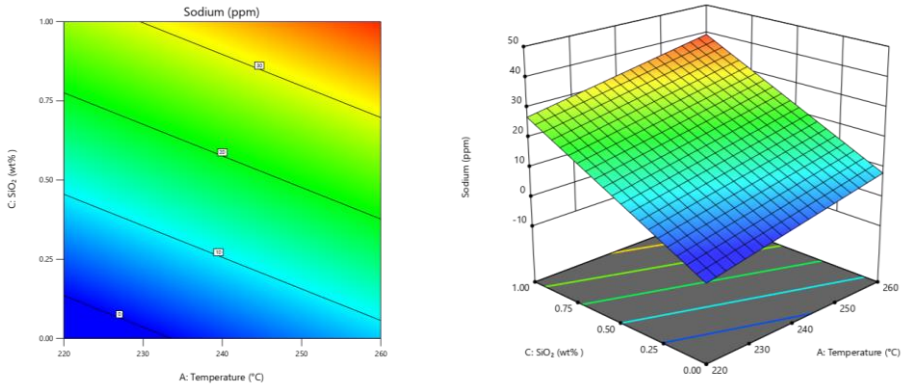


Figure 17. Contour plots (**left**) and the 3D surfaces (**right**) of the regression function for the sodium, varying the temperature and the heat-exposure time for a conventional lubricant ((**a**,**b**); in this case the SiO_2 concentration is set at 0.00%) and the temperature and concentration of SiO_2 nanoparticles ((**c**,**d**); in this case the time is set at 180 h).





(**c**) (**d**)

Figure 18. Contour plots (**left**) and the 3D surfaces (**right**) of the regression function for the sodium varying the temperature and the heat-exposure time for a biolubricant ((**a**,**b**); in this case the SiO_2 concentration is set at 0.00%) and the temperature and concentration of SiO_2 nanoparticles ((**c**,**d**); in this case the time is set at 180 h).

The contour plot (Figures 17c and 18c) and the 3D surface plot (Figures 17d and 18d) illustrate how temperature and concentration of SiO_2 nanoparticles affect sodium. Sodium levels steadily rise with increasing SiO_2 concentrations, showing an association between SiO_2 concentration and the measured sodium content under the investigated conditions. However, the present measurements do not establish a specific interaction or retention mechanism. This trend is more pronounced at higher temperatures, although the respective contributions of evaporation, matrix changes, contamination, and nanoparticle-related effects cannot be distinguished from the present data.

As temperature, time, and SiO_2 concentration increase, sodium levels in nanolubricants also increase. For instance, sodium levels rose from 0 ppm at 0.0% SiO_2 to 17 ppm at 1.0% SiO_2 after 120 h at 220 °C. Sodium levels were 24 ppm without SiO_2 and 34 ppm with 1.0% SiO_2 at 260 °C at 168 h. Although it varies slightly, sodium exhibits a similar trend in nanobiolubricants. Sodium levels rose from 0 ppm (0% SiO_2) to 30 ppm (1.0% SiO_2) at 220 °C at 240 h, and the same increased from 0 ppm (0% SiO_2) to 41 ppm (1.0% SiO_2) at 260 °C at 168 h.

3.4.3. Analysis of Additives: Calcium

The results of the ICP-OES analysis of the calcium content in both nanolubricants and nanobiolubricants offer valuable information about the behaviour of additives under various temperature and time conditions. In order to neutralize acids and preserve lubricant cleanliness, calcium-based additives are initially present and function as detergents. When the concentration of SiO_2 nanoparticles increases in fresh samples, there is minimal variation in the calcium levels, suggesting that the nanoparticles and the calcium-based additives interact only weakly. As confirmed in our previous study [28], in both fresh nanolubricants and nanobiolubricants, the calcium levels are relatively stable, indicating the presence of calcium-based additives.

The best fit to the calcium data for nanolubricants and nanobiolubricants was a 2FI regression model at various concentrations and ageing conditions (120, 168, and 240 h at 220 °C and 260 °C). However, an ANOVA on the 2FI model showed that several of the components were not statistically significant. The model was improved by employing a backward elimination process, which retained just the crucial terms. A summary of the achieved numerical regression models is given in Table 14. Figures 19 and 20 display 2D/3D graphical representations of these models that highlight significant patterns and overall values.

The contour plot (Figures 19a and 20a) and the 3D surface plot (Figures 19b and 20b) demonstrate how temperature and time affect calcium in both lubricants and biolubricants, regardless of the SiO_2 content. As the lubricant and biolubricant age, their calcium levels rise in tandem with rising temperatures and longer periods of time. This increase in calcium content over time and at higher temperatures raises the possibility that calcium-based additives could partially degrade and release calcium ions into the lubricant matrix.

Table 14. Main data on both nanolubricants and nanobiolubricants for a response-surface reduced 2FI model based on the calcium data.

Quantity	Nanolubricants Regression Equation	Nanobiolubricants Regression Equation
Calcium [ppm]	$+9632.99 - 24.6606 \cdot T - 50.986 \cdot t - 302.926 \cdot C_{SiO2} + 0.219012 \cdot T \cdot t$	$+2249.6 - 1.34591 \cdot T - 14.0846 \cdot t + 563.7 \cdot C_{SiO2} + 0.061536 \cdot T \cdot t - 2.83409 \cdot T \cdot C_{SiO2}$
Fit Statistics, Std. Dev.	169.69	26.77
Mean	3686.47	1916.13
C.V. %	4.60	1.40
R^2	0.7857	0.9778
Adjusted R^2	0.6999	0.9655
Predicted R^2	0.5046	0.8858
Adeq Precision	10.1063	27.1025

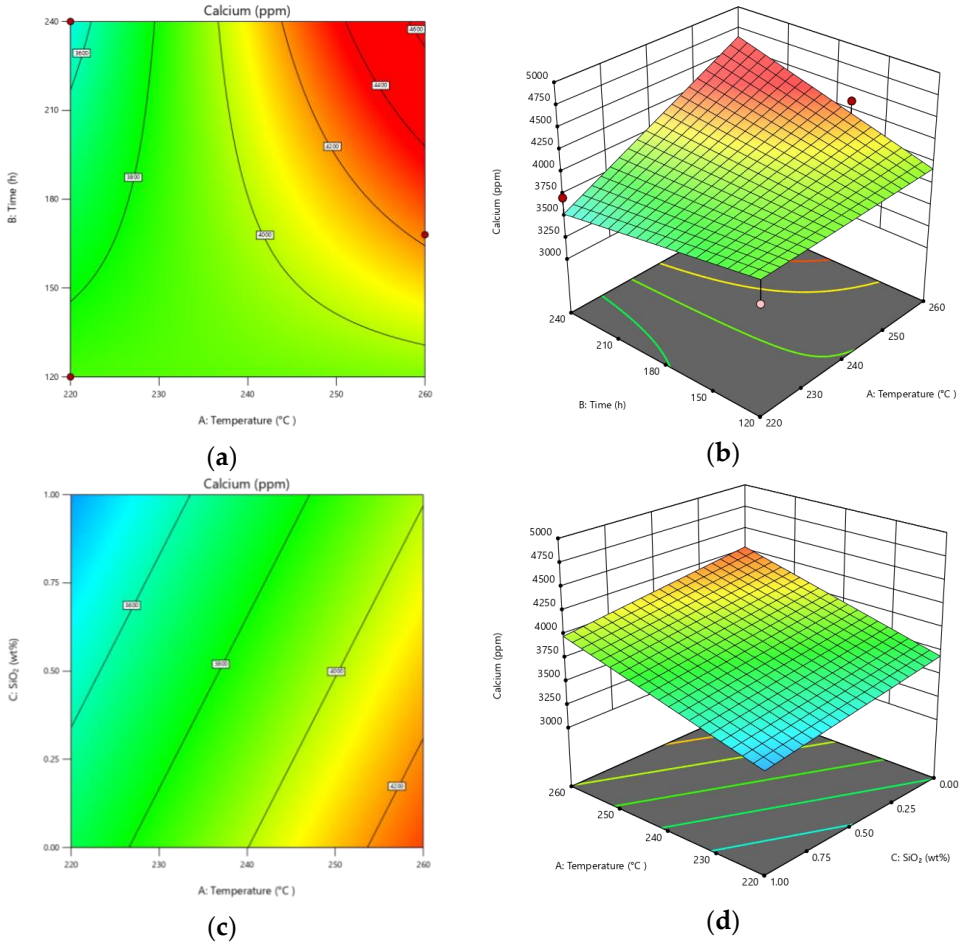


Figure 19. Contour plots (**left**) and the 3D surfaces (**right**) of the regression function for the calcium, varying the temperature and the heat-exposure time for a conventional lubricant ((**a**,**b**); in this case the SiO_2 concentration is set at 0.00%) and the temperature and concentration of SiO_2 nanoparticles ((**c**,**d**); in this case the time is set at 180 h).

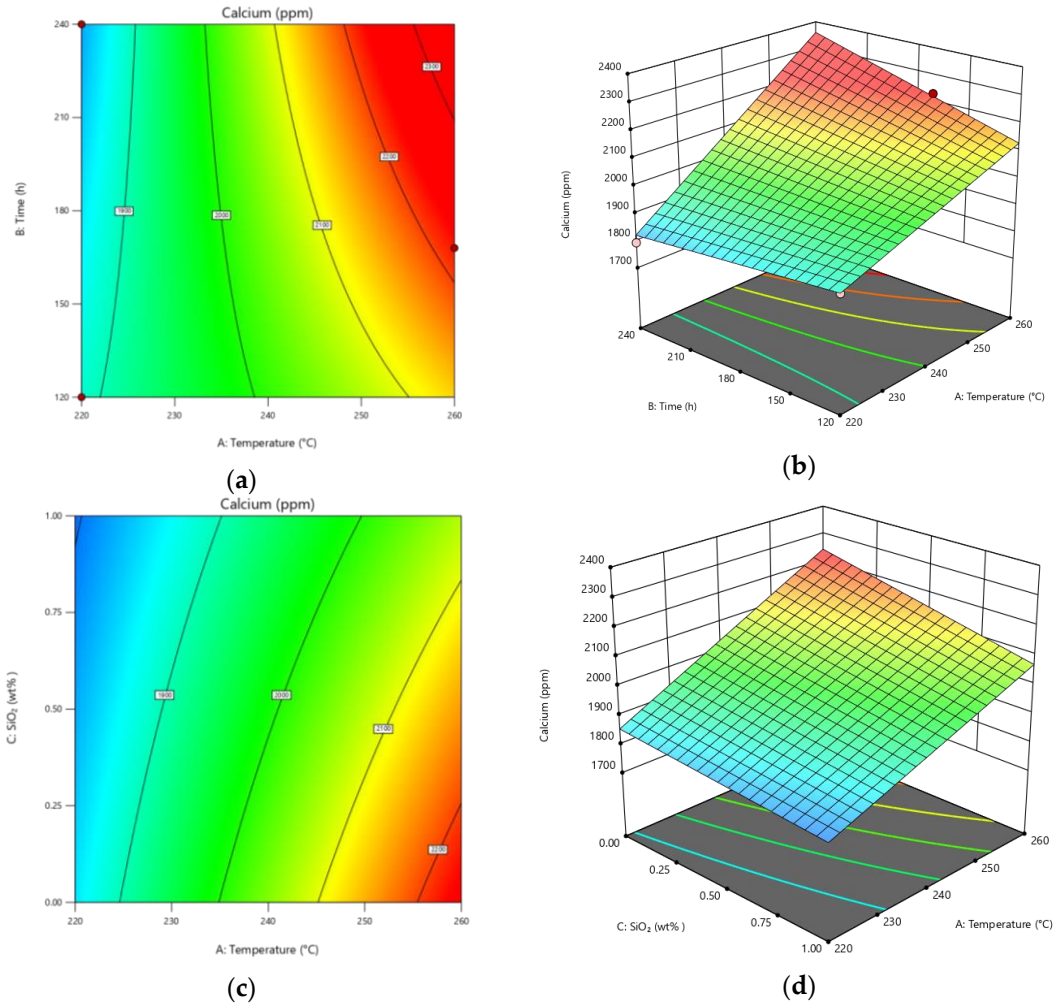


Figure 20. Contour plots (**left**) and the 3D surfaces (**right**) of the regression function for the calcium, varying the temperature and the heat-exposure time for a biolubricant ((**a**,**b**); in this case the SiO_2 concentration is set at 0.00%) and the temperature and concentration of SiO_2 nanoparticles ((**c**,**d**); in this case the time is set at 180 h).

The effects of temperature and SiO_2 nanoparticle concentration on calcium are depicted in Figures 19 and 20 by the contour plot (Figures 19c and 20c) and the 3D surface plot (Figures 19d and 20d). When SiO_2 nanoparticles are introduced, the levels of calcium show a modest drop, especially at high temperatures and extended ageing durations (e.g., 260 °C, 168 h). After ageing, calcium increases when no nanoparticles are present. This implies that the temperature stability offered by the nanoparticles prevents calcium-based compounds from degrading. Since these additives break down with age, the calcium concentration usually rises. However, the presence of nanoparticles seems to counteract this rise, keeping the calcium levels in both nanolubricants and nanobiolubricants more constant. This suggests that SiO_2 nanoparticles aid in maintaining additive performance, especially in situations involving high temperatures and extended periods of time.

3.4.4. Analysis of Additives: Magnesium

As a component of detergent additives, magnesium is frequently added to lubricants to neutralize acids and maintain the cleanliness of engine parts. After adding SiO_2 nanoparticles, magnesium levels in fresh samples are rather steady for nanolubricants, and more slightly so in the case of nanobiolubricants, as shown in our previous study [28].

A 2FI regression model provided the best match to the magnesium data for nanolubricants and nanobiolubricants at various concentrations and ageing conditions

(120, 168, and 240 h at 220 °C and 260 °C). However, an ANOVA on the 2FI model showed that several of the components were not statistically significant. The model was improved by employing a backward elimination process, which retained just the crucial terms. A summary of the achieved numerical regression models is given in Table 15. Figures 21 and 22 display 2D/3D graphical representations of these models that highlight significant patterns and overall values.

Table 15. Main data on both nanolubricants and nanobiolubricants for a response-surface reduced 2FI model based on the magnesium data.

Quantity	Nanolubricants Regression Equation	Nanobiolubricants Regression Equation
Magnesium [ppm]	+133.4 − 0.238636 · T − 1.07625 · t + 63.9 · C $_{SiO2}$ + 0.00483144 · T · t − 0.291364 · T · C $_{SiO2}$	+445.4 − 0.29 · T − 2.595 · t + 145 · C $_{SiO2}$ + 0.0115833 · T · t − 0.65 · T · C $_{SiO2}$
Fit Statistics, Std. Dev.	2.99	4.72
Mean	83.00	389.47
C.V. %	3.61	1.21
R^2	0.9049	0.9746
Adjusted R^2	0.8521	0.9605
Predicted R^2	0.7120	0.9053
Adeq Precision	12.7233	23.3329

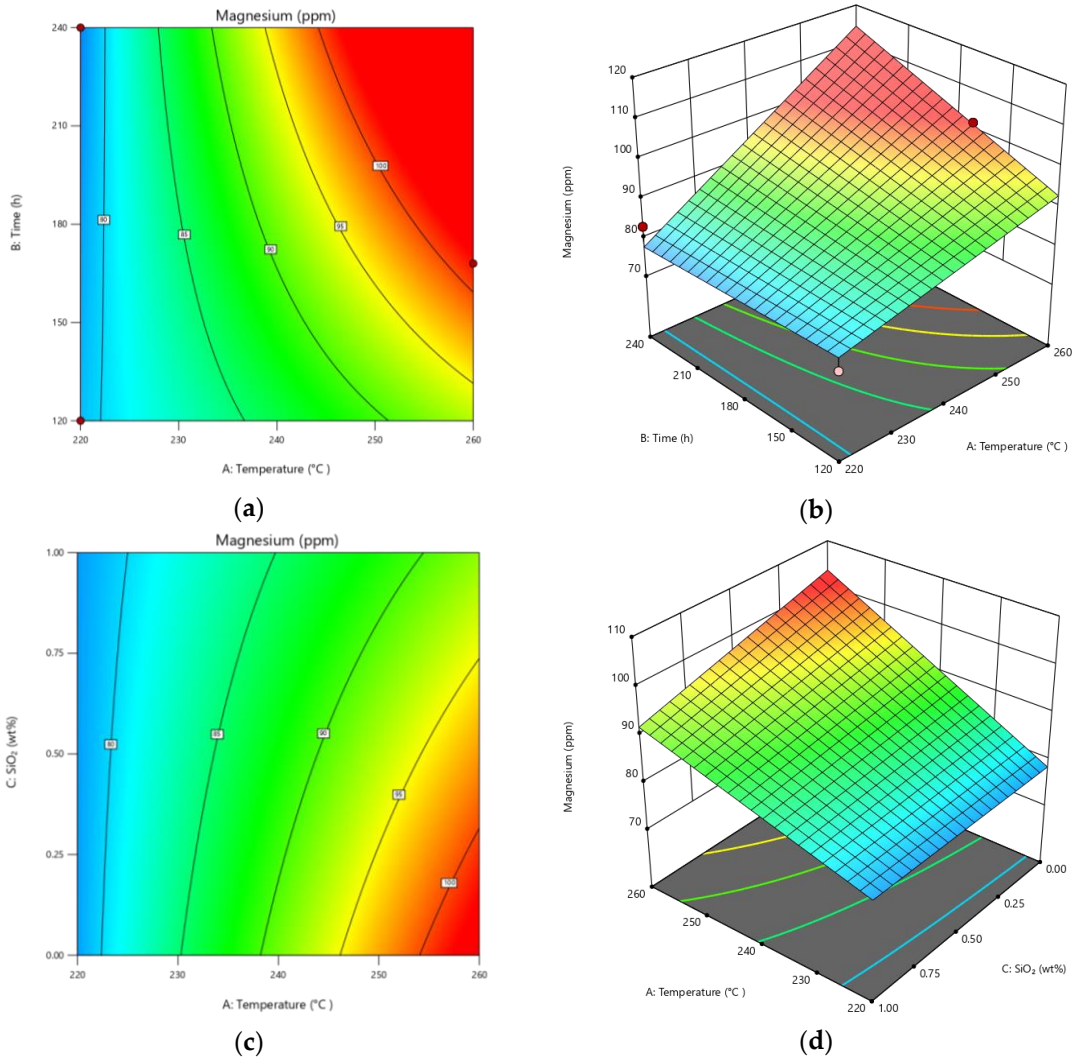


Figure 21. Contour plots (**left**) and the 3D surfaces (**right**) of the regression function for the magnesium, varying the temperature and the heat-exposure time for a conventional lubricant ((**a**,**b**); in this

case the SiO_2 concentration is set at 0.00%) and the temperature and concentration of SiO_2 nanoparticles ((**c**,**d**); in this case the time is set at 180 h).

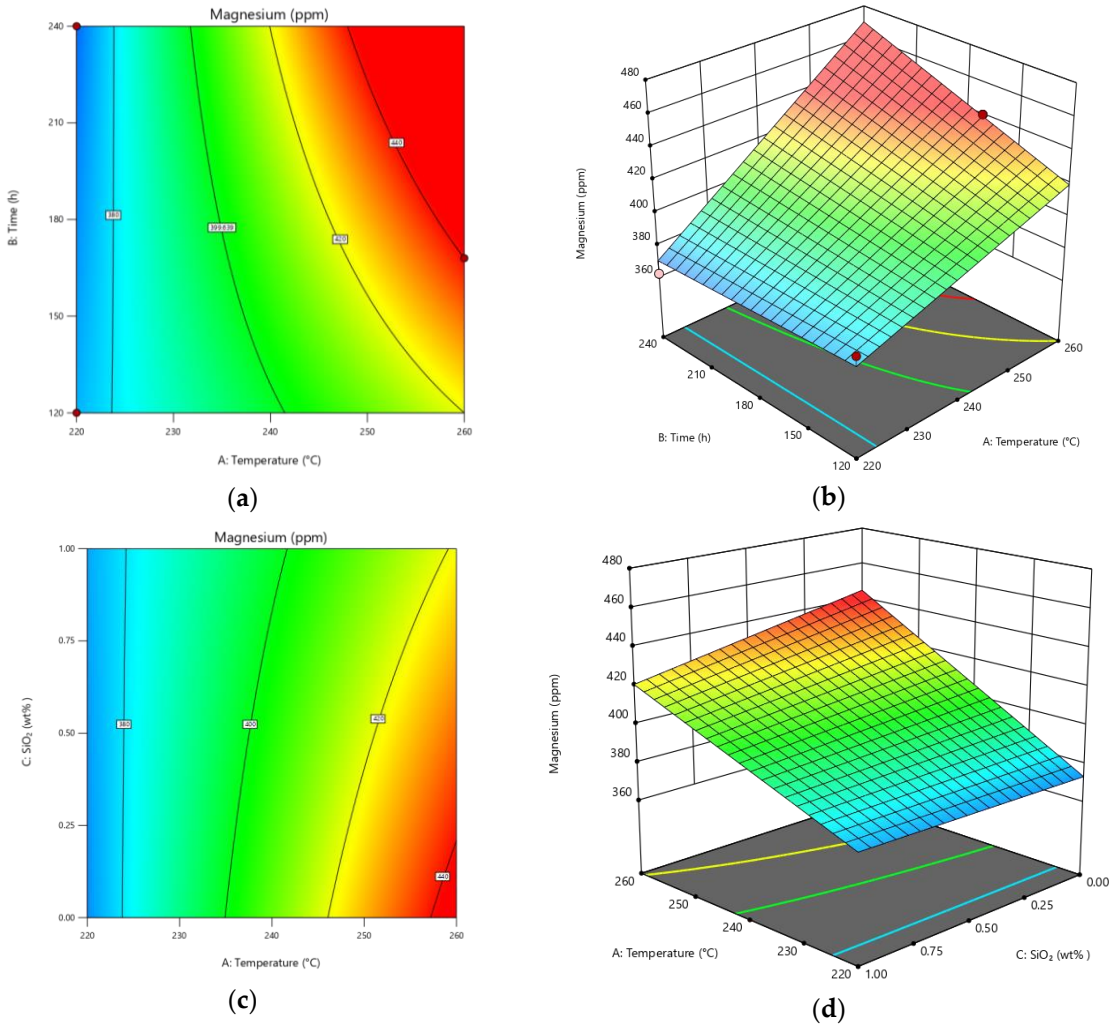


Figure 22. Contour plots (**left**) and the 3D surfaces (**right**) of the regression function for the magnesium, varying the temperature and the heat-exposure time for a biolubricant ((**a**,**b**); in this case the SiO_2 concentration is set at 0.00%) and the temperature and concentration of SiO_2 nanoparticles ((**c**,**d**); in this case the time is set at 180 h).

Regardless of the SiO_2 content, the contour plot (Figures 21a and 22a) and the 3D surface plot (Figures 21b and 22b) show how temperature and time impact magnesium in both lubricants and biolubricants. It is evident that magnesium levels rise with age, temperature, and time. When 0.0% nanoparticles are included in the formulation, magnesium levels rise with age, indicating that magnesium compounds may break down or leak out in the absence of SiO_2, eventually leading to higher detectable magnesium levels. This pattern suggests that extended exposure and higher temperatures encourage the release of additives based on magnesium, which may have an impact on the lubricant's stability and functionality. Therefore, it appears that the stabilizing function of nanoparticles is essential in formulations that need constant magnesium levels during long ageing times.

The contour plot (Figures 21c and 22c) and the 3D surface plot (Figures 21d and 22d) show how temperature and the concentration of SiO_2 nanoparticles affect magnesium. In general, magnesium levels exhibit a constant response to temperature and SiO_2 concentration increases, suggesting some resistance to these factors. However, the magnesium levels exhibit a slight decline when nanoparticles are present during prolonged ageing,

particularly at 260 °C. According to this pattern, the SiO_2 nanoparticles may have a stabilizing effect and slow the breakdown or leaching out of compounds based on magnesium. In order to preserve the integrity of the magnesium additions in the formulation, SiO_2 nanoparticles appear to aid in maintaining magnesium stability during extended exposure to high temperatures.

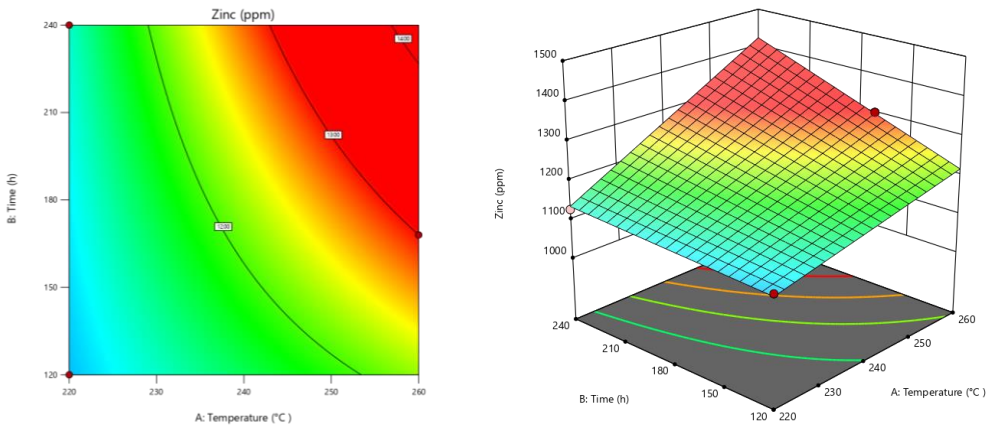
3.4.5. Analysis of Additives: Zinc

Zinc dialkyldithiophosphate (ZDDP), an anti-wear and anti-oxidation ingredient, is widely used in lubricants. Because zinc forms a protective film on metal surfaces, it lowers friction and prevents wear, especially when engine parts are subjected to high pressure. As reported in our previous study [28], the zinc level in fresh samples is marginally lower when SiO_2 nanoparticles are added than when using the base lubricant. This could be the result of a reaction or dispersion that lowers the measurable zinc concentration caused by interactions between the ZDDP additive and the nanoparticles.

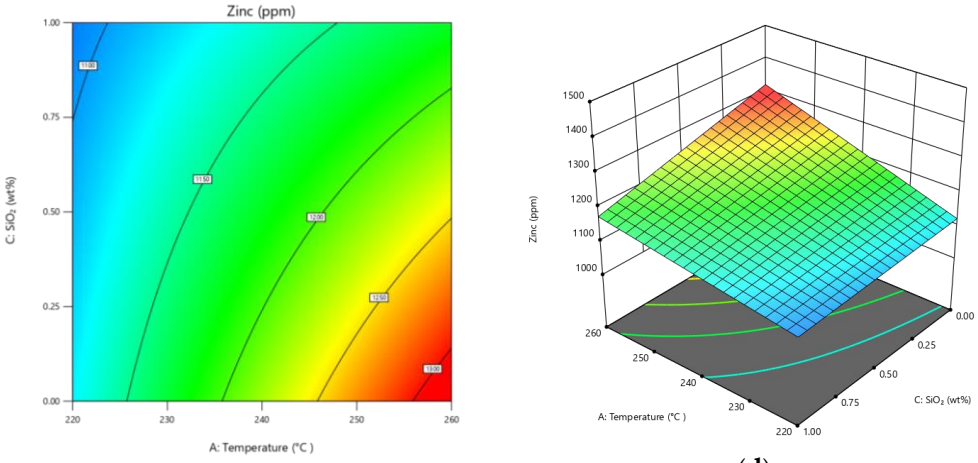
A 2FI regression model provided the best match to the zinc data for nanolubricants, and a full-linear model for nanobiolubricants, at various concentrations and ageing conditions (120, 168, and 240 h at 220 °C and 260 °C). However, an ANOVA on the 2FI model showed that several of the components were not statistically significant. The model was improved by employing a backward elimination process, which retained just the crucial terms, but the full linear model showed that all of the terms were statistically significant. A summary of the achieved numerical regression models is given in Table 16. Figures 23 and 24 display 2D/3D graphical representations of these models that highlight significant patterns and overall values.

Table 16. Main data on both nanolubricants and nanobiolubricants for a response-surface reduced 2FI and linear model based on the zinc data.

Quantity	Nanolubricants Regression Equation	Nanobiolubricants Regression Equation
Zinc [ppm]	+1454.7 − 1.69682 · T − 7.92333 · t + 610.6 · C $_{SiO2}$ + 0.0370303 · T · t − 2.90818 · T · C $_{SiO2}$	+142.782 + 2.48974 · T + 0.320182 · t − 23.9158 · C $_{SiO2}$
Fit Statistics, Std. Dev.	16.66	12.18
Mean	1136.13	766.07
C.V. %	1.47	1.59
R^2	0.9459	0.9509
Adjusted R^2	0.9158	0.9376
Predicted R^2	0.8286	0.8970
Adeq Precision	20.9649	22.0807

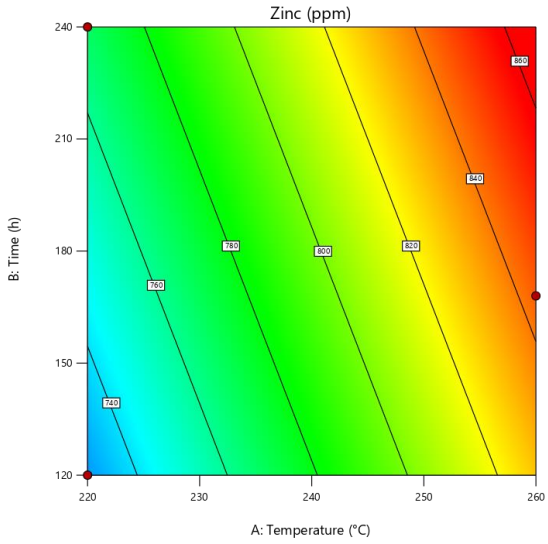


(**a**) (**b**)

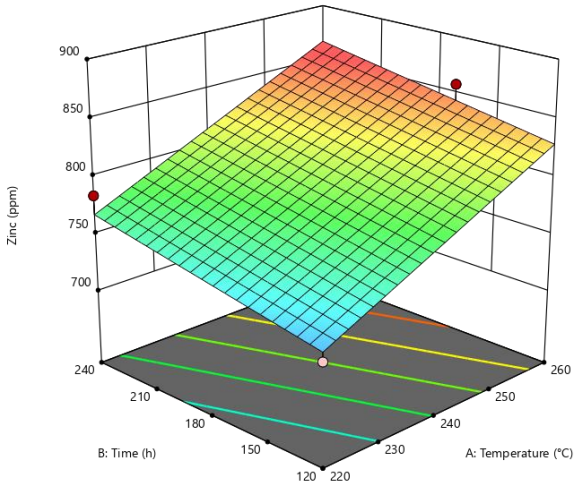


(**c**) (**d**)

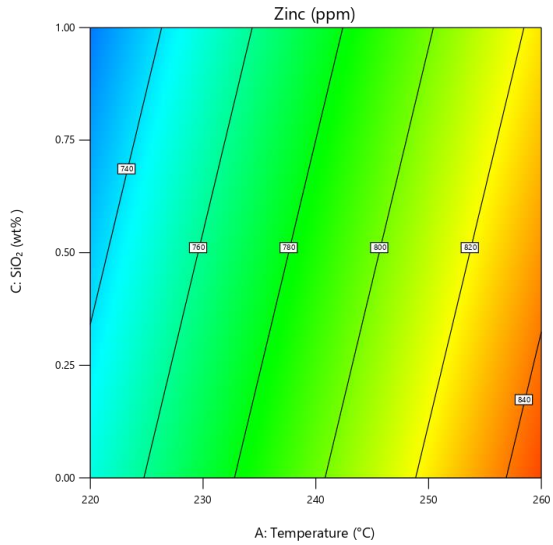
Figure 23. Contour plots (**left**) and the 3D surfaces (**right**) of the regression function for zinc as a function of temperature and the heat-exposure time for a conventional lubricant ((**a**,**b**); in this case the SiO_2 concentration is set at 0.00%) and the temperature and concentration of SiO_2 nanoparticles ((**c**,**d**); in this case the time is set at 180 h).



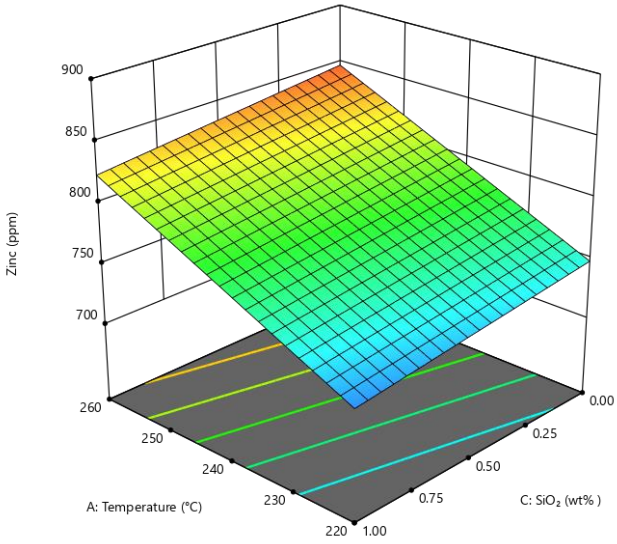
(**a**)



(**b**)



(**c**)



(**d**)

Figure 24. Contour plots (**left**) and the 3D surfaces (**right**) of the regression function for the zinc, varying the temperature and the heat-exposure time for a biolubricant ((**a**,**b**); in this case the SiO_2 concentration is set at 0.00%) and the temperature and concentration of SiO_2 nanoparticles ((**c**,**d**); in this case the time is set at 180 h).

The contour plot (Figures 23a and 24a) and the 3D surface plot (Figures 23b and 24b) demonstrate the effects of temperature and time on zinc in lubricants and biolubricants, regardless of the SiO_2 content. In samples lacking nanoparticles, there is a discernible increase in zinc content as the lubricants age, especially at higher temperatures (260 °C). This is probably because zinc is released into the lubricant as a result of ZDDP's heat breakdown.

Figures 23 and 24 illustrate the effects of temperature and SiO_2 nanoparticle concentration on zinc through the contour plot (Figures 23c and 24c) and the 3D surface plot (Figures 23d and 24d). With ageing, the zinc content slightly decreases in samples that contain nanoparticles. This indicates that SiO_2 nanoparticles maintain ZDDP additives by delaying their degradation and reducing zinc release after extended exposure to high temperatures. This stabilization suggests that the nanoparticles might be involved in preserving the zinc additions' protective qualities in harsh environments.

3.4.6. Analysis of Additives: Phosphorus

Phosphorus is frequently included in lubricants as an additive for anti-oxidation and anti-wear. As investigated in our previous study [28], phosphorus levels are comparatively stable in fresh samples at all SiO_2 concentrations, suggesting that phosphorus-based additives are initially completely functional and well-preserved in nanobiolubricants as well as nanolubricants.

A 2FI regression model provided the best match to the phosphorus data for nanolubricants and nanobiolubricants at various concentrations and ageing conditions (120, 168, and 240 h at 220 °C and 260 °C). However, an ANOVA on the 2FI model showed that several of the components were not statistically significant. The model was improved by employing a backward elimination process, which retained just the crucial terms. A summary of the achieved numerical regression models is given in Table 17. Figures 25 and 26 display 2D/3D graphical representations of these models that highlight significant patterns and overall values.

Regardless of the SiO_2 content, the contour plot (Figures 25a and 26a) and the 3D surface plot (Figures 25b and 26b) show how temperature and time impact phosphorus in both lubricants and biolubricants. Phosphorus content changes noticeably as the samples age, especially when they are heated to high temperatures (260 °C). Phosphorus levels in samples free of nanoparticles typically rise with age. This rise can be the result of additives containing phosphorus breaking down and releasing phosphorus into the lubricant.

Table 17. Main data on both nanolubricants and nanobiolubricants for a response-surface reduced 2FI model based on the phosphorus data.

Quantity	Nanolubricants Regression Equation	Nanobiolubricants Regression Equation
Phosphorus [ppm]	$+1584.25 - 2.91205 \cdot T - 8.55958 \cdot t + 403.6 \cdot C_{SiO2} + 0.0400966 \cdot T \cdot t - 2.08545 \cdot T \cdot C_{SiO2}$	$+667.254 - 0.0952717 \cdot T - 2.58723 \cdot t + 9.41169 \cdot C_{SiO2} + 0.0123644 \cdot T \cdot t - 0.262544 \cdot t \cdot C_{SiO2}$
Fit Statistics, Std. Dev.	19.88	7.67
Mean	987.20	674.33
C.V. %	2.01	1.14
R^2	0.9167	0.9730
Adjusted R^2	0.8703	0.9580

Predicted R^2	0.6773	0.8994
Adeq Precision	17.5545	25.4237

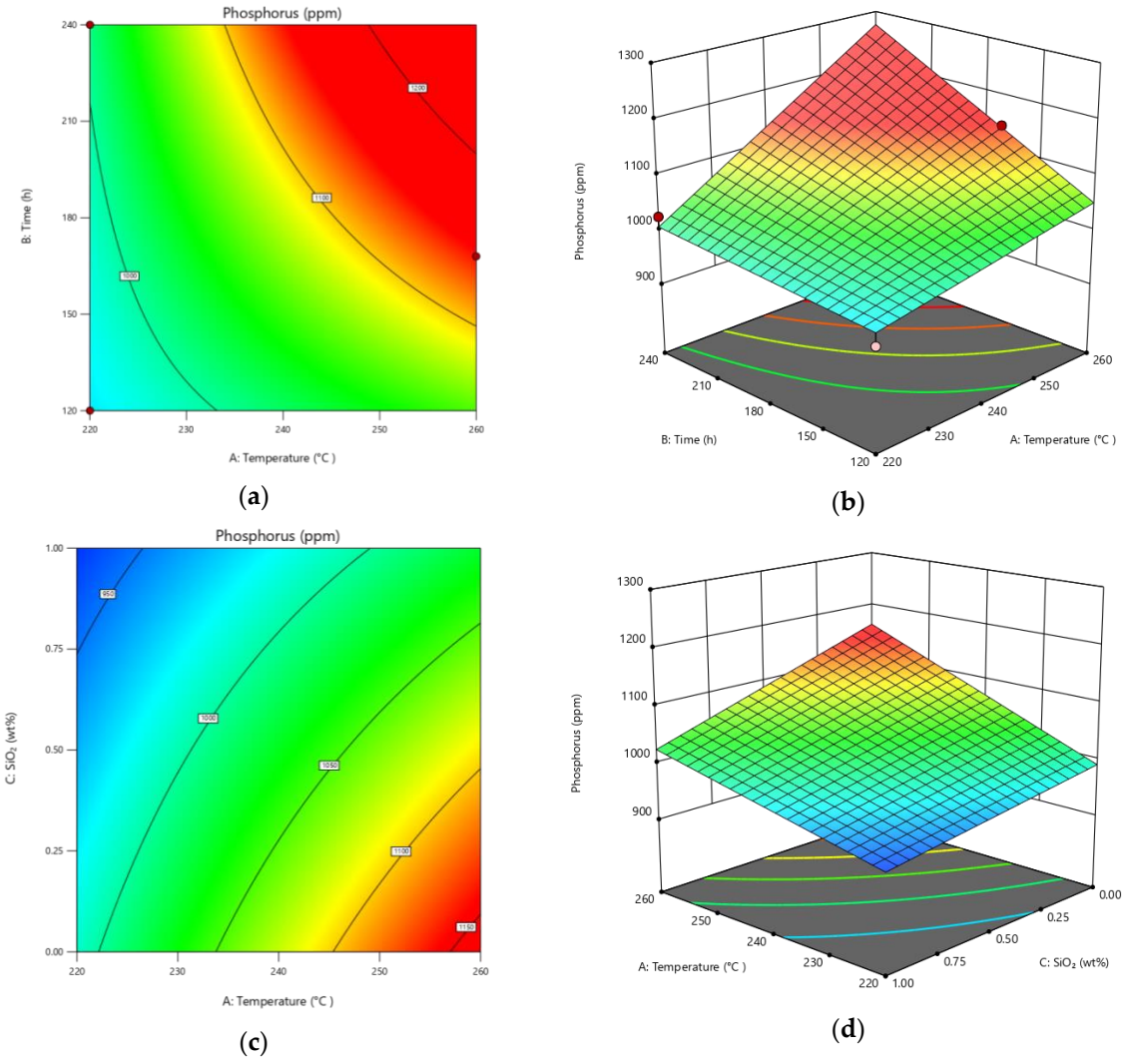


Figure 25. Contour plots (**left**) and the 3D surfaces (**right**) of the regression function for the phosphorus, varying the temperature and the heat-exposure time for a conventional lubricant ((**a**,**b**); in this case the SiO_2 concentration is set at 0.00%) and the temperature and concentration of SiO_2 nanoparticles ((**c**,**d**); in this case the time is set at 180 h).

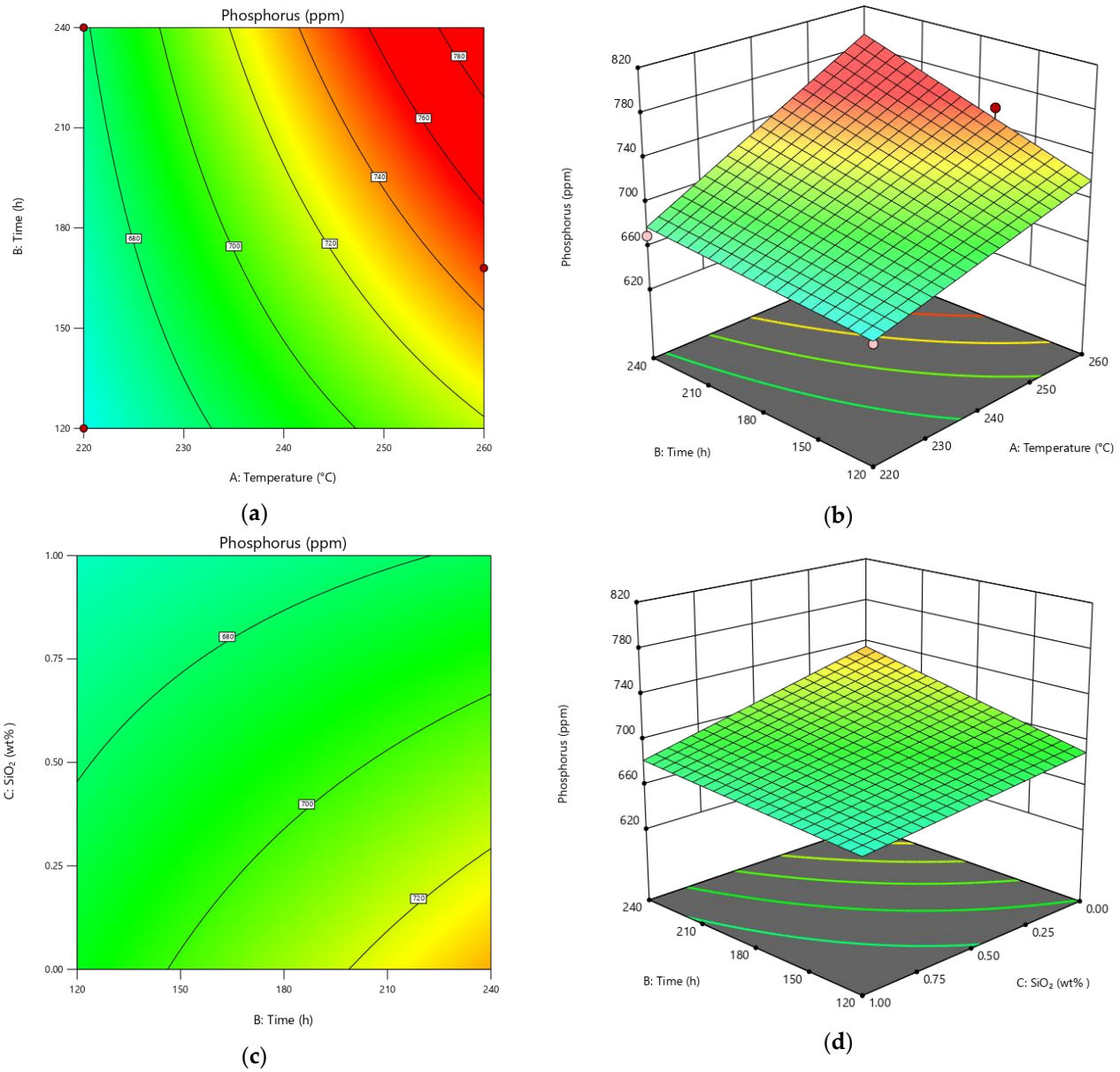


Figure 26. Contour plots (**left**) and the 3D surfaces (**right**) of the regression function for the phosphorus, varying the temperature and the heat-exposure time for a biolubricant ((**a**,**b**); in this case the SiO_2 concentration is set at 0.00%) and the time and concentration of SiO_2 nanoparticles ((**c**,**d**); in this case the temperature is set at 240 °C).

The contour plot (Figure 25c) and the 3D surface plot (Figure 25d) show how temperature and the concentration of SiO_2 nanoparticles affect phosphorus in lubricants. The contour plot (Figure 26c) and the 3D surface plot (Figure 26d) show the time and concentration of SiO_2 nanoparticles impacts in biolubricants. The addition of SiO_2 nanoparticles causes the phosphorus levels to drop, especially in samples that have been aged for a long time (168 h) at high temperatures (260 °C). This pattern is seen in both nanobiolubricants and nanolubricants, and it implies that the phosphorus-containing additives may be stabilized by the presence of nanoparticles, which would restrict the amount of phosphorus released into the lubricant by preventing the additives from degrading. The reason phosphorus levels are lower in samples containing SiO_2 is probably that the nanoparticles interact with the additives, prohibiting their breakdown under high conditions.

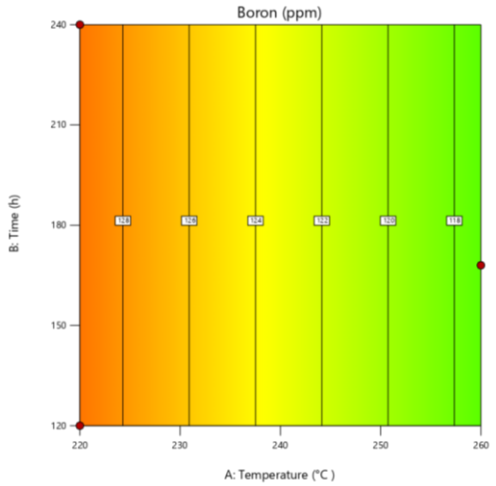
3.4.7. Analysis of Additives: Boron

Boron-based additives have anti-wear and friction-reducing qualities, which make them popular in lubricants. By creating a protective coating on metal surfaces, boron additions assist minimizing wear, especially in high-pressure environments. In our previous study [28], it is reported that after adding SiO_2 nanoparticle concentrations in fresh samples, the amounts of boron in both nanolubricants and nanobiolubricants slightly decrease. This implies that SiO_2 nanoparticles may interact with boron additives at first, changing their availability or behaviour in the lubricant to a slight extent.

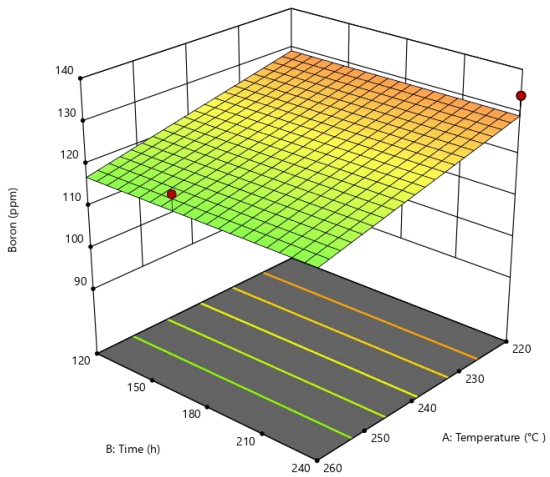
A linear regression model provided the best match to the boron data for nanolubricants and nanobiolubricants at various concentrations and ageing conditions (120, 168, and 240 h at 220 °C and 260 °C). However, an ANOVA on the linear model showed that one term (time) of the components was not statistically significant for nanolubricants. Consequently, the model was improved by employing a backward elimination process, which retained just the crucial terms. In contrast, for nanobiolubricants, all of the terms were statistically significant. A summary of the achieved numerical regression models is given in Table 18. Figures 27 and 28 display 2D/3D graphical representations of these models that highlight significant patterns and overall values.

Table 18. Main data on both nanolubricants and nanobiolubricants for a response-surface reduced and linear model based on the boron data.

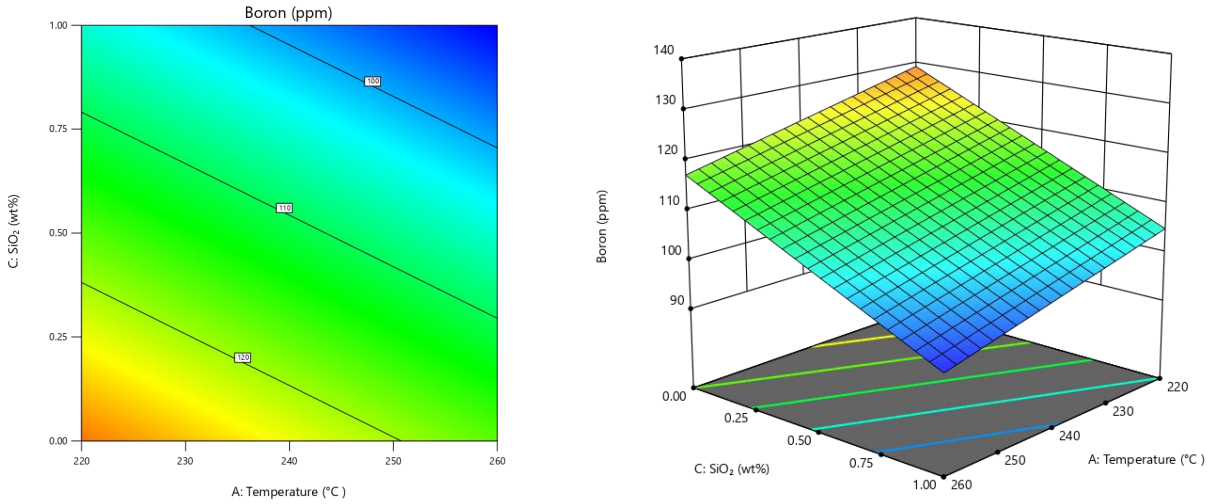
Quantity	Nanolubricants Regression Equation	Nanobiolubricants Regression Equation
Boron [ppm]	+195.85 − 0.3025 · T − 24.4 · C $_{SiO2}$	+489.968 − 0.295452 · T + 0.150062 · t − 67.3604 · C $_{SiO2}$
Fit Statistics, Std. Dev.	2.90	6.82
Mean	113.07	412.80
C.V. %	2.56	1.65
R^2	0.9410	0.9516
Adjusted R^2	0.9312	0.9384
Predicted R^2	0.9010	0.9006
Adeq Precision	28.1883	25.5684



(**a**)

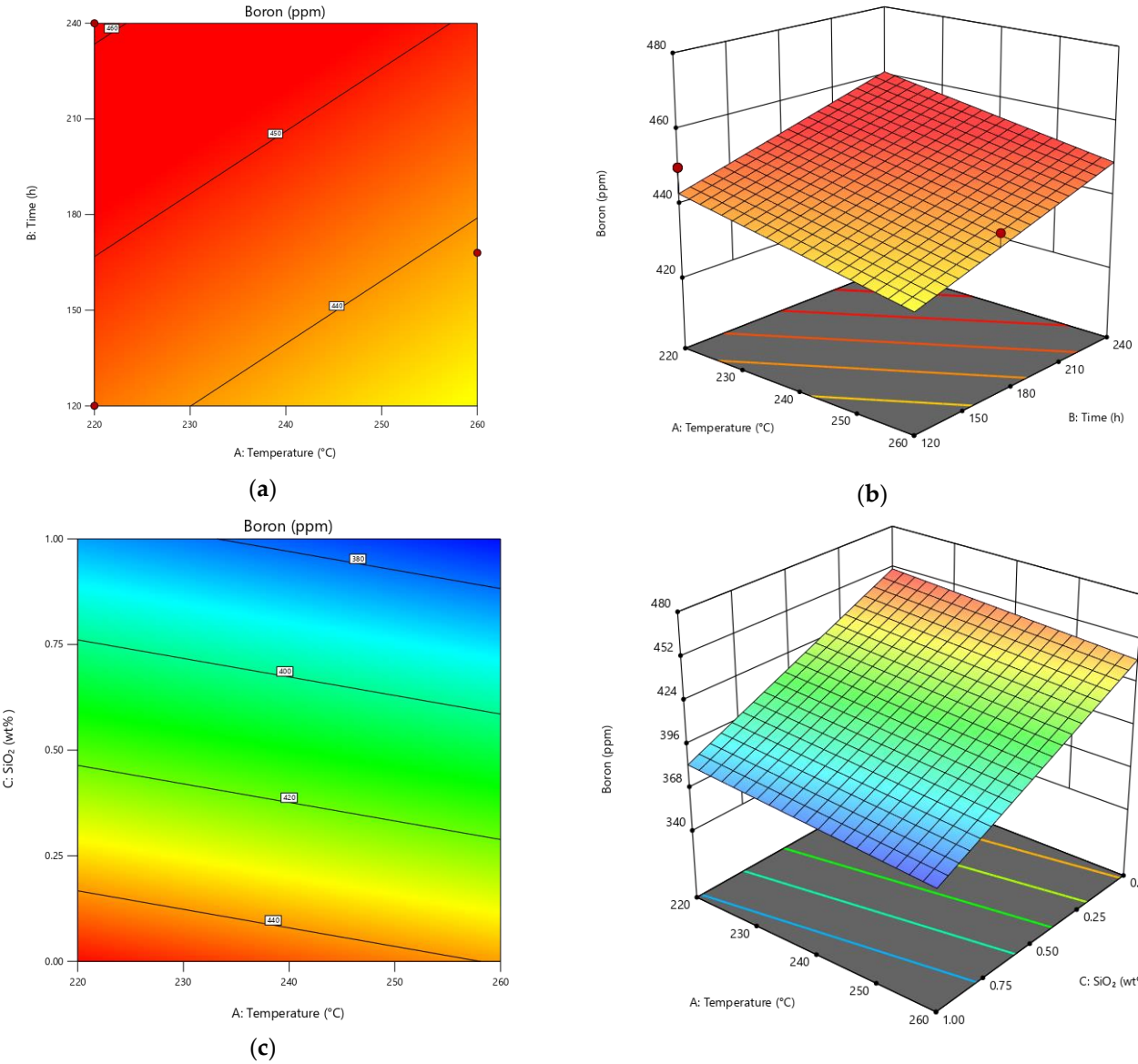


(**b**)



(**c**) (**d**)

Figure 27. Contour plots (**left**) and the 3D surfaces (**right**) of the regression function for the boron, varying the temperature and the heat-exposure time for a conventional lubricant ((**a**,**b**); in this case the SiO_2 concentration is set at 0.00%) and the temperature and concentration of SiO_2 nanoparticles ((**c**,**d**); in this case the time is set at 180 h).



(**a**) (**b**)

(**c**)

https://doi.org/10.3390/lubricants14110416

(**d**)

Figure 28. Contour plots (**left**) and the 3D surfaces (**right**) of the regression function for the boron, varying the temperature and the heat-exposure time for a biolubricant ((**a**,**b**); in this case the SiO_2 concentration is set at 0.00%) and the temperature and concentration of SiO_2 nanoparticles ((**c**,**d**); in this case the time is set at 180 h).

Regardless of the SiO_2 content, the contour plot (Figures 27a and 28a) and the 3D surface plot (Figures 27b and 28b) show how temperature and time affect boron in lubricants and biolubricants. Boron levels gradually decline with increasing temperature and ageing time. This decrease may reflect volatilization, thermal degradation, redistribution, or other concentration-related effects affecting the measured boron content. Boron levels gradually decline with increasing temperature and ageing time. This decrease may reflect volatilization, thermal degradation, redistribution, or other concentration-related effects affecting the measured boron content. However, the present measurements do not establish the specific mechanism responsible for this decrease.

The contour plot (Figures 27c and 28c) and the 3D surface plot (Figures 27d and 28d) show how temperature and the concentration of SiO_2 nanoparticles affect boron. The total content of boron dropped with age in both nanolubricants and nanobiolubricants, and the quantity appeared to drop significantly after the addition of nanoparticles. The observed decrease in boron content during ageing may be associated with thermal degradation, redistribution, volatilization, or other concentration-related effects; however, the available measurements do not allow these contributions to be distinguished. The observed changes in boron concentration indicate modifications in the elemental profile during ageing; however, the present ICP-OES measurements do not establish whether these changes translate into improved protective-film formation, friction reduction, or wear resistance.

3.4.8. Analysis of Additives: Molybdenum

Molybdenum disulphide (MoS_2), a well-known anti-wear additive that lowers friction between metal surfaces, especially at high pressures, is often added to lubricants. As demonstrated in our previous study [28], the fresh samples of nanobiolubricants exhibited relatively stable molybdenum concentrations, suggesting that nanoparticle addition had only a limited effect on the measured molybdenum concentration under these conditions. However, a slight increase was observed in the nanolubricant samples. This indicates a difference in molybdenum concentration under the investigated conditions, but the present measurements do not establish whether this translates into improved anti-wear or friction-reduction performance.

A 2FI regression model provided the best match to the molybdenum data for nanolubricants and a linear model for nanobiolubricants at various concentrations and ageing conditions (120, 168, and 240 h at 220 °C and 260 °C). However, an ANOVA on the 2FI model showed that several of the components were not statistically significant. The model was improved by employing a backward elimination process, which retained just the crucial terms, but on the linear model showed that all of the terms were statistically significant. A summary of the achieved numerical regression models is given in Table 19. Figures 29 and 30 display 2D/3D graphical representations of these models that highlight significant patterns and overall values.

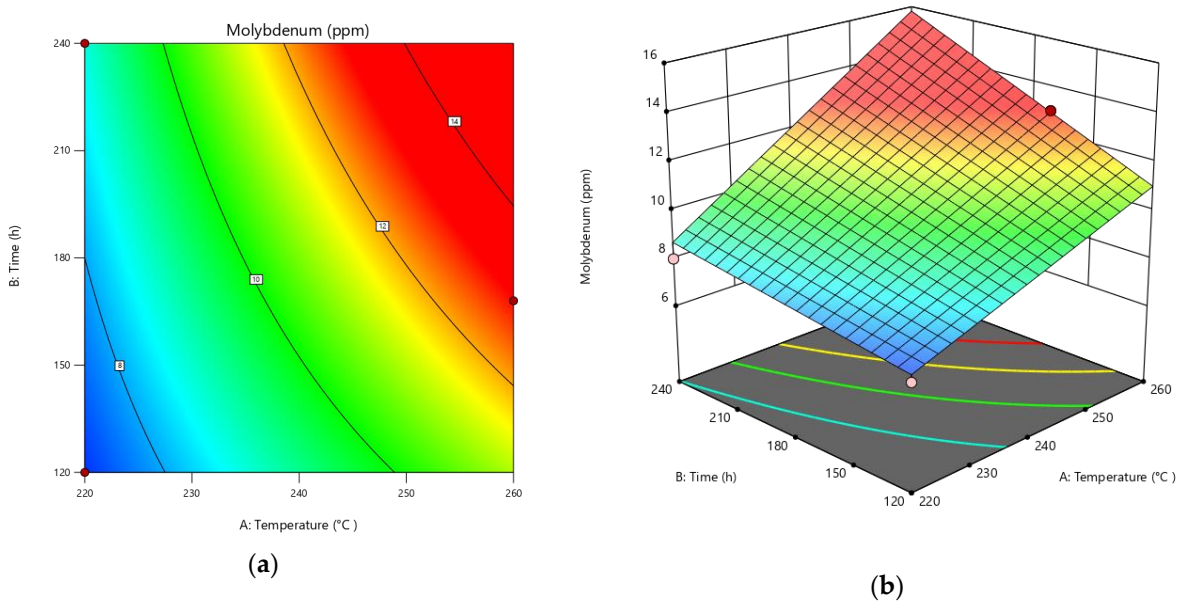
The contour plot (Figures 29a and 30a) and the 3D surface plot (Figures 29b and 30b) illustrate the effects of temperature and time on molybdenum in lubricants and biolubricants, independent of the SiO_2 content. Both the lubricant and biolubricant without nanoparticles tend to have greater molybdenum contents as they age, particularly at higher temperatures (260 °C). This increase may reflect thermal degradation, redistribution, concentration effects, or changes in the measured availability of molybdenum-containing

species; however, the present measurements do not establish the specific mechanism responsible for this trend.

The contour plot (Figures 29c and 30c) and 3D surface plot (Figures 29d and 30d) illustrate the effects of temperature and SiO_2 nanoparticle concentration on molybdenum. The molybdenum content of aged lubricants appears to be slightly stabilized upon the addition of SiO_2 nanoparticles. When samples containing nanoparticles are ageing for a longer period of time at 260 °C, the molybdenum levels stay more stable at greater concentrations of SiO_2. This comparatively more stable molybdenum concentration in some SiO_2-containing samples is consistent with a possible moderating effect under severe ageing conditions; however, the present measurements do not demonstrate reduced additive degradation or extended additive service life. Overall, some SiO_2-containing formulations exhibited more consistent measured molybdenum concentrations under severe ageing conditions, although the underlying cause cannot be determined from the present ICP-OES measurements alone.

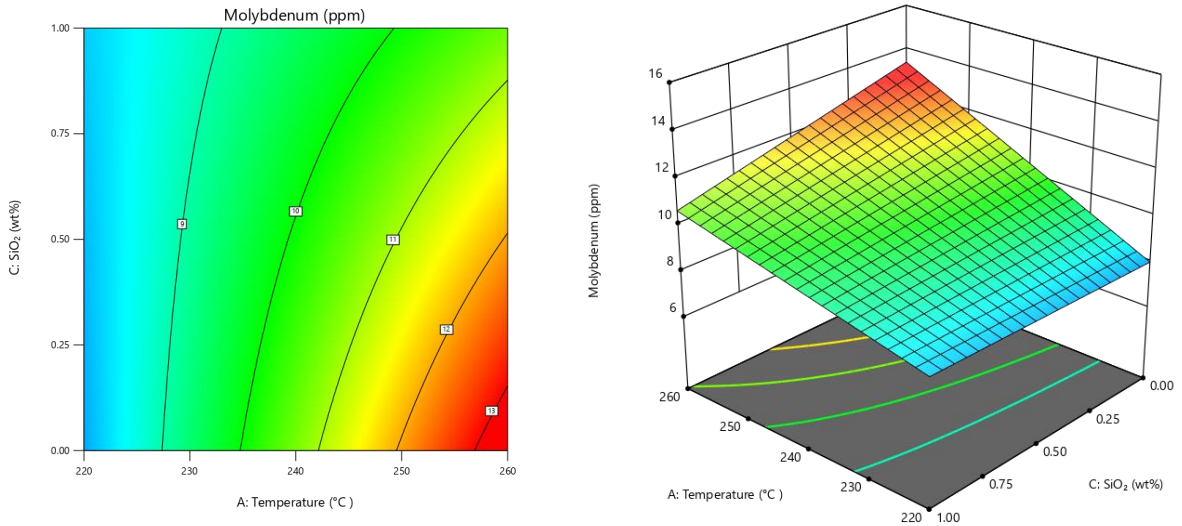
Table 19. Main data on both nanolubricants and nanobiolubricants for a response-surface reduced 2FI and linear model based on the molybdenum data.

Quantity	Nanolubricants Regression Equation	Nanobiolubricants Regression Equation
Molybdenum [ppm]	$+3.9 + 0.00909091 \cdot T - 0.142917 \cdot t + 16.5 \cdot C_{SiO2} + 0.000702652 \cdot T \cdot t - 0.0740909 \cdot T \cdot C_{SiO2}$	$+2.14516 + 0.295645 \cdot T + 0.0489041 \cdot t - 5.77965 \cdot C_{SiO2}$
Fit Statistics, Std. Dev.	0.4990	1.46
Mean	9.00	76.53
C.V. %	5.54	1.91
R^2	0.9410	0.9552
Adjusted R^2	0.9083	0.9430
Predicted R^2	0.8383	0.9057
Adeq Precision	17.8887	26.4126



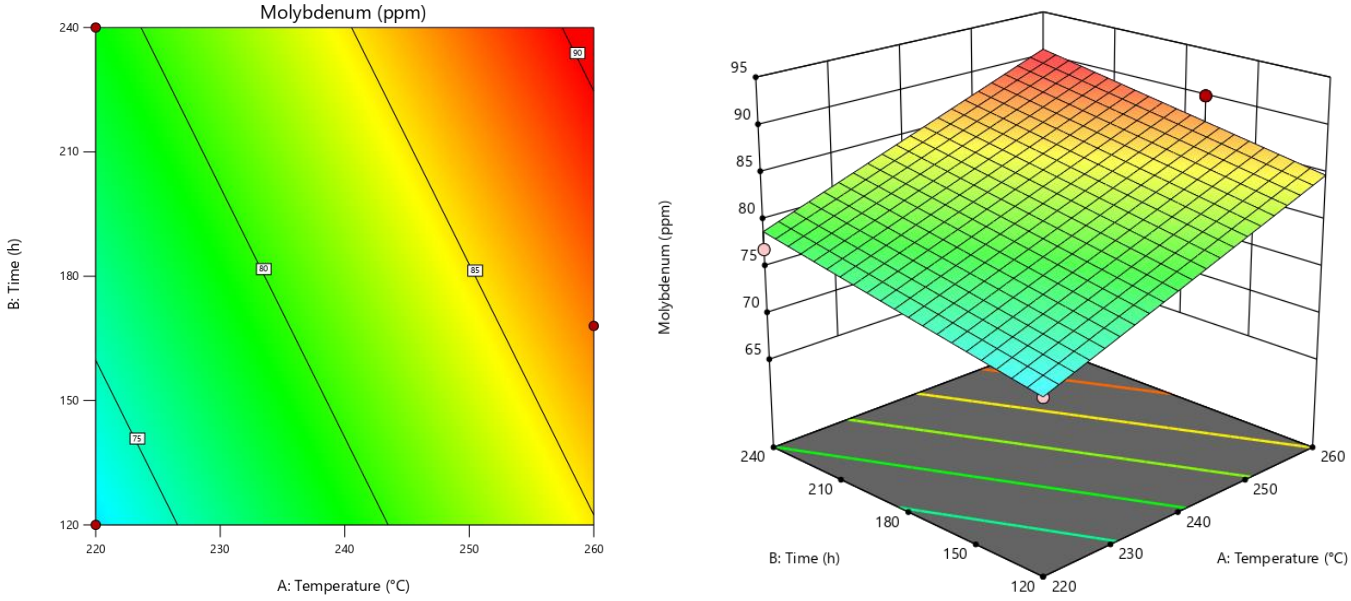
(**a**) (**b**)

https://doi.org/10.3390/lubricants14110416



(**c**) (**d**)

Figure 29. Contour plots (**left**) and the 3D surfaces (**right**) of the regression function for the molybdenum, varying the temperature and the heat-exposure time for a conventional lubricant ((**a**,**b**) and in this case the SiO_2 concentration is set at 0.00%), the temperature and concentration of SiO_2 nanoparticles ((**c**,**d**); in this case the time is set at 180 h).



(**a**) (**b**)

https://doi.org/10.3390/lubricants14110416

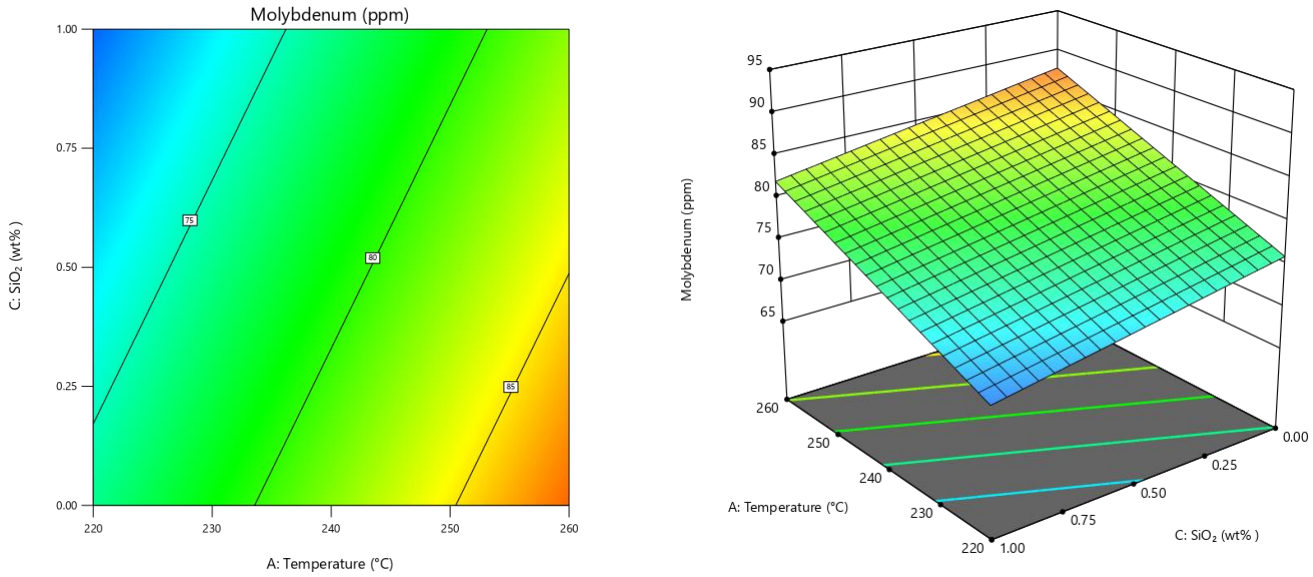


Figure 30. Contour plots (**left**) and the 3D surfaces (**right**) of the regression function for the molybdenum, varying the temperature and the heat-exposure time for a biolubricant ((**a**,**b**); in this case the SiO_2 concentration is set at 0.00%) and the temperature and concentration of SiO_2 nanoparticles ((**c**,**d**); in this case the time is set at 180 h).

4. Conclusions

This study comparatively investigated the ageing behaviour of a conventional lubricant and a biolubricant containing 0–1.00 wt.% KH570-modified SiO_2 nanoparticles under controlled thermal exposure at 220 and 260 °C for 120–240 h. The combined experimental and response-surface analyses showed that temperature, exposure time, nanoparticle concentration, and base-oil chemistry jointly controlled the physicochemical and chemical ageing responses. The main findings are summarized as follows:

- Density and viscosity: Ageing severity increased density and viscosity, while SiO_2-containing formulations generally showed lower increases under severe conditions, particularly for the biolubricant.
- Viscosity index and acid–base properties: SiO_2 partly preserved viscosity-index behaviour and produced formulation-dependent TAN/TBN responses, with more favourable trends generally observed in the biolubricant.
- Oxidation: FTIR oxidation increased with temperature and exposure time, while SiO_2 reduced oxidation under selected severe-ageing conditions, again with a more consistent response in the biolubricant.
- Elemental composition: ICP-OES showed formulation-dependent changes in elemental composition during ageing; however, these results do not establish a unique degradation mechanism.

Overall, the results demonstrate that KH570-modified SiO_2-containing formulations exhibited mitigation of several changes associated with thermo-oxidative ageing, including excessive viscosity growth, density increase, viscosity-index loss, and oxidation. Nevertheless, their effectiveness was strongly dependent on the lubricant chemistry and nanoparticle concentration. It should also be emphasized that the observed differences between the conventional lubricant and the biolubricant reflect formulation-level differences and cannot be attributed solely to their mineral- versus bio-based nature, since the two commercial products also differ in SAE grade, initial physicochemical properties, additive package, and base-oil chemistry. The most favourable range was generally between 0.75

and 1.00 wt.%, although the optimum concentration varied substantially among the investigated responses and between the two lubricant formulations. In particular, the biolubricant exhibited more favourable comparative responses under several severe-ageing conditions, including viscosity control, TAN reduction, TBN preservation, and oxidation resistance, whereas the conventional lubricant showed a more variable response.

The present findings were obtained under accelerated static ageing conditions using open sample containers and should not be directly interpreted as predictions of lubricant lifetime or as equivalent to field service intervals in an operating engine, since no experimentally validated relationship between the applied temperature–time combinations and actual service life was established. Because mass loss was not quantified, evaporation and the resulting concentrations of the remaining less-volatile lubricant components may have contributed to some of the observed changes. Nevertheless, all nanoparticle-free and SiO_2-containing formulations were subjected to the same nominal ageing conditions, allowing the results to be interpreted comparatively across formulations. Future work should therefore include gravimetric monitoring of sample mass loss and control or monitoring of the ageing atmosphere, in addition to validation under real-engine conditions involving temperature cycling, mechanical shear, variable load, fuel dilution, combustion contaminants, and repeated ageing cycles. Since no direct tribological measurements were performed in the present study, future work should include friction and wear testing to determine whether the observed physicochemical and chemical ageing trends translate into improved tribological performance.

Author Contributions: Conceptualization, H.P., S.M., M.R. and M.B.; Methodology, H.P.; Validation: H.P., S.M., M.R. and M.B.; Formal Analysis, H.P.; Investigation, H.P. and S.M.; Resources: H.P.; Data Curation, H.P.; Writing—Original Draft Preparation, H.P.; Writing—Review and Editing, H.P., M.R. and M.B.; Visualization, H.P.; Supervision, M.R. and M.B. All authors have read and agreed to the published version of the manuscript.

Funding: This research received no external funding.

Data Availability Statement: The original contributions presented in this study are included in the article. Further inquiries can be directed to the corresponding author.

Acknowledgments: The authors wish to thank Ivo Cordioli for his useful suggestions about lubricants, and the company management of NILS S.p.A. (Postal, Bolzano, Italy) for allowing Homeyra Piri to be hosted for an 8-month internship period, thus allowing her to develop expertise in lubricants. Furthermore, the authors wish also to thank NILS S.p.A. and FUCHS LUBRICANTS GERMANY GmbH for providing the lubricant and biolubricant used in the tests, free of charge.

Conflicts of Interest: The authors declare no conflicts of interest.:

References

1. Deepika. Nanotechnology implications for high performance lubricants. *SN Appl. Sci.* **2020**, *2*, 1128. https://doi.org/10.1007/s42452-020-2916-8.
2. Duan, L.; Li, J.; Duan, H. Nanomaterials for lubricating oil application: A review. *Friction* **2023**, *11*, 647–684. https://doi.org/10.1007/s40544-022-0667-9.
3. Piri, H.; Renzi, M.; Bietresato, M. Technical Implications of the Use of Biofuels in Agricultural and Industrial Compression-Ignition Engines with a Special Focus on the Interactions with (Bio)lubricants. *Energies* **2023**, *17*, 129. https://doi.org/10.3390/en17010129.
4. Pawar, R.V.; Hulwan, D.B.; Mandale, M.B. Recent advancements in synthesis, rheological characterization, and tribological performance of vegetable oil-based lubricants enhanced with nanoparticles for sustainable lubrication. *J. Clean. Prod.* **2022**, *378*, 134454. https://doi.org/10.1016/j.jclepro.2022.134454.

5. Cortes, V.; Sanchez, K.; Gonzalez, R.; Alcoutlabi, M.; Ortega, J.A. The performance of SiO_2 and TiO_2 nanoparticles as lubricant additives in sunflower oil. *Lubricants* **2020**, *8*, 10. https://doi.org/10.3390/lubricants8010010.
6. Peng, D.X.; Chen, C.H.; Kang, Y.; Chang, Y.P.; Chang, S.Y. Size effects of SiO_2 nanoparticles as oil additives on tribology of lubricant. *Ind. Lubr. Tribol.* **2010**, *62*, 111–120. https://doi.org/10.1108/00368791011025656.
7. Dembelova, T.; Badmaev, B.; Makarova, D.; Mashanov, A.; Mishigdorzhiyn, U. Rheological and Tribological Study of Polyethylsiloxane with SiO_2 Nanoparticles Additive. *Lubricants* **2023**, *11*, 9. https://doi.org/10.3390/lubricants11010009.
8. López, T.D.F.; González, A.F.; Del Reguero, Á.; Matos, M.; Díaz-García, M.E.; Badía-Laíño, R. Engineered silica nanoparticles as additives in lubricant oils. *Sci. Technol. Adv. Mater.* **2015**, *16*, 055005. https://doi.org/10.1088/1468-6996/16/5/055005.
9. Techinstro. What Are Silicon Dioxide Nano-Particles and Their Applications? Available online: https://blog.techinstro.com/what-are-silicon-dioxide-nano-particles-and-their-applications/ (accessed on 1 September 2026).
10. Shafi, W.K.; Charoo, M.S. An overall review on the tribological, thermal and rheological properties of nanolubricants. *Tribol.-Mater. Surf. Interfaces* **2021**, *15*, 20–54. https://doi.org/10.1080/17515831.2020.1785233.
11. Mariño, F.; del Río, J.M.L.; Gonçalves, D.E.P.; Seabra, J.H.O.; López, E.R.; Fernández, J. Effect of the addition of coated SiO_2 nanoparticles on the tribological behavior of a low-viscosity polyalphaolefin base oil. *Wear* **2023**, *530–531*, 205025. https://doi.org/10.1016/j.wear.2023.205025.
12. Akhter, F.; Rao, A.A.; Abbasi, M.N.; Wahocho, S.A.; Mallah, M.A.; Anees-Ur-Rehman, H.; Chandio, Z.A. A Comprehensive Review of Synthesis, Applications and Future Prospects for Silica Nanoparticles (SNPs). *Silicon* **2022**, *14*, 8295–8310. https://doi.org/10.1007/s12633-021-01611-5.
13. Navada, M.K.; Rai, R.; Shetty, A.R.; Hariharan, G.; Kumar, N.; Kumar, S.; Chandrashekar, G.S.; Aroor, G. Sol–gel-assisted synthesis of ultra-fine porous SiO_2 nanoparticles for investigation of lubricity and rheological properties of eco-friendly bio-lubricant oil. *Chem. Pap.* **2024**, *78*, 2437–2450. Correction in *Chem. Pap.* **2024**, *78*, 2451. https://doi.org/10.1007/s11696-023-03250-z.
14. Kotia, A.; Ghosh, G.K.; Srivastava, I.; Deval, P.; Ghosh, S.K. Mechanism for improvement of friction/wear by using Al_2O_3 and SiO_2/Gear oil nanolubricants. *J. Alloys Compd.* **2019**, *782*, 592–599. https://doi.org/10.1016/j.jallcom.2018.12.215.
15. Qin, C.; He, S.; Zhou, X.; Li, Q.; Li, Q.; Yang, Z. Research on the Effect of Nano/Micron SiO_2 Particles on Actual Wear of the Main Gear Box of Large-Scale Mechanical Equipment. *Tribol. Lett.* **2024**, *72*, 12. https://doi.org/10.1007/s11249-023-01814-4.
16. Haldar, A.; Kotia, A.; Kumar, N.; Ghosh, S.K. Enhancing the tribological properties of hydraulic oil-based nanolubricants using MWCNT-SiO_2 hybrid nanoparticles. *J. Braz. Soc. Mech. Sci. Eng.* **2022**, *44*, 223. https://doi.org/10.1007/s40430-022-03484-0.
17. Dai, W.; Kheireddin, B.; Gao, H.; Liang, H. Roles of nanoparticles in oil lubrication. *Tribol. Int.* **2016**, *102*, 88–98. https://doi.org/10.1016/j.triboint.2016.05.020.
18. Gaur, R.; Kumar, A.; Suhane, A. Effect of Addition of Nano Particles on Tribological Properties of Lubricants—A Review. *Int. Res. J. Eng. Technol.* **2018**, *5*, 4045–4047.
19. Chaudhary, S.; Singh, R.C.; Chaudhary, R. An Experimental Investigation of the Impact of Nanoparticles on the Tribological Properties of 15W40 Lubricating Oil. Available online: www.tjprc.org (accessed on 1 September 2026).
20. Tang, Z.; Li, S. A review of recent developments of friction modifiers for liquid lubricants (2007–present). *Curr. Opin. Solid State Mater. Sci.* **2014**, *18*, 119–139. https://doi.org/10.1016/j.cossms.2014.02.002.
21. Ali, Z.A.A.A.; Takhakh, A.M.; Al-Waily, M. A review of use of nanoparticle additives in lubricants to improve its tribological properties. *Mater. Today Proc.* **2022**, *52*, 1442–1450. https://doi.org/10.1016/j.matpr.2021.11.193.
22. Ismail, M.F.; Hamzah, W.A.W. Tribological Performance Effect of SiO_2 and TiO_2 Nanoparticles as Lubricating Oil Additives. In *Lecture Notes in Mechanical Engineering*; Springer Science and Business Media Deutschland GmbH: Berlin/Heidelberg, Germany, 2023; pp. 223–231. https://doi.org/10.1007/978-981-19-4425-3_20.
23. Lue, Y.F.; Hsiao, W.L.; Chen, Y.S. Tribology Performance of Silica Nanoparticles as Lubricant Additives in a Reciprocating Four-Stroke Engine Motorcycle. *Int. J. Automot. Technol.* **2023**, *24*, 435–444. https://doi.org/10.1007/s12239-023-0036-3.
24. Ismail, M.F.; Azmi, W.H.; Mamat, R.; Ali, H.M. Thermal and Tribological Properties Enhancement of PVE Lubricant Modified with SiO_2 and TiO_2 Nanoparticles Additive. *Nanomaterials* **2023**, *13*, 42. https://doi.org/10.3390/nano13010042.
25. Sankar, E.; Duraivelu, K. The effect of SiO_2-Al_2O_3-TiO_2 nanoparticle additives on lubrication performance: Evaluation of wear and coefficient of friction. *Mater. Today Proc.* **2022**, *68*, 2387–2392. https://doi.org/10.1016/j.matpr.2022.09.107.
26. Tan, K.-H.; Awala, H.; Mukti, R.R.; Wong, K.-L.; Ling, T.C.; Mintova, S.; Ng, E.-P. Zeolite nanoparticles as effective antioxidant additive for the preservation of palm oil-based lubricant. *J. Taiwan Inst. Chem. Eng.* **2016**, *58*, 565–571. https://doi.org/10.1016/j.jtice.2015.06.032.
27. Nagarajan, T.; Sridewi, N.; Wong, W.P.; Walvekar, R.; Khalid, M. Enhanced tribological properties of diesel-based engine oil through synergistic MoS_2-graphene nanohybrid additive. *Sci. Rep.* **2023**, *13*, 17424. https://doi.org/10.1038/s41598-023-43260-1.

28. Piri, H.; Renzi, M.; Bietresato, M. Enhancing Performance and Sustainability of Engine Lubricants and Biolubricants by Dispersing SiO_2 Nanoparticles Coated with KH570-Silane Coupling Agent. *Appl. Sci.* **2024**, *14*, 7943. https://doi.org/10.3390/app14177943.
29. Piri, H.; Moradi, S.; Renzi, M.; Bietresato, M. An Experimental–Numerical Study on Oxidation Inhibition of SiO_2 Nanoparticles in Biolubricants for Internal Combustion Engines. *Appl. Sci.* **2026**, *16*, 4208. https://doi.org/10.3390/app16094208.
30. Piri, H.; Caligiuri, C.; Brolpasino, M.; Renzi, M.; Bietresato, M. Biolubricant ageing analysis: Proposal for a real-engine test and chemical characterization. *J. Energy Inst.* **2025**, *121*, 102121. https://doi.org/10.1016/j.joei.2025.102121.
31. Piri, H.; Benedetti, V.; Moradi, S.; Renzi, M.; Bietresato, M. Enhancing thermal stability and oxidation resistance of engine lubricants by incorporating SiO_2 nanoparticles. *Sustain. Energy Technol. Assess.* **2026**, *91*, 105038. https://doi.org/10.1016/j.seta.2026.105038.
32. *ASTM D445-24*; Standard Test Method for Kinematic Viscosity of Transparent and Opaque Liquids (and Calculation of Dynamic Viscosity). ASTM: West Conshohocken, PA, USA, 2024. Available online: https://www.astm.org/d0445-24.html (accessed on 30 October 2024).
33. *ISO 2909:2002*; Petroleum Products–Calculation of Viscosity Index from Kinematic Viscosity. International Organization for Standardization: Geneva, Switzerland, 2002.
34. *ASTM D4052-22*; Standard Test Method for Density, Relative Density, and API Gravity of Liquids by Digital Density Meter. ASTM: West Conshohocken, PA, USA, 2022. Available online: https://www.astm.org/d4052-22.html (accessed on 30 October 2024).
35. *ASTM D4739-17*; Standard Test Method for Base Number Determination by Potentiometric Hydrochloric Acid Titration. ASTM: West Conshohocken, PA, USA, 2017. https://doi.org/10.1520/D4739-17.
36. *ASTM D664-18e2*; Standard Test Method for Acid Number of Petroleum Products by Potentiometric Titration. ASTM: West Conshohocken, PA, USA, 2018. Available online: https://www.astm.org/d0664-18e02.html (accessed on 30 October 2024).
37. Gulzar, M.; Masjuki, H.H.; Kalam, M.A.; Varman, M.; Zulkifli, N.W.M.; Mufti, R.A.; Zahid, R.; Yunus, R. Dispersion Stability and Tribological Characteristics of TiO_2/SiO_2 Nanocomposite-Enriched Biobased Lubricant. *Tribol. Trans.* **2017**, *60*, 670–680. https://doi.org/10.1080/10402004.2016.1202366.
38. Bietresato, M.; Caligiuri, C.; Bolla, A.; Renzi, M.; Mazzetto, F. Proposal of a predictive mixed experimental-numerical approach for assessing the performance of farm tractor engines fuelled with diesel-biodiesel-bioethanol blends. *Energies* **2019**, *12*, 2287. https://doi.org/10.3390/en12122287.
39. Caligiuri, C.; Bietresato, M.; Algieri, A.; Baratieri, M.; Renzi, M. Experimental Investigation and RSM Modeling of the Effects of Injection Timing on the Performance and NOx Emissions of a Micro-Cogeneration Unit Fueled with Biodiesel Blends. *Energies* **2022**, *15*, 3586. https://doi.org/10.3390/en15103586.
40. Bietresato, M.; Bolla, A.; Caligiuri, C.; Renzi, M.; Mazzetto, F. The kinematic viscosity of conventional and bio-based fuel blends as a key parameter to indirectly estimate the performance of compression-ignition engines for agricultural purposes. *Fuel* **2021**, *298*, 120817. https://doi.org/10.1016/j.fuel.2021.120817.
41. Available online: https://www.engineeringclicks.com/kinematic-viscosity/ (accessed on 1 September 2026).
42. Available online: https://www.britannica.com/science/density (accessed on 1 September 2026).
43. Vidrio, R.; Mastromarino, S.; Still, E.; Chapdelaine, L.; Scarlat, R.O. Density and Thermal Expansivity of Molten 2LiF-BeF2(FLiBe): Measurements and Uncertainty Quantification. *J. Chem. Eng. Data* **2022**, *67*, 3517. https://doi.org/10.1021/acs.jced.2c00212.
44. Available online: https://sciencenotes.org/viscosity-definition-and-examples/ (accessed on 1 September 2026).
45. Romano, M.R.; Cuomo, F.; Massarotti, N.; Mauro, A.; Salahudeen, M.; Costagliola, C.; Ambrosone, L. Temperature Effect on Rheological Behavior of Silicone Oils. A Model for the Viscous Heating. *J. Phys. Chem. B* **2017**, *121*, 7048–7054. https://doi.org/10.1021/acs.jpcb.7b03351.
46. Chang, T.S.; Yunus, R.; Rashid, U.; Choong, T.S.Y.; Biak, D.R.A.; Syam, A.M. Palm oil derived trimethylolpropane triesters synthetic lubricants and usage in industrial metalworking fluid. *J. Oleo Sci.* **2015**, *64*, 143–151. https://doi.org/10.5650/jos.ess14162.
47. Sharma, U.C.; Sachan, S.; Trivedi, R.K. Viscous flow behaviour of karanja oil based biolubricant base oil. *J. Oleo Sci.* **2018**, *67*, 105–111. https://doi.org/10.5650/jos.ess17140.
48. Available online: https://en.wikipedia.org/wiki/Viscosity_index (accessed on 1 September 2026).
49. Hu, C.; Ai, J.; Ma, L.; Wen, P.; Fan, M.; Zhou, F.; Liu, W. Ester Oils Prepared from Fully Renewable Resources and Their Lubricant Base Oil Properties. *ACS Omega* **2021**, *6*, 16343–16355. https://doi.org/10.1021/acsomega.1c00808.

50. Gan, Z.; Yao, T.; Zhang, M.; Hu, J.; Liao, X.; Shen, Y. Effect of temperature on the composition of a synthetic hydrocarbon aviation lubricating oil. *Materials* **2020**, *13*, 1606. https://doi.org/10.3390/ma13071606.
51. Barbera, E.; Hirayama, K.; Maglinao, R.L.; Davis, R.W.; Kumar, S. Recent developments in synthesizing biolubricants—A review. *Biomass Convers. Biorefin.* **2022**, *14*, 2867–2887. https://doi.org/10.1007/s13399-022-02438-9.
52. Salimon, J.; Abdullah, B.M.; Yusop, R.M.; Salih, N. Synthesis, reactivity and application studies for different biolubricants. *BMC Chem.* **2014**, *8*, 16. https://doi.org/10.1186/1752-153X-8-16.
53. Khan, S.; Das, P.; Quadir, M.A.; Thaher, M.; Annamalai, S.N.; Mahata, C.; Hawari, A.H.; Al Jabri, H. A comparative physicochemical property assessment and techno-economic analysis of biolubricants produced using chemical modification and additive-based routes. *Sci. Total Environ.* **2022**, *847*, 157648. https://doi.org/10.1016/j.scitotenv.2022.157648.
54. Nogales-Delgado, S.; Cabanillas, A.G.; Romero, Á.G.; Martín, J.M.E. Monitoring tert-Butylhydroquinone Content and Its Effect on a Biolubricant during Oxidation. *Molecules* **2022**, *27*, 8931. https://doi.org/10.3390/molecules27248931.
55. Oil Analysis and Testing TAN & TBN. Available online: https://www.oil-analysis.org/tan-tbn/ (accessed on 8 November 2024).
56. Available online: https://360.lubrizol.com/2023/Measuring-Lubricant-Lifetime-Are-Current-Measures-Telling-the-Whole-Story (accessed on 1 September 2026).
57. Polaris Laboratories. Optimizing Drain Intervals Using TBN vs. TAN. Available online: https://www.machinerylubrication.com/Read/2170/oil-drain-interval-tan-tbn (accessed on 7 September 2024).
58. Cecilia, J.A.; Plata, D.B.; Saboya, R.M.A.; de Luna, F.M.T.; Cavalcante, C.L.; Rodríguez-Castellón, E. An overview of the biolubricant production process: Challenges and future perspectives. *Processes* **2020**, *8*, 257. https://doi.org/10.3390/pr8030257.
59. Wang, W.; Chang, W.; Ding, S.; Qu, Y.; Gao, Y.; Wang, K. Preparation and tribological properties of multi-layer graphene/silicon dioxide composites-based solid lubricant coatings at elevated temperatures. *R. Soc. Open Sci.* **2023**, *10*, 220740. https://doi.org/10.1098/rsos.220740.
60. Determination of Metals in Lubricating Oil by ICP-OES. Available online: https://www.agilent.com/cs/library/applications/ICPES-2.pdf (accessed on 1 September 2026).
61. Bietresato, M.; Friso, D. Durability test on an agricultural tractor engine fuelled with pure biodiesel (B100). *Turk. J. Agric. For.* **2014**, *38*, 214–223. https://doi.org/10.3906/tar-1302-51.

Disclaimer/Publisher's Note: The statements, opinions and data contained in all publications are solely those of the individual author(s) and contributor(s) and not of MDPI and/or the editor(s). MDPI and/or the editor(s) disclaim responsibility for any injury to people or property resulting from any ideas, methods, instructions or products referred to in the content.